COULOMBIC INTERACTIONS IN RIBONUCLEASE A

by

Barbra Mindy Templer

A dissertation submitted in partial fulfillment

of the requirements for the degree of

Doctor of Philosophy

(Biochemistry)

at the

UNIVERSITY OF WISCONSIN–MADISON

1998

A dissertation entitled

Coulombic Interactions in Ribonuclease A

submitted to the Graduate School of the
University of Wisconsin-Madison
in partial fulfillment of the requirements for the
degree of Doctor of Philosophy
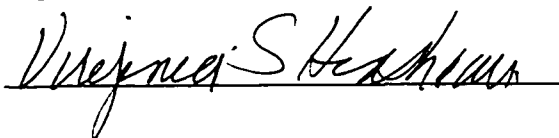
by

Barbra Mindy Templer

Date of Final Oral Examination: May 21, 1998

Month & Year Degree to be awarded: **December**   **May**   **August**   1998

* *

Approval Signatures of Dissertation Readers: **Signature, Dean of Graduate School**

COULOMBIC INTERACTIONS IN RIBONUCLEASE A

Barbra Mindy Templer

Under the supervision of Associate Professor Ronald T. Raines

At the University of Wisconsin–Madison

The interactions between bovine pancreatic ribonuclease (RNase) A and its RNA substrate extend beyond the scissile $P–O_{5'}$ bond. Enzymic subsites interact with the bases and phosphoryl groups of the substrate. Those residues interacting with the phosphoryl groups comprise the P0, P1, and P2 subsites, with the scissile bond residing in the P1 subsite. In this Dissertation, the function of the P0 and P2 subsites of RNase A is characterized in detail. A new subsite, P(−1), is also described.

Lys66 (P0 subsite) and Lys7 and Arg10 (P2 subsite) were replaced with alanine residues. Wild-type RNase A and the K66A, K7A/R10A, and K7A/R10A/K66A variants were evaluated as catalysts for the cleavage of poly(cytidylic acid) and for their abilities to bind to single-stranded DNA, a substrate analog (Chapter Two). The values of k_{cat}, K_m, and k_{cat}/K_m for poly(C) cleavage were affected by altering the P0 and P2 subsites as were the values of K_d for RNase A•d(AUAA) complex formation. Nucleic acid binding to wild-type RNase A is strongly dependent on NaCl concentration (values of K_d range from 0.82 μM – 88 μM), but this dependence is diminished upon alteration of the P0 and P2 subsites. Similar experiments with NaF and wild-type RNase A indicate that the anion has little effect on nucleic acid binding. Structures of K7A/R10A/K66A RNase A and the K7A/R10A/K66A• uridine 3′-phosphate RNase A complex were determined by X-ray diffraction analyses to resolutions of 2.0 Å and 2.1 Å, respectively (Chapter Three). Little change is observed between these structures and that of wild-type RNase A, either free or with bound cytidine 3′-phosphate. The

P0 and P2 subsites depress the pK_a values of the two active-site histidine residues and decrease their interaction with each other. These effects are sensitive to salt concentration. For these reasons, K7A/R10A/K66A RNase A cleaves UpA and binds uridine 3′-phosphate, neither of which span the P0 or P2 subsites, less efficiently than does wild-type RNase A. In Chapter Four, a new RNase A subsite, comprised of Arg85, is described. Together these results provide a detailed picture of the role of Coulombic interactions in catalysis by RNase A.

ACKNOWLEDGEMENTS

TABLE OF CONTENTS

LIST OF FIGURES

LIST OF TABLES

LIST OF ABBREVIATIONS

A .... anisotropy

EDN .... eosinophil-derived neurotoxin

3′-CMP.. cytidine 3′-phosphate

DCl ....deuterium chloride

D_2O ....deuterium oxide

DSS........................ sodium 2,2-dimethyl-2-silapentane-5-sulfonate

DTT..dithiothreitol

Fl...fluorescein

^{1}H NMR ....proton nuclear magnetic resonance

HPLC .... high pressure liquid chromatography

I...intensity

IPTG isopropyl-1-thio-β-D-galactopyranoside

IEF..isoelectric focusing

K_d.....................................equilibrium dissociation constant

MES ....2-(N-morpholino)ethanesulfonic acid

NaOD.. sodium deuteroxide

OD ....optical density

PAGE ....polyacrylamide gel electrophoresis

pdb.......................................Brookhaven Protein Data Bank

pI... isoelectric point

PLP... pyridoxal 5′-phosphate

poly(C)..poly(cytidylic acid)

ppm .... parts per million

pUp .... 5′-phosphouridine 3′-phosphate

pU>p .... 5′-phosphouridine 2′,3′-cyclic phosphate

RNase A .... bovine pancreatic ribonuclease A

SDS .... sodium dodecyl sulfate

SOD .... superoxide dismutase

SSB .... single-stranded binding protein

TB .... terrific broth

T_m .... midpoint in a thermal denaturation curve

3′-UMP .... uridine 3′-phosphate (otherwise Up)

Up .... uridine 3′-phosphate

UpA .... uridylyl(3′→5′)adenosine

U>p .... uridine 2′,3′-cyclic phosphate

Chapter One

Introduction

Overview. Proteins serve essential roles in biology. These biopolymers provide a large part of the structural framework of cells and tissues, transport and store small molecules, control metabolic pathways, regulate gene transcription and translation, and protect against attack by foreign bacteria and viruses. Proteins are able to perform such diverse functions due to their unique three-dimensional structures, which are encoded by their amino acid sequences (*i.e.*, their primary structure). A regular motif of covalent bonds between amino acid residues forms the backbone of a protein. All twenty naturally-occurring amino acids have a central carbon atom to which an amino group, a carboxyl group and a variable side chain are covalently attached. The chemical nature of the side chain distinguishes each amino acid from the nineteen others. Additionally, cysteine residues can form covalent crosslinks via the sulfur atoms in their side chains.

Although 25 years have elapsed since Anfinsen demonstrated that the three-dimensional structure of a protein is determined by its primary structure (Anfinsen, 1973), the details of protein folding pathways and the ability to predict a protein structure from its amino acid sequence remain inaccessible. The ability to predict the function of a protein strictly from its three-dimensional structure is also out of reach. The protein folding problem and the relationship between protein structure and function are two central questions in biochemistry that remain elusive. Both questions are related to how atoms interact with each other through noncovalent, rather than covalent, interactions.

In this Dissertation, the importance of noncovalent interactions between charged residues (*i.e*, Coulombic interactions) in enzymology is examined using bovine pancreatic ribonuclease A (RNase A) as a model system. The ensuing introduction (Chapter One) provides a historical account of the study of Coulombic interactions in proteins, including a discussion of the work of Charles Augustin Coulomb and descriptions of several studies undertaken more recently that demonstrate the importance of Coulombic interactions in biological systems. In Chapter Two, Coulombic interactions between three RNase A cationic

residues (Lys7, Arg10, and Lys66) and the anionic phosphoryl groups of a bound nucleic acid are characterized. Crystalline structures of K7A/R10A/K66A RNase A, both free and with a bound nucleotide, are reported in Chapter Three. Long-range Coulombic interactions between the side chains of Lys7, Arg10, and Lys66 and active-site residues His12 and His119 are also described in Chapter Three. In Chapter Four, the identification of a new remote subsite in RNase A is described. This subsite is comprised of Arg85, whose cationic side chain is postulated to interact with a phosphoryl group of a bound nucleic acid via a Coulombic interaction. Together, these results elucidate how one type of noncovalent interaction affects the structure – function relationships of RNase A.

Noncovalent Interactions. Interactions between covalently bonded atoms are much stronger than are noncovalent interactions. For example, the homolytic bond strength for each C–H bond in methane is > 100 kcal/mol whereas the strength of a typical hydrogen bond is in the range of 2 – 10 kcal/mol (Pauling, 1960) and the strength of a $Glu^-\cdots Lys^+$ ion pair is ~0.5 kcal/mol (Scholtz *et al.*, 1993; Smith & Scholtz, 1998). Although energetically weak, noncovalent interactions are the glue that holds the covalently bonded atoms of a protein together in a functional three-dimensional assembly. Biology as we know it depends on water. The interactions between biological molecules in an aqueous environment involve noncovalent interactions both with each other and with the solvent.

Noncovalent interactions can be divided into two categories: hydrophobic and electrostatic. The hydrophobic effect describes the tendency of nonpolar groups to associate with each other and thereby exclude water when in this polar solvent. This effect provides a meaningful description for the tendency of nonpolar amino acids to cluster in the interior of proteins. [For reviews, see: Kauzmann (1959) and Rose and Wolfenden (1993).] "Electrostatic" tends to be an all-inclusive term that describes all noncovalent interactions that are not hydrophobic (Burley & Petsko, 1988; Matthews & van Holde, 1990; Nakamura, 1996). These types of interactions can be divided further into the categories of hydrogen

bonds, London (also called dispersion or van der Waals), dipole – induced dipole, charge – induced dipole, dipole – dipole, charge – dipole, and charge – charge interactions. The energies of electrostatic interactions decrease as the distances (r) between interacting atoms increase. The energy of London forces decreases as a function of $1/r^6$. Interactions between point charges are the strongest of the non-hydrogen bond electrostatic interactions, with their energies dependent on the inverse of the distance between the charges (*i.e.*, $1/r$). These interactions are called Coulombic interactions and will be described in detail.

Coulombic Interactions. The law that describes the forces between two point charges is named after Charles Augustin Coulomb (Figure 1.1), who in the late eighteenth century, wrote seven important memoirs related to electricity and magnetism (Coulomb, 1884). Although several scientists had postulated that the force between two point charges is inversely proportional to the square of the distance between them (the inverse square law), Coulomb was the first to support this hypothesis with experimental data (Gillmor, 1971). In his experiments, Coulomb used a torsion balance that he had developed to study many other fundamental problems in physics and engineering. In his first memoir, read to the Académie des Sciences in France in 1785, Coulomb proved that like charges are repulsive. In his second memoir, read to this academy two years later, he proved that opposite charges are attractive. In these memoirs, Coulomb implied, but never stated explicitly, that the forces between charges are proportional to the product of their charges. Although he never recorded Coulomb's law as it appears in physics books today, this important equation, eq 1.1, is given his name in recognition of his significant contributions.

$$F = \frac{kq_1q_2}{r^2} \qquad (1.1)$$

In eq 1.1, k is Boltzmann's constant, q_1 and q_2 are the two point charges, and r is the distance separating the two charges. If q_1 and q_2 have the same sign, the force between them will be positive, which corresponds to repulsion. If q_1 and q_2 have opposite signs, the force between them will be negative, and thus attractive. Equation 1.1 describes the force between two point charges in a vacuum. A term must be added to this equation to account for solvent, which has the capacity to shield charges from each other. To account for medium effects, a term describing the dielectric constant of the solvent (ε) is inserted into the denominator of eq 1.1 to give eq 1.2:

$$F = \frac{kq_1q_2}{\varepsilon r^2} \tag{1.2}$$

Dielectric constants range typically between the values of $2 - 110$ (Creighton, 1993), with that of water being 78.5. From eq 1.2, it is apparent that Coulombic interactions are favored in solvents with low dielectric constants. The protein surface and interior are often regarded as regions whose dielectric constant is lower than that of water. The strength of a Coulombic interaction may be stronger in proteins than is the interaction between analogous groups examined free in solution because the charged groups in the protein are attached to regions of lower dielectric (Kauzmann, 1959). Still, choosing an appropriate dielectric constant for modeling protein clefts in theoretical studies has been the subject of much controversy (Mehler & Eichele, 1984; Gilson *et al.*, 1985; Gilson & Honig, 1988; Warshel & Åqvist, 1991).

Applications to Protein Chemistry. Coulomb's basic principles have been applied to protein chemistry via two main avenues: theoretical studies and experimental studies. Both are rooted in the work of Linderstrøm-Lang (1924), who first proposed a quantitative model of Coulombic interactions in native proteins. He applied the theory of electrolyte solutions described by Debye and Hückel (1923) one year earlier to polyvalent acids and ampholytes. By

treating a protein as a multivalent spherical particle with charges distributed uniformly on its surface, Linderstrøm-Lang predicted that the number of protons that bind to a protein (and hence its net charge) varies as a function of the solution pH. In addition, he showed that the pH titration behavior of a protein varies with salt concentration. Although this model was grossly oversimplified, it provided a valuable starting point for applying basic principles of physics to protein chemistry.

Studies of Coulombic interactions in proteins have focused primarily on the determination of pK_a values of titratable groups in folded proteins. The side chains of four (or five, if histidine is included) of the twenty amino acids bear a charge under physiological conditions. The environment in which these side chains reside affects their pK_a values. In a denatured protein, the polypeptide chain adopts random conformations wherein residues do not interact with each other through the ordered noncovalent interactions that stabilize the folded protein. In contrast, residues that are distal in primary structure but proximal in tertiary structure can interact with each other in a folded protein. By comparing the pK_a values of titratable residues in native proteins to those in analogous model compounds, one can ascertain the extent of environmental influence on the protonation state of the residue. For such a comparison to be valid, the model compounds used in these comparisons must take into account the inductive effect of the polypeptide on the acid dissociation constant of the titratable group. For instance, N-acetylaspartic acid α-amide (pK_a 4.0) is a good mimic of the side chain of an aspartic acid residue in a polypeptide chain (pK_a 4.0) whereas the completely aliphatic model compound acetic acid (pK_a 4.75) underestimates the acidity of the β-carboxylic acid group. Tables of pK_a values for titratable amino acid residues (Asp, Arg, Asn, Cys, Gln, Glu, His, Lys, Ser, Thr, Tyr, and Trp) in random polypeptide chains are available (Edsall & Wyman, 1958; Tanford, 1962; Kyte, 1995).

Intramolecular Coulombic Interactions. Perturbed pK_a values of titratable groups arise often from Coulombic interactions with proximal acidic or basic residues. Coulombic interactions can either stabilize or destabilize the charged form of the titratable group. Attractive interactions between a cationic residue and an anionic residue tend to stabilize the charged form of the residues while repulsive interactions between two anionic or two cationic residues tend to destabilize the charged form of each. For example, the pK_a of the xylanase active-site residue Glu172 is raised 1.2 units (to 6.7) by its proximity to Glu78 (McIntosh *et al.*, 1996). Electrostatic repulsion between the Glu78 carboxylate group and that of Glu172 is responsible for this elevation. Evolution appears to have favored spatial proximity of two acidic residues in the glycosidase family to effect catalysis. Lysozyme has an aspartic acid residue, Asp52, rather than a glutamic acid residue as in xylanase, near the active-site residue Glu35 to help elevate its pK_a value (Inoue *et al.*, 1992; Bartik *et al.*, 1994). In these enzymes, one of the two active-site acidic residues (Glu78 in xylanase and Glu35 in lysozyme) functions as a nucleophile during a double-displacement reaction while the other active-site residue (Glu172 in xylanase or Asp52 in lysozyme) cycles between its role as an acid and a base during the two-step reaction. The perturbed pK_a values result in the efficient cycling between these roles under physiological conditions. Coulombic interactions between neighboring active-site residues may be a common feature of enzymatic catalysis.

Coulombic interactions between some nearby, interacting titratable groups are described more completely by microscopic pK_a values than by macroscopic pK_a values such as those reported for members of the glycosidase family of enzymes. Microscopic pK_a values arise from Coulombic interactions that create either positive or negative cooperativity during acid dissociation, and describe the protonation state of one residue when the neighboring residue is either protonated or unprotonated. For example, Cys32 in thioredoxin is affected by the protonation state of Asp26 (Chivers *et al.*, 1997). When Asp26 is protonated, the microscopic pK_a of Cys32 is 7.5. When Asp26 is unprotonated, the microscopic pK_a of Cys32 is 9.2.

Likewise, when Cys32 is protonated, the microscopic pK_a of Asp26 is 7.5. When Cys32 is unprotonated, the microscopic pK_a of Asp26 is 9.2. These residues interact with negative cooperativity, *i.e.*, the deprotonation of one residue disfavors deprotonation of the other, due to the unfavorable Coulombic interaction between neighboring anionic groups. Microscopic pK_a values for the active-site histidine residues in RNase A were demonstrated many years ago (Markley & Finkenstadt, 1975) and will be discussed in detail in Chapter Three. Still, recent studies examining the pH-titration behavior of these residues in RNase A (and the homologous protein angiogenin) failed to account for these microscopic pK_a values (Cederholm *et al.*, 1991; Lequin *et al.*, 1997).

Early theoretical studies on Coulombic interactions were performed even before the first protein crystalline structure was determined (Tanford, 1957; Tanford & Kirkwood, 1957). In these studies, not only were the distribution of protein charges not known, but also the overall shape of proteins was still regarded as strictly spherical. Protein structure determinations have advanced both theoretical and experimental studies on Coulombic interactions significantly. Structural information was utilized in an early study on the pH titration of lysozyme (Tanford & Roxby, 1972); The positions of individual titratable groups on the protein were taken into account during both the theoretical studies and the interpretation of experimental results. Similarly, theoretical calculations that describe the pH titration curve of hemoglobin were improved dramatically upon the determination of a 2.8 Å-resolution structure of this protein (Orttung, 1969; Orttung, 1970).

The introduction of protein engineering was another significant advance in the study of Coulombic interactions within proteins. With protein crystalline structures, interactions between residues could be postulated based on the spatial proximity of charged residues. Replacing charged residues with other aliphatic residues by protein engineering makes possible the direct testing of such hypotheses. For example, Glu139 is 3.6 Å from the imidazole nitrogens of His66 in bovine protein tyrosine phosphatase (Tishmack *et al.*, 1997). In the

wild-type protein, the pK_a of His66 is 8.3. The proximity of the Glu139 carboxylate group to the His66 imidazole group was hypothesized to be one of the causes of this elevated pK_a value. The replacement of Glu139 with alanine resulted in a pK_a of 7.1 for His66 in the E139A protein variant. Although the pK_a value of His66 remains elevated in the protein variant, indicating interactions with additional residues, a favorable interaction between the anionic glutamic acid residue and the cationic histidine residue clearly exists.

In addition to advancing the study of Coulombic interactions between neighboring groups, protein engineering has afforded the means to study long-range Coulombic interactions within a protein. From crystalline structures, it is difficult to determine if non-neighboring residues are interacting with each other. By replacing the residue in question with an alanine residue, the existence of long-range interactions can be evaluated. Fersht and coworkers used the protease subtilisin BPN′ in pioneering work in this area (Russell & Fersht, 1987). Several anionic residues 13 – 15 Å from the active site of this enzyme were replaced individually with neutral or cationic residues. The resultant protein variants were examined for their abilities to form complexes with a transition-state analog (Jackson & Fersht, 1993). Experimental results showed that long-range Coulombic interactions contribute 0.1 – 0.46 kcal/mol each to the binding energy of the transition-state analog. These studies illustrate the importance of long-range Coulombic interactions in transition-state stabilization during enzymatic catalysis. A similar study has been performed with the nuclease barnase. In barnase, charged residues 12 Å from the active site were shown to interact with active-site residue His64 with free energies in the range of 0.3 – 0.5 kcal/mol (Loewenthal *et al.*, 1993). Chapter Three in this Dissertation examines the role of long-range Coulombic interactions in catalysis by RNase A.

Salt-Concentration Dependence of pK_a Values. Determining the salt-concentration dependence of pK_a values is an effective means to detect the presence of Coulombic interactions between protein residues. Coulombic interactions are masked by concentrated

solutions of electrolytes such that Coulombic effects are most apparent in solutions of low salt concentration (Russell *et al.*, 1987). Although obtaining quantitative data for the dependence of pK_a values on the salt concentration is difficult (see Section 3.5 in this Dissertation), qualitative results support this theory. In a model peptide of 26 amino acid residues designed by Blasie and Berg (1997), a Coulombic interaction between Arg3 and Asp10 is influenced dramatically by salt concentration. The strength of this interaction decreases five-fold, from –0.5 kcal/mol to –0.1 kcal/mol, upon raising the salt concentration from 0 M NaCl to 0.1 M NaCl. The effect of salt concentration on intraprotein Coulombic interactions has also been investigated. One such study examined the interaction between subtilisin BPN′ residues His64 and Glu156 (Loewenthal *et al.*, 1993). At 0.001 M salt, the measured interaction energy between these two residues is 0.5 kcal/mol. When the salt concentration was increased to 0.5 M, the interaction energy decreased to a value of 0.1 kcal/mol. In these types of experiments, proper controls must be performed to insure that the apparent salt concentration-dependence of pK_a values is a result of Coulombic interactions and not a result of specific ion binding to the protein (Lohman, 1986).

Protein–Ligand Interactions. The importance of Coulombic interactions in biology extends beyond those that are intramolecular. Intermolecular Coulombic interactions, such as those between enzymes and small-molecule substrates or proteins and nucleic acids, are an essential component of molecular recognition and often contribute significantly to the stability of protein•ligand complexes.

An isolated charge on a substrate may form a specific Coulombic interaction with an enzymic residue or interact Coulombically with several enzymic residues at once. An example comes from ornithine decarboxylase, a pyridoxal 5′-phosphate (PLP)-dependent enzyme that catalyzes the conversion of ornithine to putrescine (Osterman *et al.*, 1997). The phosphate group of PLP is stabilized by interactions with a glycine-rich loop and by a Coulombic

interaction with the side chain of Arg277. Replacing Arg277 with an alanine residue results in a value of K_m that is 270-fold larger than that of the wild-type enzyme. Thus, a single Coulombic interaction is important for the binding of PLP. In contrast, superoxide dismutase (SOD) attracts the radical substrate O_2^- by a mechanism that has been named electrostatic guidance (Getzoff et al., 1983; Sharp et al., 1987). In this mechanism of molecular recognition, several enzymic residues form an electrostatically-focused region that attracts the anionic substrate. In an SOD variant designed to have an enhanced local positive charge, the diffusion-limited rate of radical dismutation is increased (Getzoff et al., 1992).

Multiple Coulombic interactions between the anionic phosphoryl group-backbone of a nucleic acid strand and cationic residues on nucleic acid-binding proteins contribute to protein•nucleic acid complex formation. Similar to the electrostatic guidance mechanism used by SOD to attract its anionic substrate, nucleic acid-binding proteins often have cationic regions dedicated to interacting with the anionic nucleic-acid ligand. For example, a common motif in RNA-binding proteins is an arginine-rich "basic domain" (Varani, 1997). In the HIV-1 Tat protein, a nine-residue basic domain helps mediate complex formation with its TAR RNA hairpin substrate (Frankel, 1992; Frankel, 1994). Model peptide studies have shown that these domains confer substrate specificity to complex formation. Peptides comprised of 10 – 15 basic residues bind RNA with comparable affinity to the corresponding protein, but fail to discriminate cognate binding sites from noncognate RNAs (Varani, 1997). In the deoxyribonuclease T4 endonuclease V, a basic amino acid cluster participates in substrate binding (Doi et al., 1992). Upon removal of the Arg3, Arg22, Arg26, Arg117, or Lys121 side chains, a significant increase in the value of K_m for a specific substrate is observed. The β-subunit of Escherichia coli DNA polymerase III binds to DNA non-specifically (Kuriyan & O' Donnell, 1993). This protein has a ring-shaped tertiary structure lined with cationic residues on its inner surface (Kong et al., 1992). Complex formation between this subunit and DNA

depends primarily on contacts formed between these cationic protein residues and the anionic nucleic acid phosphoryl groups. Coulombic interactions between the cationic active-site cleft of RNase A and a bound nucleic acid are examined in Chapters Two and Four.

Thermodynamic Signature of Coulombic Interactions. In aqueous solvents, the formation of an ion pair is entropically-favored and enthalpically-disfavored (Kauzmann, 1959). When an ion pair is formed, immobilized ions and water molecules are released into solvent, thus increasing the "disorder" or configurational freedom in the solvent. This disorder gives rise to a large increase in the overall entropy change associated with complex formation. In contrast, energetically favorable ion–water interactions are disrupted upon complex formation, resulting in a positive (*i.e.*, unfavorable) enthalpy change associated with ion pair formation. Thus, in water, favorable Coulombic interactions are always entropically-driven (Cantor & Schimmel, 1980).

Studies on the thermodynamics of intermolecular Coulombic interactions in biological systems have focused primarily on the formation of protein•nucleic acid complexes. The dominant factor driving complex formation is the favorable gain in entropy arising from the release of accumulated counterions. Theory predicts that a protein•nucleic acid complex will dissociate with increasing cation concentration (Record *et al.*, 1976). Similar to the detection of intramolecular Coulombic interactions by varying the salt concentration and measuring pK_a values of titratable residues, intermolecular Coulombic interactions can be detected by measuring equilibrium binding constants at varying cation concentrations. If the nucleic acid strand is a polymer (> 36 phosphoryl groups), the number of cations released and number of ion pairs formed upon complex formation can be determined from the slope of a $\log(K_a)$ versus $\log([cation])$ plot (Olmsted *et al.*, 1989).

The binding of several different proteins to polymeric DNA has been examined as a function of salt concentration. For example, the binding of *Escherichia coli* single-stranded binding protein (SSB) to poly(dT) has been examined as a function of NaCl concentration

(Lohman & Overman, 1985; Bujalowski & Lohman, 1986; Overman *et al.*, 1988). Upon varying the NaCl concentration, it became apparent that SSB binds poly(dT) in multiple binding modes, where 35, 56, or 65 nucleotides are bound per tetramer. This latter mode of binding is designated $(SSB)_{65}$. More recent experiments with this system revealed that significant Coulombic interactions occur in the $(SSB)_{65}$ complexes with several different single-stranded DNA polymers, resulting in a net release of both cations and anions as well as contributions due to cation and anion uptake (Overman *et al.*, 1988; Overman & Lohman, 1994). A similar study was undertaken with the intron-encoded endonuclease I-*Ppo*I, an enzyme which binds and cleaves double-stranded DNA. Binding assays in the presence of varying NaCl concentrations revealed that 6.3 ± 1.4 ion pairs are formed upon complex formation (Wittmayer & Raines, 1996). The interaction of the *lac* repressor protein with nonspecific DNA and with its specific DNA ligand, the *lac* operator, has been examined in detail as well. In the nonspecific *lac* repressor•DNA complex, 12 ± 2 DNA phosphoryl groups are involved in Coulombic interactions with the protein (deHaseth *et al.*, 1977). In the specific *lac* repressor•*lac* operator complex, 8 ± 1 Coulombic interactions are formed (Record *et al.*, 1977). The binding of RNase A to a heterogeneous ssDNA polymer also shows a strong dependence on the NaCl concentration (Jensen & von Hippel, 1976). From an analysis similar to those described above, it was shown that seven ion pairs are formed between polymeric ssDNA and RNase A (Record *et al.*, 1976). In Chapters Two and Four of this Dissertation, the binding of a small (4-base), single-stranded DNA oligonucleotide to RNase A is examined in detail.

RNase A as a Model System. In this Dissertation, the role of Coulombic interactions in the RNase A-catalyzed cleavage of RNA is described. RNase A (Figure 1.2) catalyzes the hydrolytic cleavage of the $P–O_{5'}$ bond of single-stranded RNA specifically after pyrimidine residues (Figure 1.3). His12 and His119 are the base and acid, respectively, in this

transphosphorylation reaction (Findlay *et al.*, 1961; Thompson & Raines, 1994) and the side chain of Lys41 donates a hydrogen bond to stabilize the transition state (Messmore *et al.*, 1995). RNase A has been the object of landmark work on the folding, stability, and chemistry of proteins and in enzymology. [For reviews, see: (Richards & Wyckoff, 1971; Karpeisky & Yakovlev, 1981; Blackburn & Moore, 1982; Beintema, 1987; Raines, 1998).] RNase A was one of the first enzymes whose structure was determined by X-ray diffraction analysis (Kartha *et al.*, 1967). In total, over 70 sets of three-dimensional coordinates (from both X-ray diffraction analysis and ^{1}H NMR spectroscopy) related to RNase A have been deposited in the Brookhaven Protein Data Bank (Raines, 1998), including structures of RNase A with bound oligonucleotides, dinucleotides, and mononucleotides (Gilliland, 1997). The recent cloning of the RNase A gene and its overexpression in *Escherichia coli* make this protein amenable to protein engineering studies (delCardayré *et al.*, 1995). The wealth of structural and mechanistic information available on this small (13.7 kDa), stable, cationic (at physiological pH) and readily available protein make RNase A an excellent model for such studies.

Conclusions. Intra- and intermolecular Coulombic interactions are prevalent in biological systems. Such interactions are a general feature of enzymatic catalysis and play a key role in protein•nucleic acid complex formation. The continued examination of Coulombic interactions, via the determination of pK_a values for protein titratable groups or the salt concentration-dependence of protein•nucleic acid complex formation, will further our understanding of this important noncovalent interaction.

Figure 1.1   Charles Augustin Coulomb (1736–1806). This picture was reproduced from

Gilmor (1971).
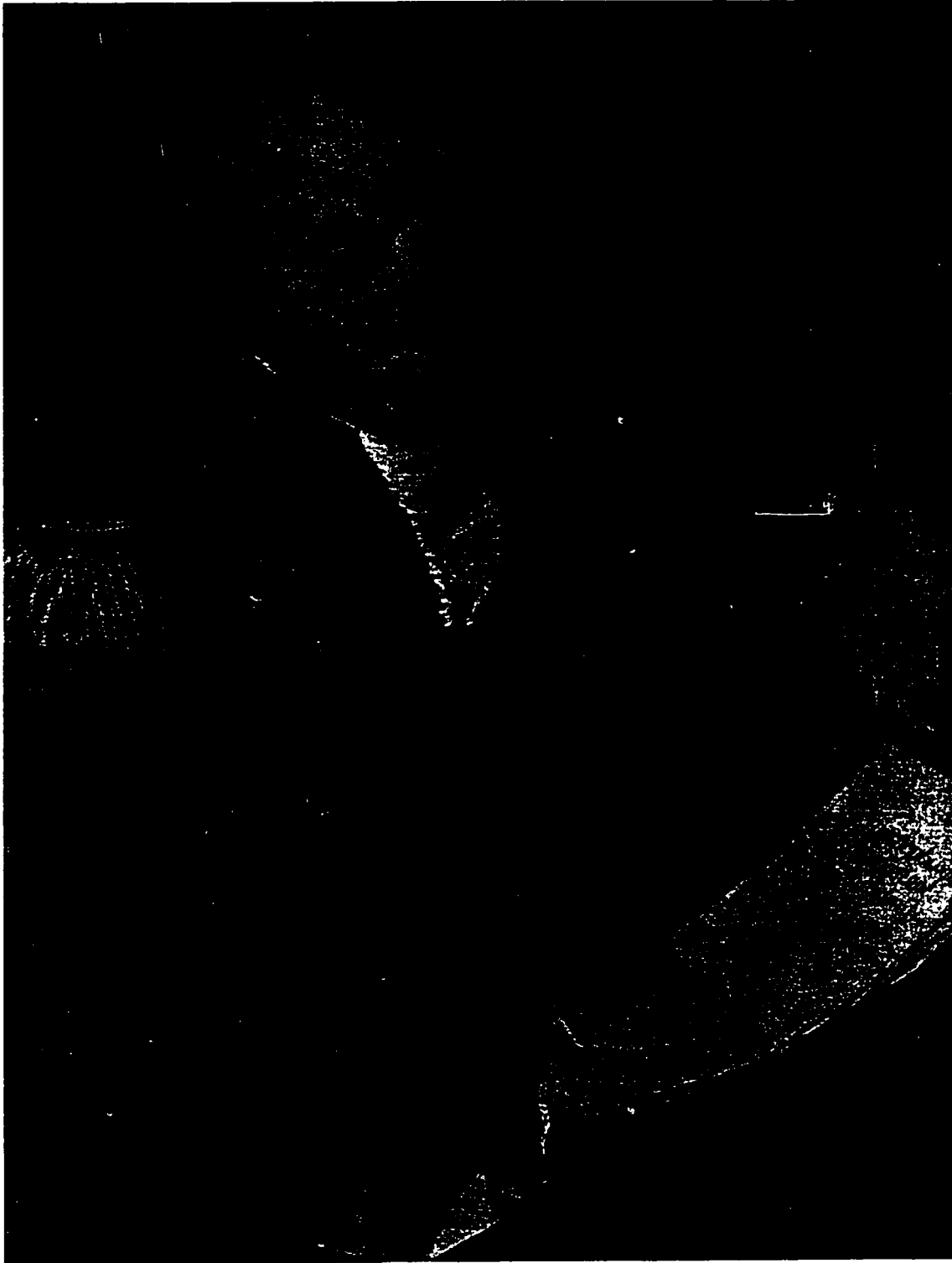
Figure 1.2   Ribbon diagram of the structure of RNase A. The positions of the active-site

residues His12, His119, and Lys41 are indicated. The four disulfide bonds in

RNase A are indicated in yellow.

Lys41

His119

His12

19
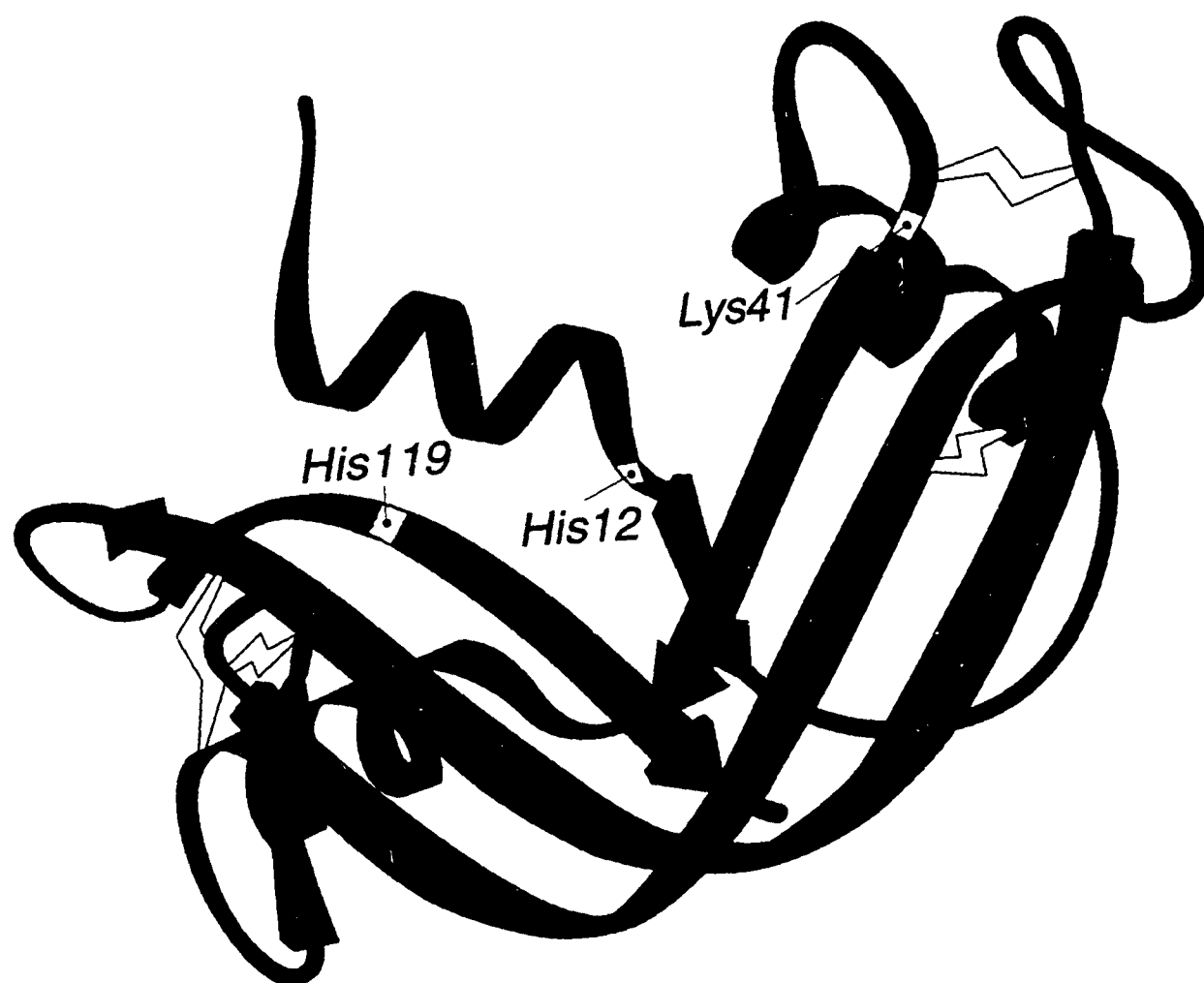
Figure 1.3   Mechanism of the transphosphorylation (A) and hydrolysis (B) reactions

catalyzed by RNase A. B is His12; A is His119; py is a pyrimidine base

(Findlay *et al.*, 1961; Thompson *et al.*, 1994).

A
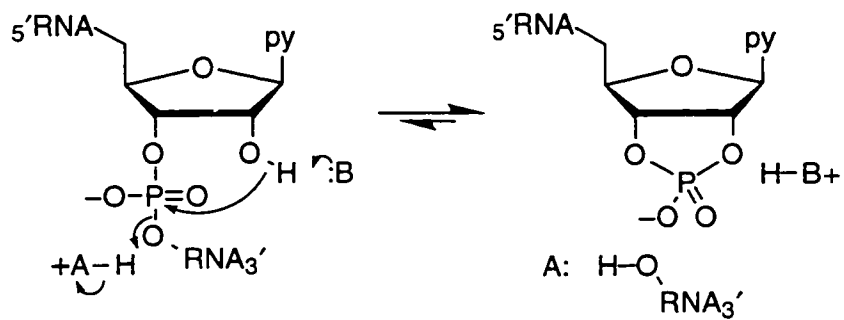
B
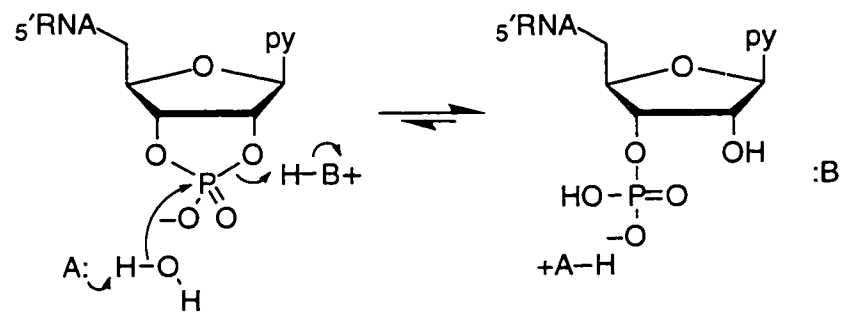
Chapter Two

Coulombic Forces in Protein – RNA Interactions:

Binding and Cleavage by Ribonuclease A

and Variants at Lys7, Arg10, and Lys66

2.1 ABSTRACT: The interactions between bovine pancreatic ribonuclease A (RNase A) and its RNA substrate extend beyond the scissile $P–O_{5'}$ bond. Enzymic subsites interact with the bases and phosphoryl groups of the bound substrate. Those residues interacting with the phosphoryl group comprise the P0, P1, and P2 subsites, with the scissile bond residing in the P1 subsite. Here, the function of the P0 and P2 subsites of RNase A is characterized in detail. Lys66 (P0 subsite) and Lys7 and Arg10 (P2 subsite) were replaced with alanine residues. Wild-type RNase A and the K66A, K7A/R10A, and K7A/R10A/K66A variants were evaluated as catalysts for the cleavage of poly(cytidylic acid) [poly(C)] and for their abilities to bind to single-stranded DNA, a substrate analog. The values of k_{cat} and K_m for poly(C) cleavage were affected by altering the P0 and P2 subsites. The k_{cat}/K_m values for poly(C) cleavage by the K66A, K7A/R10A, and K7A/R10A/K66A variants were 3-fold, 60-fold, and 300-fold lower, respectively, than that of wild-type RNase A. These values indicate that the P0 and P2 subsites contribute 0.70 kcal/mol and 2.46 kcal/mol, respectively, to transition-state binding. Binding experiments indicate that the P0 and P2 subsites contribute 0.92 kcal/mol and 1.21 kcal/mol, respectively, to ground-state binding. Thus, the P0 subsite makes a uniform contribution toward binding the ground state and the transition state, whereas the P2 subsite differentiates—binding more tightly to the transition state than to the ground state. In addition, nucleic acid binding to wild-type RNase A is strongly dependent on NaCl concentration, but this dependence is diminished upon alteration of the P0 or P2 subsites. The logarithm of K_d is a linear function of the logarithm of $[Na^+]$ over the range 0.010 M < $[Na^+]$ < 0.10 M, with slopes of 2.3 ± 0.1, 1.8 ± 0.1, 1.4 ± 0.1, and 0.9 ± 0.2 for nucleic acid binding to wild-type RNase A and the K66A, K7A/R10A, and K7A/R10A/K66A variants, respectively. Similar experiments with NaF and the wild-type enzyme yield a slope of 2.0 ± 0.2, indicating that the anion has little effect on nucleic acid binding. Together these data provide a detailed picture of

the contributions of Coulombic interactions to binding and catalysis by RNase A, and illuminate the general role of Coulombic forces between proteins and nucleic acids.

2.2 INTRODUCTION

The viability of organisms relies on protein – nucleic acid interactions. Somatic cells undergo division, a process that requires the replication and transcription of DNA and the translation of RNA. These chemical reactions are catalyzed and regulated by proteins. A complete understanding of the forces involved in nucleic acid recognition and complex formation by proteins is therefore necessary for delineating the chemical basis of life.

Selective recognition of nucleic acids by proteins involves both sequence-dependent and sequence-independent interactions. Sequence-dependent interactions usually arise from direct contacts between the protein and the exposed edges of nucleic acid bases, primarily in the major groove of B-DNA or the minor groove of duplex RNA. These contacts may involve hydrogen bonds or van der Waals interactions between the protein and the nucleic acid. For example, the amino group of a cytosine base can form a hydrogen bond with the side chain of a threonine residue or with a main-chain carbonyl group. Sequence-dependent malleability of duplex DNA or RNA also results in structural features that are recognized by proteins. These features include kinks, bends, and twists in the duplex strands, and melting of base pairs (Steitz, 1993). Protein folding transitions and other protein conformational changes are also coupled to DNA binding (Spolar & Record, 1994). Attractive forces between the anionic phosphoryl groups of nucleic acids and cationic side chains of proteins are a primary source of sequence-independent interactions between these biopolymers.

Sequence selectivity can be quantitated as the difference between the binding free energies for the sequence-dependent and sequence-independent components of the protein – nucleic acid complex (Travers, 1993). This selectivity can vary widely. For example, a single base-pair change in a critical operator sequence can reduce its affinity for a repressor protein by more than 10^3-fold (Mossing & Record, 1985), and a similar change in the recognition site of an

endonuclease can eliminate all detectable enzymatic activity (Taylor & Halford, 1989). In these systems, sequence selectivity is critical, as formation of a specific complex is a prerequisite for biological function. Still, not all nucleic acid-binding proteins employ strict sequence specificity. The β-subunit of *Escherichia coli* DNA polymerase III binds to DNA non-specifically (Kuriyan & O' Donnell, 1993). This protein has a ring-shaped tertiary structure lined with cationic residues on its inner surface (Kong *et al.*, 1992). Complex formation between this subunit and DNA depends primarily on contacts formed between these cationic protein residues and the anionic nucleic acid phosphoryl groups.

Ribonuclease A (RNase A; EC 3.1.27.5) is an endonuclease that catalyzes the cleavage and hydrolysis of single-stranded RNA in two distinct steps (Findlay *et al.*, 1961; Cuchillo *et al.*, 1993; Thompson *et al.*, 1994). Catalysis by RNase A results in the cleavage of the $P-O_{5'}$ bond specifically on the 3'-side of pyrimidine residues (Aguilar *et al.*, 1992). This enzyme has been the object of landmark work on the folding, stability, and chemistry of proteins; in enzymology; and in molecular evolution (Raines, 1998). Because RNase A has been so well-characterized, it serves as an excellent model system for studying the details of protein – nucleic acid interactions.

Several studies have suggested that the interactions between RNase A and its RNA substrate extend beyond the scissile bond. RNase A has been shown to destabilize double-stranded DNA by binding to single strands (Jensen & von Hippel, 1976). Using monovalent cation titration, Record and co-workers have shown that seven ion pairs form between denatured DNA and RNase A (Record *et al.*, 1976). The structures of crystalline complexes between RNase A and d(pA)$_4$ (McPherson *et al.*, 1986), d(pT)$_4$ (Birdsall & McPherson, 1992), and d(ApTpApApG) (Figure 2.1) (Fontecilla-Camps *et al.*, 1994) also show that there are many interactions between RNase A and polynucleotide ligands. In addition, chemical modification and mutagenesis experiments have divulged the existence of several enzymic subsites (Nogués *et al.*, 1995).

The subsites of RNase A interact with the bases and phosphoryl groups of the bound substrate (Figure 2.2). There are three known base-binding subsites, B1, B2 and B3. The B1 subsite imparts RNase A with its specificity for cleavage after pyrimidine residues (McPherson *et al.*, 1986; Aguilar *et al.*, 1992). The B2 subsite has a preference for an adenine base (Katoh *et al.*, 1986), and the B3 subsite has a preference for a purine base (Rushizky *et al.*, 1961; Irie *et al.*, 1984). The important residues in the B1 and B2 subsites have been identified by site-directed mutagenesis experiments (Tarragona-Fiol *et al.*, 1993; delCardayré & Raines, 1994; delCardayré *et al.*, 1994; delCardayré & Raines, 1995). The existence of the B3 subsite has been proposed based on kinetic data and chemical modification studies (Rushizky *et al.*, 1961; Parés *et al.*, 1980; Irie *et al.*, 1984; Boqué *et al.*, 1994). The residues comprising the phosphoryl group binding subsites, P0, P1, and P2, have been inferred from similar types of experiments. The phosphoryl group containing the scissile $P-O_{5'}$ resides in the P1 subsite (Parés *et al.*, 1991), which is the enzymic active site. Residues that comprise the P0 and the P2 subsites have been identified by chemical modification, site-directed mutagenesis, and molecular modeling studies. Chemical modification of RNase A by reaction with pyridoxal 5'-phosphate and cyclohexane-1,2-dione implicated Lys7 and Arg10 in the P2 subsite (Richardson *et al.*, 1990). Only recently have Lys7 and Arg10 been altered by site-directed mutagenesis (to glutamine residues) to confirm these results (Boix *et al.*, 1994). Lys66 has been proposed as the single residue comprising the P0 subsite, based on molecular modeling and comparison of binding affinities and cleavage rates of varying-length substrates (Parés *et al.*, 1991).

In this study, we characterize in detail the function of the P0 and P2 binding subsites of RNase A. We have removed the side chains of Lys7, Arg10, and Lys66 by site-directed mutagenesis of the cDNA encoding the wild-type protein, and produced wild-type RNase A and its K66A, K7A/R10A, and K7A/R10A/K66A variants in *Escherichia coli*. By analyzing catalysis of RNA cleavage, we show directly that the residues comprising the P0 and P2

subsites interact with the phosphoryl groups adjacent to the scissile bond. In addition, we used fluorescence anisotropy to probe the interaction between a fluorescein-labeled, single-stranded DNA substrate analog and the wild-type protein and three variants. By comparing the values of the equilibrium dissociation constants (K_d) for the protein•nucleic acid complexes at various salt concentrations, we demonstrate that strong Coulombic interactions exist between Lys7, Arg10, and Lys66 and the bound nucleic acid. In addition, by comparing values of K_d for complex formation in the presence of NaCl to those in the presence of NaF, we find that the anion has little effect on binding.

2.3 EXPERIMENTAL PROCEDURES

Materials. *E. coli* strain BL21(DE3) (F⁻ ompT r$_B$-m$_B$-) was from Novagen (Madison, WI). *E. coli* strain CJ236 and helper phage M13K07 were from Bio-Rad (Richmond, CA). *E. coli* strain JM109 was from Promega (Madison, WI). All enzymes for the manipulation of recombinant DNA were from either Promega or New England Biolabs (Beverly, MA). Reagents for mutagenesis oligonucleotides were from Applied Biosystems (Foster City, CA), except for acetonitrile, which was from Baxter Healthcare (McGaw Park, IL). Mutagenesis oligonucleotides were synthesized on an Applied Biosystems 392 DNA/RNA synthesizer, and purified using Oligo Purification Cartridges from Applied Biosystems (Foster City, CA). DNA was sequenced with a Sequenase 2.0 kit from United States Biochemicals (Cleveland, OH). Poly(cytidylic acid) [poly(C)] was from Midland Certified Reagent (Midland, TX) and was precipitated from aqueous ethanol (70% v/v) before use. Bacto yeast extract, Bacto tryptone, Bacto peptone, and Bacto agar were from Difco (Detroit, MI). Bacterial terrific broth (TB) (Tartof, 1992) contained (in 1 L) Bacto tryptone (12 g), Bacto yeast extract (24 g), glycerol (4 mL), KH_2PO_4 (2.31 g), and K_2HPO_4 (12.54 g). All media were prepared in distilled,

deionized water and autoclaved. Isopropyl-1-thio-β-D-galactopyranoside (IPTG) was from

Gold Biotechnology (St. Louis, MO). MES, obtained as the free acid, was from ICN

Biomedicals (Aurora, OH). Gel-purified oligonucleotides used for fluorescence anisotropy

experiments were obtained from Promega. Sigmacote was from Sigma (St. Louis, MO). All

other chemicals and reagents were of commercial grade or better and used without further

purification.

General Methods. Ultraviolet and visible absorbance measurements were made with a Cary

Model 3 spectrophotometer equipped with a Cary temperature controller from Varian (Sugar

Land, TX). RNase A concentrations were determined by assuming that $\varepsilon^{0.1\%} = 0.72$ at 277.5

nm (Sela *et al.*, 1957). pH was measured with a Beckman pH meter fitted with a Corning

electrode, calibrated at room temperature with standard buffers from Fisher (Chicago, IL).

Buffer solutions were prepared from the free acid of MES. The Na^+ concentration of the

solution was determined using the Henderson–Hasselbalch equation[1] and assuming a pK_a

value of 6.15 for MES at 25 °C (Scopes, 1994).

Site-Directed Mutagenesis. Oligonucleotide-mediated site-directed mutagenesis (Kunkel *et

al.*, 1987) was performed on single-stranded DNA isolated from *E. coli* strain CJ236. To

produce the DNA coding for K66A RNase A, the AAG codon for Lys66 in wild-type plasmid

pBXR (delCardayré & Raines, 1995) was replaced with one coding for alanine (GCT; reverse

complement in bold) using the oligonucleotide RR59:

TCTGCCCATTAGC<u>GCATGC</u>AACATTTT, which also incorporates a translationally silent

*Sph*I site (underlined). K7A/R10A RNase A and the triple variant K7A/R10A/K66A RNase A

were created by replacing the AAG codon for Lys7 and the CGG codon for Arg10 with ones

---

[1] Using the Henderson–Hasselbalch equation, 0.10 M MES-NaOH buffer, pH 6.0, has $[Na^+]$

$= 0.042$ M.

coding for alanine (GCT; GCG; reverse complements in bold) in the wild-type or K66A

RNase A cDNA using the oligonucleotide BT1:

TCCATGTGCTGCGCCTCAAACG<u>CAGCTG</u>CTGCAGTT, which also incorporates a

translationally silent *Pvu*II site (underlined). Mutagenesis reaction mixtures were transformed

into competent JM109 cells, and the isolated plasmid DNA of the transformants was analyzed

by sequencing.

Protein Production and Purification. A glycerol freeze of *E. coli* strain BL21(DE3)

harboring wild-type or mutant plasmids was prepared from a mid-log phase culture grown in

LB medium containing ampicillin (400 μg/mL). Wild-type and variant proteins were produced

and purified essentially as described elsewhere (Kim & Raines, 1993; delCardayré & Raines,

1995), except on a larger scale. To produce protein, glycerol freezes were streaked onto LB-

agar plates containing ampicillin (100 μg/mL). A single colony was then used to inoculate a

starter culture (20 mL) of LB medium containing ampicillin (400 μg/mL). Upon reaching mid-

log phase (*OD* = 1.0 at 600 nm), this culture was used to inoculate a larger starter culture (500

mL) of TB medium containing ampicillin (400 μg/mL). Both inoculated cultures were shaken

(250 rpm) at 37 °C. This starter culture was used to inoculate a 12 L fermenter flask of TB

containing ampicillin (400 μg/mL). cDNA expression was induced by the addition of IPTG (to

0.5 mM) at late log phase (*OD* = 2.0 at 600 nm). Cells were harvested by centrifugation 2 – 4 h

after induction and resuspended in 1/100 volume of cell lysis buffer, which was 20 mM Tris-

HCl buffer, pH 8.0, containing EDTA (10 mM). Cells were broken by passing through a

French pressure cell three times. Proteins were solubilized from inclusion bodies, denatured

and reduced, folded/oxidized *in vitro*, concentrated by ultrafiltration, and purified by loading

on a Pharmacia FPLC HiLoad™ 26/60 Superdex 75 gel filtration column (Piscataway, NJ) that

had been equilibrated with 50 mM sodium acetate buffer, pH 5.0, containing 0.10 M NaCl and

0.02% NaN$_3$ (w/v). Fractions corresponding to monomeric protein, which eluted at 192 –

220 mL, were pooled and loaded onto an FPLC mono-S cation exchange column (15 cm ×

1.8 cm^2) that had been equilibrated with 50 mM sodium acetate buffer, pH 5.0. RNase A was eluted with a linear gradient (50 mL + 50 mL) of NaCl (0.1 – 0.3 M) in sodium acetate buffer, pH 5.0. Protein fractions were pooled and characterized. SDS-polyacrylamide gel electrophoresis, zymogram electrophoresis (Blank *et al.*, 1982; Ribó *et al.*, 1991; Kim & Raines, 1993), and A_{280}/A_{260} ratios greater than 1.8 (Layne, 1957) indicated that the proteins were > 99% pure. K7A/R10A RNase A and K7A/R10A/K66A RNase A migrated more slowly during SDS-PAGE than did wild-type protein. The N-terminus of K7A/R10A RNase A was determined by Edman degradation (Protein and Nucleic Acid Chemistry Laboratory, Washington University; St. Louis, MO). The sequence revealed that the pelB leader sequence was indeed removed by endogenous *E. coli* proteases, suggesting that these proteins migrated more slowly during SDS-PAGE because of their lower positive charge.

Thermal Denaturation. The stabilities of the wild-type and variant enzymes were determined by thermal denaturation studies. As RNase A is denatured, its six tyrosine residues become exposed to solvent and its molar absorptivity at 287 nm decreases significantly (Hermans & Scheraga, 1961). By monitoring the change in absorbance at 287 nm with temperature, the thermal stability of RNase A can be assessed (Pace *et al.*, 1989; delCardayré *et al.*, 1994; Eberhardt *et al.*, 1996). Solutions of protein (70 – 210 μM) were prepared in 0.030 M sodium acetate buffer, pH 6.0, containing 0.10 M NaCl. The absorbance at 287 nm was recorded as the temperature was increased from 25 to 90 °C in 1-°C increments, with a 5-min equilibration at each temperature. Similarly, the absorbance at 287 nm was recorded as the temperature was decreased from 90 to 25 °C. The data were fit to a two-state model for denaturation, and T_m (the midpoint in the thermal denaturation curve) was calculated using the program SIGMA PLOT 4.16 (Jandel Scientific; San Rafael, CA).

Steady-State Kinetic Analysis. Spectrophotometric assays were used to determine the steady-state kinetic parameters for the cleavage of poly(C). The cleavage of poly(C) was monitored by following a change in ultraviolet hyperchromicity. The $\Delta\varepsilon$ for this reaction,

calculated from the difference in molar absorptivity of the polymeric substrate and the mononucleotide cyclic phosphate product, is 2380 $M^{-1}cm^{-1}$ at 250 nm (delCardayré *et al.*, 1994). Assays were performed at 25 °C in 0.10 M MES-NaOH buffer, pH 6.0, containing NaCl (0.10 M). The values of k_{cat} K_m, and k_{cat}/K_m were determined from initial velocity data with the program HYPERO (Cleland, 1979).

Thermodynamic Cycles. The degree of interaction between altered residues in RNase A can be determined by examining thermodynamic cycles calculated from steady-state kinetic parameters for the cleavage of poly(C). The change in the contribution of free energy ($\Delta\Delta G$) to catalysis due to a particular protein variation was calculated from eq 2.1, where f is the ratio of a particular kinetic or thermodynamic parameter for the two enzymes being compared:

$$\Delta\Delta G = RT \ln f \tag{2.1}$$

For example, the contribution of free energy to binding of the rate-limiting transition state (Radzicka & Wolfenden, 1995; Thompson *et al.*, 1995) by the side chain of Lys66 was calculated from eq 2.2:

$$\Delta\Delta G_{wt \to K66A} = RT \ln\left[\frac{(k_{cat}/K_m)_{wt}}{(k_{cat}/K_m)_{K66A}}\right] \tag{2.2}$$

The contribution of free energy to catalysis from the interaction between the residues under investigation was calculated from eq 2.3 as described previously (Carter *et al.*, 1984; Horowitz & Fersht, 1990; Horowitz *et al.*, 1990; Mildvan *et al.*, 1992).

$$\Delta\Delta G_{int} = \Delta\Delta G_{wt \to K7A/R10A/K66A} - \Delta\Delta G_{wt \to K7A/R10A} - \Delta\Delta G_{wt \to K66A} \tag{2.3}$$

Fluorescence Anisotropy. Fluorescence anisotropy assays are based on the increase in the rotational correlation time of a fluorophore upon binding of a fluorophore-labelled oligonucleotide to a protein (LeTilly & Royer, 1993; Heyduk *et al.*, 1996). The protein•oligonucleotide complex, due to its increased molecular volume, tumbles more slowly than does the free, labelled oligonucleotide. The ensuing reduction in the rotational correlation time of the fluorophore causes an increase in anisotropy, which allows binding to be monitored (Wittmayer & Raines, 1996). As shown in eq 2.4, anisotropy (*A*) is defined as the ratio of the difference between the vertical (‖) and horizontal (⊥) emission components with respect to the total intensity (*I*) when vertically polarized excitation is used.

$$A = 10^3 \times mA = \frac{I_\parallel - I_\perp}{I_\parallel + 2I_\perp} \qquad (2.4)$$

The oligonucleotide used in the fluorescence anisotropy assays was fluorescein~d(AUAA) [Fl~d(AUAA); Figure 2.3]. Fluorescein, incorporated via a phosphoramidite derivative during the final coupling step of DNA synthesis, was attached to the 5′ end of the oligonucleotide by a six-carbon spacer to the terminal 5′-OH. Following synthesis, the oligonucleotide was gel-purified, de-salted, and analyzed for homogeneity by reversed-phased HPLC and capillary electrophoresis (D. Leland, personal communication). The oligonucleotide concentration was determined by assuming that $\varepsilon = 52650$ M^{-1} cm^{-1} at 260 nm (Wallace & Miyada, 1987).

Fluorescence anisotropy was measured at room temperature (23 ± 2 °C) on a Beacon Fluorescence Polarization System from PanVera (Madison, WI) with excitation at 488 nm and emission at 520 nm. Protein that had been dialyzed exhaustively against water and lyophilized was dissolved in 1.8 mL of 0.020 M or 0.10 M MES-NaOH buffer, pH 6.0, containing NaCl (0.010 – 0.10 M). Fluorescein-labeled oligonucleotide, diluted in the same buffer, was added to half of the protein solution to a final concentration of 2.5 nM. The sample volume was then

adjusted to 1.0 mL by the addition of buffer. Similarly, a blank tube was prepared by diluting the remaining half of the protein solution with buffer to 1.0 mL. Sigmacote was used to prepare silinized glass tubes, which were used for all anisotropy measurements to reduce the adhering of protein to the glass. Measurements (6 – 8) were made at this protein concentration before diluting the sample and the blank. Dilution of the sample entailed removing an aliquot (0.25 mL) and replacing it with an aliquot (0.25 mL) of a 2.5 nM oligonucleotide solution. The blank was diluted similarly, except that buffer, rather than oligonucleotide solution, was used. Reading of the blank, then sample, followed by the dilution step, was repeated up to thirty times for each binding experiment. At the end of each experiment, the RNase A concentration in an aliquot of sample tubes 1, 4, and 7 was determined. The remaining protein concentrations were calculated by assuming constant dilutions of three-fourths for each concentration. The equilibrium dissociation constants were determined by fitting the average anisotropy value at each protein concentration to eq 2.5, which describes binding to a single specific site (Attie & Raines, 1995). Binding parameters were determined by a non-linear least squares analysis, which was weighted by the inverse of the standard deviation of each reading, using the program DELTA GRAPH 4.0 (DeltaPoint; Monterey, CA).

$$A = \frac{\Delta A \cdot [\text{RNaseA}]}{K_d + [\text{RNaseA}]} + A_{min} \qquad (2.5)$$

In eq 2.5, A is the average of the measured fluorescence anisotropy values, ΔA ($= A_{max} - A_{min}$) is the total change in anisotropy, and A_{min} is the anisotropy value of the unbound oligonucleotide. [RNase A] is protein concentration, and K_d is the equilibrium dissociation constant.

2.4 RESULTS

Protein Production and Purification. A recombinant DNA system developed in our laboratory was used to direct the expression of wild-type, K66A, K7A/R10A, and K7A/R10A/K66A RNase A (delCardayré *et al.*, 1995). This system utilizes the *E. coli* T7 RNA polymerase expression system, and after several purification steps yields approximately 50 mg of pure wild-type protein per L of culture. Following expression of appropriately mutated cDNA in *E. coli* strain BL21(DE3), similar protein yields were obtained of pure K66A RNase A, K7A/R10A RNase A, and K7A/R10A/K66A RNase A. K66A RNase A migrated similarly to the wild-type protein during SDS-PAGE. In contrast, both the double and triple variants migrated more slowly than did the wild-type protein (data not shown). To ascertain that the pelB leader sequence had been cleaved properly from the N-terminal of the protein, the double variant K7A/R10A RNase A was subjected to N-terminal sequence analysis. The sequence of the eight N-terminal amino acid residues indicated that proper proteolytic processing had occurred. Because both the double and the triple variant migrated similarly, we assume that the slower migration during SDS-PAGE in comparison to wild-type protein is a result of removing the positive charges at residues 7 and 10. This result is consistent with the slower migration during SDS-PAGE seen by Cuchillo and co-workers for R7Q/R10Q RNase A (Boix *et al.*, 1994).

Steady-State Kinetic Parameters. Steady-state kinetic parameters for the cleavage of poly(C) are listed in Table 2.1. Also listed in this table are the values of T_m determined for the three variant proteins. These values, which are all within 6 °C of the T_m for the wild-type protein, suggest that the tertiary structure of the variant proteins are not markedly different than that of the wild-type protein. Further, the values of T_m indicate that the kinetic parameters determined at 25 °C are indeed those of the native proteins.

Replacing Lys66, Lys7, and Arg10, or all three of these residues with alanine has an effect on the values of both K_m and k_{cat} for cleavage of poly(C). The k_{cat} for poly(C) cleavage by K66A RNase A is similar to that of the wild-type protein, and the K_m is increased by 2- to 3-fold. The k_{cat} for poly(C) cleavage by K7A/R10A RNase A is reduced by 20-fold, and the K_m increased by 2- to 3-fold as compared to the values for cleavage by the wild-type enzyme. The K7A/R10A/K66A variant showed a 20-fold reduction in k_{cat} for poly(C) cleavage and a 10-fold increase in K_m. The values of k_{cat}/K_m for catalysis of poly(C) cleavage by the K66A, K7A/R10A, and K7A/R10A/K66A variants were observed to be 3-fold, 60-fold, and 300-fold lower, respectively, than that of wild-type RNase A.

Thermodynamic Cycles for the Cleavage of Poly(C). Thermodynamic cycles that relate the free energies corresponding to k_{cat}, K_m, and k_{cat}/K_m for the cleavage of poly(C) by wild-type RNase A and the K66A, K7A/R10A, and K7A/R10A/K66A variants are shown in Figure 2.4. The effect of a substitution on the free energy relating to K_m or k_{cat}/K_m (which reports on the binding of the rate-limiting transition state) can be determined from the $1/K_m$ and k_{cat}/K_m thermodynamic cycles, respectively. The P0 subsite, which consists of Lys66, contributes 0.50 kcal/mol to the value of K_m and 0.70 kcal/mol to the binding of the rate-limiting transition state. The P2 subsite, which consists of Lys7 and Arg10, makes a similar contribution to the free energy corresponding to K_m but a larger contribution to the binding of the rate-limiting transition state than does the P0 subsite. The contribution of the P2 subsite to the K_m value is 0.56 kcal/mol and to transition state binding is 2.46 kcal/mol. The P0 and P2 subsites interact during catalysis of poly(C) cleavage. The contributions to the free energy of the K_m value and the binding of the transition state due to this interaction are 0.35 kcal/mol and 0.34 kcal/mol, respectively.

DNA Binding to Wild-Type and Three RNase A Variants. RNase A binds to single-stranded DNA (Walz, 1971), but cannot cleave this biopolymer. Therefore, single-stranded DNA is an excellent analog of RNA with which to investigate the binding (without turnover) of

a substrate to RNase A. The three-dimensional structure of the crystalline complex of d(ATAAG) with wild-type RNase A [Brookhaven Protein Data Bank (pdb) entry 1rcn; (Fontecilla-Camps *et al.*, 1994)] shows that this oligomer binds to both the active site and distal subsites of RNase A. Thus this or a similar oligomer can be used to reveal meaningful aspects of substrate binding to RNase A.

The results of fluorescence anisotropy assays with Fl~d(AUAA) binding to the wild-type protein demonstrated that this technique was suitable for assaying complex formation. The affinity of Fl~d(AUAA) to wild-type RNase A in four aqueous solutions that differ in [Na^+] is shown in Figure 2.5. As the [Na^+] increased, the affinity of this oligomer for RNase A decreased. The difference in anisotropy values between free and bound oligomer, which was approximately $\Delta A = 120$ mA units, was constant in all of the binding experiments with the wild-type protein. In addition, this value was similar to the change in anisotropy seen when Fl~d(UAA) binds to wild-type RNase A (Kelemen & Raines, 1997). The total fluorescence intensity decreased at the beginning of the titrations, but remained constant at the end of the titrations, when protein concentrations were low. This change in total intensity, which was observed in all binding experiments, could have resulted from light scattering at high protein concentrations.

Binding of Fl~d(AUAA) to K66A RNase A, K7A/R10A RNase A, and K7A/R10A/K66A RNase A at varying salt conditions was also examined by using fluorescence anisotropy. It was not possible to saturate the oligomer with K7A/R10A RNase A or K7A/R10A/K66A RNase A at high salt concentrations, due to weak binding. The solubility of protein precluded a direct determination of anisotropy values for completely bound oligomer to these variants under these conditions. To fit the data for these titrations, we used the $\Delta A = 120$ mA value that was determined for binding of this oligomer to the wild-type protein. The dissociation constants for these binding experiments are listed in Table 2.2.

As listed in Table 2.2, Fl~d(AUAA) bound more tightly to wild-type protein than to any of the variants at solution conditions equivalent to those used for the kinetic experiments [that is, 0.10 M MES-NaOH, pH 6.0, containing NaCl (0.10 M)]. The K_d values increased in the order: wild-type RNase A < K66A RNase A < K7A/R10A RNase A < K7A/R10A/K66A RNase A. At lower [Na^+], the same trend was seen, but the differences in K_d values were larger. These trends are more apparent when plotted on a logarithmic scale, as shown in Figure 2.6. It is apparent from the slopes of the lines in Figure 2.6 that oligomer binding to wild-type protein had the highest salt concentration-dependence, and binding to K7A/R10A/K66A RNase A had the lowest salt concentration-dependence.

Effect of NaF on ssDNA Binding. The effect of anions on the binding of RNase A to Fl~d(AUAA) was examined using fluorescence anisotropy assays. Values of K_d for the complex of wild-type protein with Fl~d(AUAA) were determined at four different NaF concentrations, in 0.020 or 0.10 M MES-NaOH buffer, pH 6.0. These K_d values are listed in Table 2.3 and plotted versus cation concentration on a log-log scale in Figure 2.7. As shown in Figure 2.7, the binding of wild-type RNase A to Fl~d(AUAA) binding was only slightly tighter in the presence of NaF than in the presence of NaCl, at all but the lowest concentration examined. In addition, the salt concentration-dependence of binding was slightly lower in the presence of NaF than in the presence of NaCl.

2.5 DISCUSSION

In native RNase A, the residues His12, His119, and Lys41 are in close proximity to each other (Kartha *et al.*, 1967). These residues, though being the primary residues directly involved in catalysis of RNA cleavage, do not act alone. Several other residues interact with the

RNA substrate, thereby playing important auxiliary roles in catalysis. In this work, we characterize in detail the function of three such residues: Lys7, Arg10, and Lys66.

RNase A appears to have evolved to catalyze the cleavage of RNA rather than its hydrolysis (Cuchillo *et al.*, 1993; Thompson *et al.*, 1994). Here, we used two tools to characterize the interactions involved in nucleic acid recognition and complex formation by RNase A, interactions that necessarily precede the cleavage of RNA. First, we investigated protein – nucleic acid interactions during catalysis of RNA cleavage by wild-type RNase A and three variants using spectrophotometric assays. Second, we used fluorescence anisotropy experiments to investigate binding (without turnover) of a substrate to RNase A. Fluorescence anisotropy is a useful method for studying protein – nucleic acid interactions in solution, where the effect of changing conditions such as pH, temperature, or salt concentration can be ascertained readily (LeTilly & Royer, 1993). Previous studies employing this technique have investigated the binding of a protein to a fluorescein-labeled, double-stranded DNA of > 20 base pairs (Heyduk & Lee, 1990; Heyduk *et al.*, 1993; LeTilly & Royer, 1993; Wittmayer & Raines, 1996). Here, we report the use of this technique to investigate the binding of a protein to a single-stranded DNA oligonucleotide of only 4 bases.

Lys66 Comprises the RNase A P0 Subsite. The hypothesis that Lys66 comprises the P0 subsite of RNase A had been based on the results of several studies, including a comparison of the binding affinity of 5′-phosphouridine 3′-phosphate (pUp) versus uridine 3′-phosphate (Up) to RNase A (Sawada & Irie, 1969), a comparison of the rates of cleavage of 5′-phosphouridine 2′,3′-cyclic phosphate (pU>p) versus uridine 2′,3′-cyclic phosphate (U>p) (Li & Walz, 1974), X-ray diffraction analysis (Mitsui *et al.*, 1978), and molecular modeling (de Llorens *et al.*, 1989), and its evolutionary conservation among 40 of the 41 known pancreatic ribonuclease sequences (Beintema, 1987; Beintema *et al.*, 1988). This residue had never been subjected to chemical modification or replaced with another amino acid (Raines, 1998).

Lys66 is removed from the active site of RNase A, with N_ζ of Lys66 being 7.3 Å from the nearest active-site histidine residue, His119 [pdb entry 7rsa; (Wlodawer *et al.*, 1988)]. In contrast, Lys66 is only 5.3 Å from the nearest phosphoryl group oxygen atom of a bound oligonucleotide (Fontecilla-Camps *et al.*, 1994), that which is 5' to the scissile phosphodiester bond (Figure 2.1). Thus, it is no surprise that removing the Lys66 side chain has a less profound effect on the value of k_{cat} for cleavage of a polymeric substrate than on the value of K_m. The observed > 2-fold increase in K_m for poly(C) cleavage suggests that the side chain of Lys66 does interact with this polymeric substrate during catalysis. Binding of Fl~d(AUAA) to K66A RNase A under similar solution conditions [0.10 M MES-NaOH, pH 6.0, containing NaCl (0.10 M)] yields a similar result. The value of K_d for the binding of Fl~d(AUAA) to RNase A is increased by 4.5-fold upon the removal of the Lys66 side chain. Thus, data from both kinetic and thermodynamic approaches indicate that Lys66 interacts with the substrate phosphoryl group that is 5' to the scissile phosphodiester bond.

Lys66 is not Required for Catalysis by RNase A. The conservation of a lysine residue at position 66 of RNase A implicates it as being important in catalysis. Beintema (1989) hypothesized that a cationic amino acid residue at either position 66 or position 122 is required for catalytic activity by members of the ribonuclease superfamily. He compared the more active members of the ribonuclease superfamily, such as the mammalian pancreatic and other secretory ribonucleases, to less active members of this family, such as human and bovine angiogenin and eosinophil-derived neurotoxin (EDN), and found that the less active members of this superfamily have deletions or insertions at position 66. Where a basic residue was absent at position 66 in the more active family members, a cationic residue was present at position 122. Position 122 in RNase A is a serine residue. So by this hypothesis, position 66 must be a cationic residue for RNase A to maintain high catalytic activity. The removal of the cationic side chain of Lys66 in RNase A results in only a small decrease in enzymatic

activity—the value of k_{cat}/K_m is reduced by ~3-fold for the cleavage of poly(C). In contrast, EDN cleaves poly(C) 2×10^3-fold slower than does RNase A (Sorrentino & Libonati, 1994). Apparently, a cationic residue at position 66 or position 122 is not necessary for high catalytic activity.

Roles of Lys7 and Arg10 in Catalysis. Similarly to Lys66, the role of Lys7 and Arg10 was proposed originally based on X-ray diffraction analyses and molecular modeling. But unlike with Lys66, the role of these residues has been confirmed by chemical modification and mutagenesis experiments, which showed more directly the presence of these residues in the P2 subsite. The characterization of the single variants K7Q RNase A and R10Q RNase A by Cuchillo and co-workers suggests that the side chains of Lys7 and Arg10 must both be replaced to see a significant effect on catalysis by RNase A (Boix *et al.*, 1994). N_ζ of Lys7 is 3.1 Å from the nearest phosphoryl oxygen of a bound nucleic acid, and the nearest guanido N of Arg10 is 7.7 Å from this same oxygen (Figure 2.1). Considering only proximity, one might surmise that Lys7 plays a more prominent role in interacting with the substrate, with Arg10 playing merely a compensatory role in its absence. To characterize the entire P2 subsite, we created an RNase A variant in which both Lys7 and Arg10 were changed to alanine residues.

The removal of the Lys7 and Arg10 side chains affects profoundly both the values of K_m and k_{cat} for cleavage of the polymeric substrate poly(C) and the value of K_d for binding of Fl~d(AUAA) under similar conditions. The K_m is increased by 2.5-fold and the k_{cat} is decreased by 20-fold relative to cleavage by the wild-type enzyme. The k_{cat}/K_m is decreased by 60-fold. The K_d is increased 7-fold. Cuchillo and co-workers observed similar effects on the kinetic parameters for poly(C) cleavage upon replacing Lys7 and Arg10 with glutamine residues (Boix *et al.*, 1994). They observed a 3.6-fold increase in K_m, a 17-fold decrease in k_{cat}, and a 60-fold decrease in k_{cat}/K_m. Glutamine residues do not bear a charge, but they do have the capacity to donate hydrogen bonds. Although the side chain of a glutamine residue is shorter than that of either a lysine or an arginine residue, our molecular modelling indicates that

glutamine residues at positions 7 and 10 can interact with a phosphoryl group of a bound RNA substrate. The similarity in the kinetic parameters for the glutamine and alanine variants at positions 7 and 10 in RNase A suggests that Coulombic interactions, and not hydrogen bonds, are the critical interactions formed between the P2 subsite and the phosphoryl group 3′ to the scissile phosphodiester bond on the RNA substrate.

Synergy between the P0 and P2 Subsites. Small interaction free energies ($\leq$ 1 kcal/mol) between protein residues that are not in direct contact is a common feature in proteins (LiCata & Ackers, 1995). In RNase A, the N_ζ atom of Lys66 is 16 Å from the N_ζ atom of Lys7 and 19 Å from either guanido N atom of Arg10 (Wlodawer *et al.*, 1988). From this distance, the P0 subsite cannot interact directly with the P2 subsite. From the kinetic parameters for the cleavage of poly(C) by wild-type RNase A and the three variants, we find that the free energies contributed by each of these subsites are additive in terms of k_{cat} ($\Delta\Delta G_{int} = -0.01$ kcal/mol) but are nonadditive in terms of K_m ($\Delta\Delta G_{int} = 0.34$ kcal/mol) and k_{cat}/K_m ($\Delta\Delta G_{int} = 0.35$ kcal/mol) (Figure 2.4). Analyses of multiple pairs of mutations in different proteins have, however, shown that small interaction free energies appear to be non-random and, therefore, significant (LiCata & Ackers, 1995). Although small, the interaction free energies we observe may report on a synergistic loss of entropy upon binding of both the substrate and the transition state.

Effect of NaCl on Fl~d(AUAA) Binding to Wild-Type RNase A and Three Variants. The effect of NaCl concentration on the binding affinity of ssDNA for RNase A was first demonstrated by Jensen and von Hippel (1976). Using a boundary sedimentation velocity technique, they found that single-stranded calf thymus DNA, which is heterogeneous and binds several protein molecules per strand, has a strong salt concentration-dependence for binding to RNase A. This dependence is a result of the polyanionic nature of DNA, which accumulates a high local concentration of mobile counterions (*e.g.*, Na^+) and a low local concentration of mobile co-ions (*e.g.*, Cl^-) (Anderson & Record, 1995). Accumulated cations are released from the polymeric DNA strand upon complex formation. Concomitantly, anions

are released from the protein. The accompanying increase in entropy is a driving force for binding (Record *et al.*, 1976). From the slope of a $\log(K_d)$ versus $\log([Na^+])$ plot, one can determine the number of ion pairs formed between the DNA ligand and the protein, and also the number of cations and anions released upon binding. Record and co-workers (1976) analyzed the data of Jensen and von Hippel in this manner, finding that seven ion pairs are formed between polymeric ssDNA and RNase A.

In our binding experiments, we used a small (4-base), single-stranded oligonucleotide. We based the design of our oligonucleotide, Fl~d(AUAA), on the existence of a high-resolution crystalline structure of the complex between d(ATAAG) and RNase A (Fontecilla-Camps *et al.*, 1994). Our oligonucleotide spans both the active site and distal subsites of RNase A and forms a protein•ligand complex with a stoichiometry of one. The small size of this oligonucleotide makes a quantitative analysis of our data difficult. Short oligonucleotides, such as the tetramer used here, are oligoelectrolytes, and differ strikingly from polyelectrolytes in their interactions with salt ions (Zhang *et al.*, 1996). A nucleic acid strand can be considered to be a polyelectrolyte if there are more than 18 DNA monomer units (*i.e.*, 36 phosphoryl groups) (Olmsted *et al.*, 1989); our oligomer falls well short of this value. Nevertheless, the conclusion from a qualitative analysis of our binding data is consistent with that from of our kinetic experiments—Coulombic forces mediate the interactions between the P0 and P2 subsites and a molecule of RNA.

In agreement with the results of Jensen and von Hippel (Jensen & von Hippel, 1976), we find that the affinity of ssDNA for wild-type RNase A is influenced dramatically by the concentration of NaCl (Figure 2.6). The values of K_d and cation concentration from Table 2.2 are plotted in Figure 2.6. The slope of the line representing the binding of Fl~d(AUAA) to wild-type RNase A is 2.3 ± 0.1. For the reasons described above, we cannot quantitate this value in terms of cations released from the DNA or number of ion pairs formed in the complex. Nevertheless, this slope can be compared to those for the binding of the same oligonucleotide

to the three variant proteins. Changing RNase A residues that are involved in Coulombic interactions with the substrate are expected to result in binding affinities with a weaker dependence on salt concentration. We find such an effect. The slopes of the lines in Figure 2.6 are 1.8 ± 0.1 for Fl~d(AUAA) binding to K66A RNase A, 1.4 ± 0.1 for Fl~d(AUAA) binding to K7A/R10A RNase A, and 0.9 ± 0.2 for Fl~d(AUAA) binding to K7A/R10A/K66A RNase A. From these results, we conclude that the P0 and P2 subsites engage in Coulombic interactions with the phosphoryl groups of a bound single-stranded nucleic acid.

Comparison of the K_d Values for Fl~d(AUAA) Binding to Wild-Type RNase A in Buffer Containing NaF versus NaCl. Anions can interact with proteins. Studies with several nucleic acid-binding proteins (Overman *et al.*, 1988; Ha *et al.*, 1992; Mascotti & Lohman, 1997) have shown that values of K_d for complex formation in buffers differing only in the anion tend to follow the Hofmeister series (von Hippel & Schleich, 1969), which ranks anions in the order: $F^- < SO_4^{2-} < HPO_4^{2-} < CH_3CO_2^- < Cl^- < Br^- < NO_3^- < I^- < CCl_3CO_2^- < ClO_4^- < SCN^-$. This order is similar to the ability of anions to interact with proteins, with fluoride showing the weakest preferential binding to proteins. Thus, the strongest protein•ligand complex is expected to form in fluoride-containing buffers, and the weakest in thiocyanide-containing buffers. Both individual K_d values and their salt concentration-dependence can yield information on the extent of anion binding to a protein.

Varying the anion type, while keeping the cation type constant, can reveal if anion binding by a protein contributes to an equilibrium dissociation constant (Relan *et al.*, 1997). To determine if anion binding to RNase A contributes significantly to values of K_d for complex formation in NaCl-containing buffers, we assayed the binding of Fl~d(AUAA) to wild-type RNase A in NaF-containing buffers at four [Na$^+$]. We find that the values of K_d for Fl~d(AUAA) binding to RNase A are smaller in NaF-containing buffers for all but the binding experiment performed at the lowest [Na$^+$] (Table 2.3). At this low [Na$^+$], the values of K_d are 1.1 µM for binding in NaF-containing buffer and 0.82 µM for binding in NaCl-containing

buffer. These values are within error of each other. The values of K_d, plotted on a logarithmic scale versus $\log([Na^+])$ in Figure 2.7, show only a slightly lower dependence on NaF concentration (slope 2.0 ± 0.2) than on NaCl concentration (slope 2.3 ± 0.1). We conclude that anion binding is negligible for wild-type RNase A under the solution conditions investigated herein. Thus, the binding of Fl~d(AUAA) to wild-type RNase A and (we presume) the three variants show differences in their salt concentration-dependence due to Coulombic interactions between residues 7, 10, and 66 and phosphoryl groups of the nucleic acid, and not because of differential anion release from the protein upon nucleic acid binding.

Contributions of the P0 and P2 Subsites to Catalysis. The function of the P0 and P2 subsites of RNase A is to contribute to both ground state and transition state stabilization during catalysis. Using eq 2.1 and the values of K_d for Fl~d(AUAA) binding to the wild-type and K66A proteins (at conditions similar to those used for assaying catalysis), we find that the P0 subsite contributes 0.92 kcal/mol towards the binding of Fl~d(AUAA). From a similar analysis with the K7A/R10A variant, we find that the P2 subsite contributes 1.21 kcal/mol toward the binding of Fl~d(AUAA). The contributions from the P0 and P2 subsites to transition state binding of poly(C) are 0.70 kcal/mol and 2.46 kcal/mol, respectively (Figure 2.4). Thus, the P0 subsite makes a uniform contribution toward binding the ground state and the transition state, whereas the P2 subsite differentiates—binding more tightly to the transition state than to the ground state. The energetic contributions of the P0 and P2 subsites to ground state binding are similar to those of the active-site histidine residues [His12 contributes 1.5 kcal/mol and His119 contributes 1.8 kcal/mol to ground state binding; (Thompson, 1995)], but far from the contribution to transition state stabilization from either active-site histidine residue (6 kcal/mol) (Thompson & Raines, 1994) or the active-site lysine residue (6.8 kcal/mol) (Messmore *et al.*, 1995). The P0 and P2 subsites, though distant from the active site of RNase A and contributing a relatively small amount towards transition state stabilization, play a relatively large role in ground state binding.

Why does the P2 subsite make a larger contribution to ground state and transition state binding than does the P0 subsite? The P2 subsite is comprised of two cationic residues, Lys7 and Arg10, whereas the P0 subsite contains only one cationic residue, Lys66. The presence of two positive charges may result in the release of more cations from the nucleic acid upon binding, thereby increasing the entropy more so than does the presence of a single positive charge. In addition, the B1 subsite binds nucleotides more tightly than does the B2 or B3 subsites. A pyrimidine base bound in the B1 subsite might provide an anchor for the phosphoryl group bound in the P0 subsite, providing additional binding energy that the P2 subsite must alone provide. Alternatively, another subsite beyond the P0 subsite might serve as an anchor, interacting with the phosphoryl group of the next nucleotide. Indeed, preliminary data suggests that the side chain of Arg85 of RNase A contributes significantly to nucleic acid binding and may constitute a P(−1) subsite. [For a description of the P(−1) subsite, see: Chapter 4.]

Implications. Our new knowledge of the P0 and P2 subsites of RNase A brings us one step closer to understanding the energetics of catalysis by this enzyme. In addition, our findings have implications for understanding other aspects of protein – nucleic acid interactions. For example, several restriction endonucleases rely on linear diffusion to locate their target site (Jeltsch *et al.*, 1994; Berkhout & van Wamel, 1996). By diffusing along DNA in a nonspecifically bound state, these enzymes locate target sites at rates greater than the limit set by three-dimensional diffusion (von Hippel & Berg, 1989). Likewise, we demonstrated recently that RNase A can use one-dimensional diffusion along a single-stranded nucleic acid to locate its target site, but that this routing is made inaccessible by added salt (Kelemen & Raines, 1997). This result, along with those herein, suggest that the nonspecifically bound state is likely to rely on Coulombic interactions between the protein and nucleic acid (Winter *et al.*, 1981).

2.6 ACKNOWLEDGMENT

Table 2.1: Steady-State Kinetic Parameters for the Cleavage of Poly(C) by Wild-Type RNase A, K66A RNase A, K7A/R10A RNase A, and K7A/R10A/K66A RNase A[a]

RNase A (T_m: °C)[b]	k_{cat} (s^{-1})	K_m (mM)	k_{cat}/K_m (10^6 M^{-1}s^{-1})
Wild-Type (62)	507 ± 15	0.089 ± 0.009	5.7 ± 0.5
K66A (60)	365 ± 7	0.202 ± 0.014	1.8 ± 0.1
K7A/R10A (58)	22.7 ± 1.0	0.222 ± 0.027	0.10 ± 0.01
K7A/R10A/K66A (57)	16.7 ± 0.7	0.907 ± 0.077	0.018 ± 0.002

[a] Data were obtained at 25 °C in 0.10 M MES-NaOH buffer, pH 6.0, containing NaCl (0.10 M).

[b] Values of T_m are reported ± 2 °C.

48

Table 2.2: Effect of NaCl on the Values of K_d (μM) for Binding of Fluorescein~d(AUAA) to Wild-Type RNase A, K66A RNase A, K7A/R10A RNase A, and K7A/R10A/K66A RNase A[a,b]

RNase A	[Na$^+$] (M)			
	0.018[c]	0.033[c]	0.059[c]	0.142[d]
Wild-Type	0.82	3.1	11	88
K66A	11	33	110	400
K7A/R10A	35	100	260	640
K7A/R10A/K66A	220	520	440[e]	1600

[a] All data were were collected on a Beacon Fluorescence Polarization System (Panvera; Madison, WI) at 23 ± 2 °C.

[b] The error on the curve fitting, determined using the program BIOEQS (Royer et al., 1990; Royer & Beechem, 1992; Royer, 1993), was typically < 5%. The errors determined from duplicate experiments were closer to 15%. We therefore assume the real error on each of these points to be ≤ 15% and do not report the errors determined from curve fitting, which are presumably underestimated.

[c] Determined in 0.020 M MES-NaOH buffer, pH 6.0, containing NaCl (to the indicated [Na$^+$]).

[d] Determined in 0.10 M MES-NaOH buffer, pH 6.0, containing NaCl (0.10 M).

[e] Determined in 0.10 M MES-NaOH buffer, pH 6.0, containing NaCl (0.040 M) ([Na$^+$] = 0.049 M).

Table 2.3: Comparison of the Effect of NaCl and NaF on the Values of K_d (μM) for the Binding of Fluorescein~d(AUAA) to Wild-Type RNase A[a]

Salt	[Na⁺] (M)			
	0.018^b	0.033^b	0.059^b	0.142^c
NaCl	0.82	3.1	11	88
NaF	1.1	2.4	7.1	61

[a] All data were were collected on a Beacon Fluorescence Polarization System at 23 ± 3 °C.

[b] Determined in 0.020 M MES-NaOH buffer, pH 6.0, containing NaCl (to the indicated [Na⁺]).

[c] Determined in 0.10 M MES-NaOH buffer, pH 6.0, containing NaCl (0.10 M).

Figure 2.1 Structure of RNase A complexed to the substrate analog d(ATAAG) [pdb entry 1rcn; (Fontecilla-Camps *et al.*, 1994)]. Side chains for Lys7, Arg10, and Lys66 as well as active-site residues His12, His119, and Lys41 are shown. Interactions between residues Lys7, Arg10, and Lys 66 and the nearest nonbridging phosphoryl oxygens are indicated by dashed lines.

Lys7

Arg10

Lys66
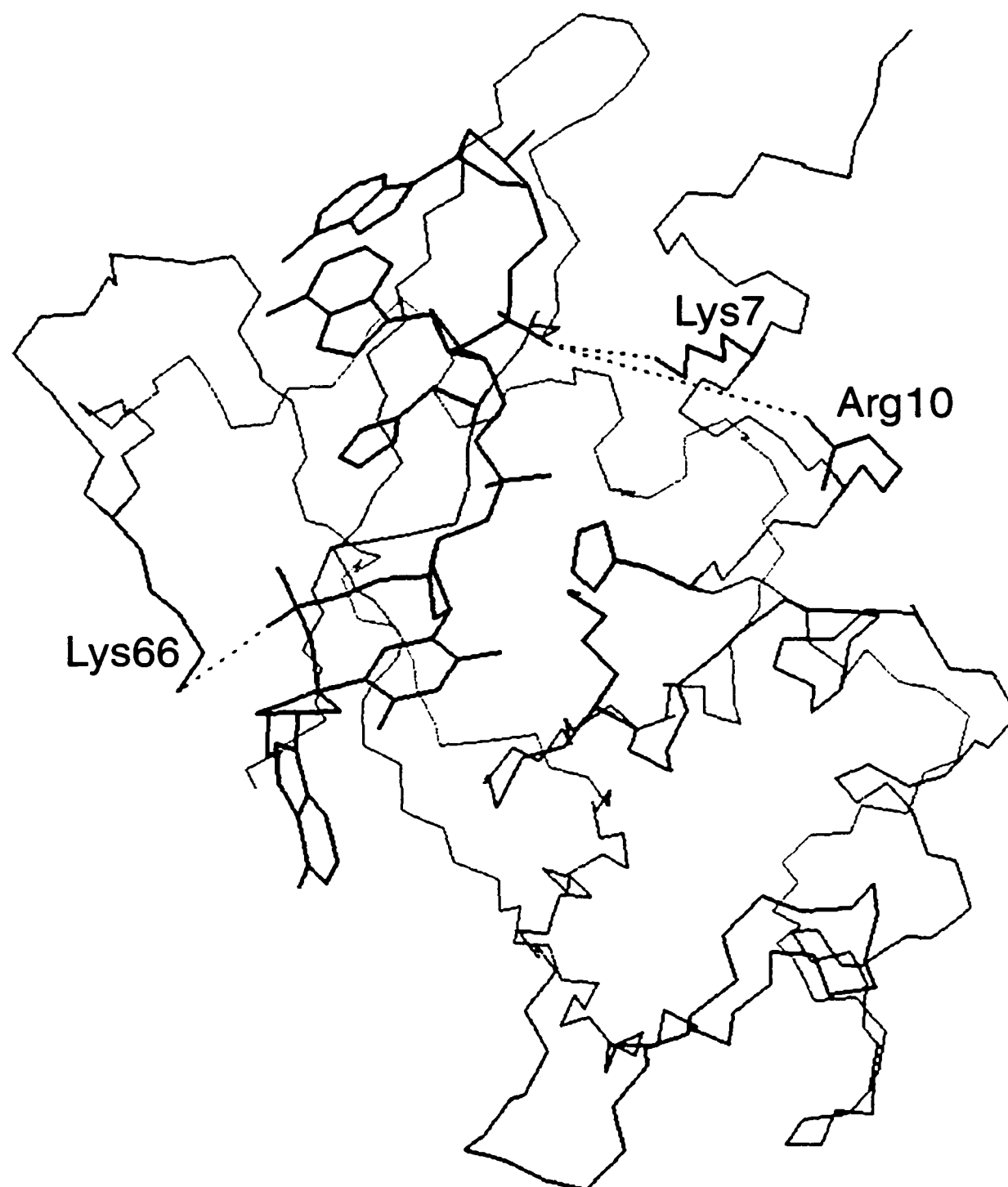
Figure 2.2 Schematic representation of the binding of an RNA fragment to RNase A. The scissile bond is indicated. B and P refer to base and phosphoryl group binding sites, respectively. The twelve indicated residues have been shown by site-directed mutagenesis to make a contribution to substrate binding or turnover (or both) (Raines, 1998).

Lys66

P0 subsite

Cyt
Ura

Thr45
Asp83

B1 subsite

OH

Gln11
His12
Lys41
His119
Asp121

⁻O−P=O *scissile*
               bond

Ade

Asn71
Glu111

P1 subsite
(*active site*)

B2 subsite

OH

Lys7
Arg10

⁻O−P=O

P2 subsite

Ade
Gua

?

B3 subsite

OH
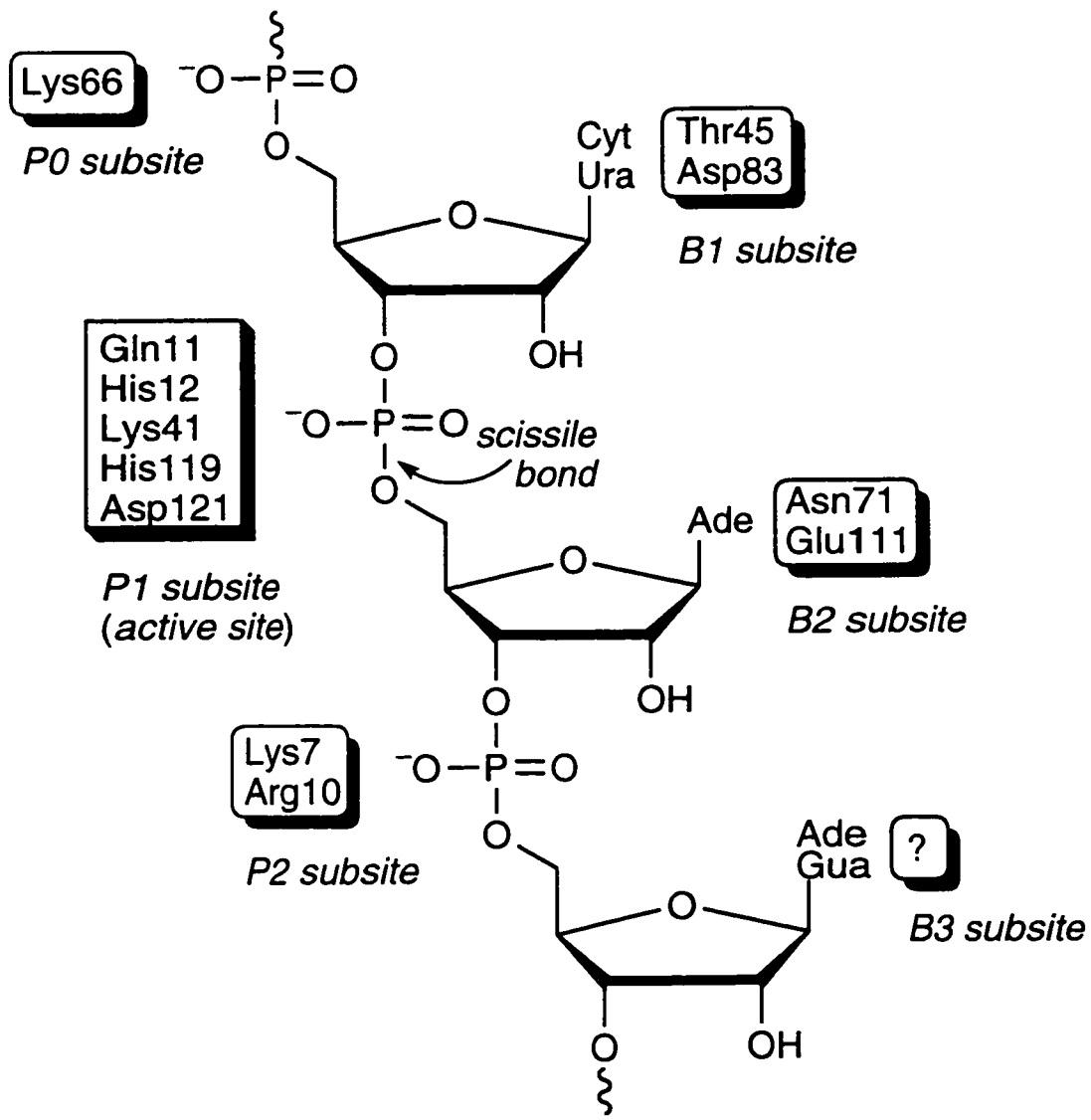
Figure 2.3 Fluorescein-labeled oligonucleotide [Fl~d(AUAA)] used for fluorescence anisotropy experiments. The design of this oligonucleotide was based on the oligonucleotide in a crystalline RNase A•d(ATAAG) complex (Fontecilla-Camps *et al.*, 1994).
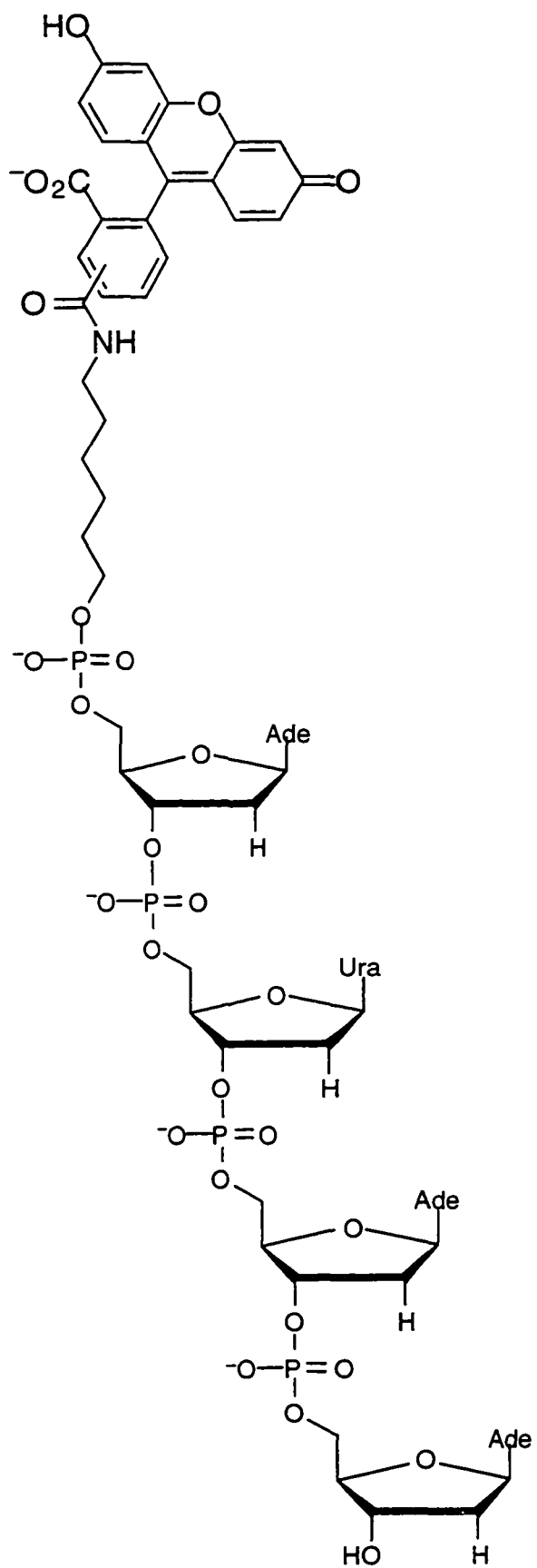
Figure 2.4 Thermodynamic cycles for the cleavage of poly(C) by RNase A upon replacing Lys7 and Arg10, Lys66, or all three residues with alanine. The cycles are drawn for the steady-state kinetic parameters k_{cat} (left), $1/K_m$ (middle) and k_{cat}/K_m (right) with values (in kcal/mol) dervied from equations analogous to eq 2.2. The values for the interaction free energies, $\Delta\Delta G_{int}$, were determined using eq 2.3.
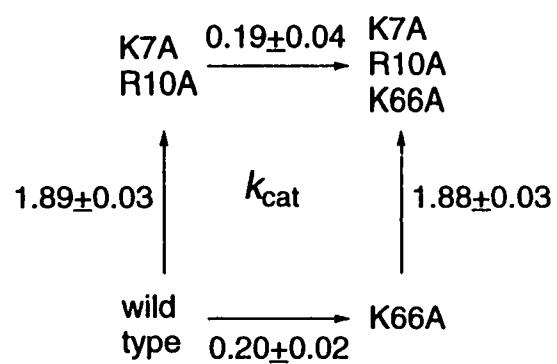
$$\Delta\Delta G_{int} = -0.01 \pm 0.05 \text{ kcal/mol} \qquad \Delta\Delta G_{int} = 0.35 \pm 0.13 \text{ kcal/mol} \qquad \Delta\Delta G_{int} = 0.34 \pm 0.13 \text{ kcal/mol}$$
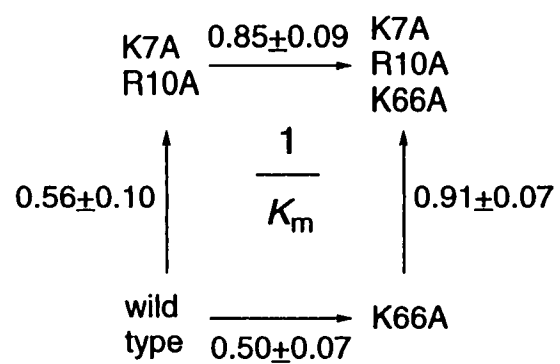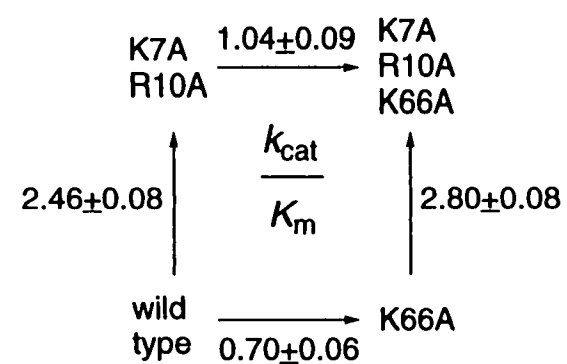
Figure 2.5 Raw data for binding of fluorescein~d(AUAA) to wild-type RNase A at four

[Na$^+$]. Binding was measured by fluorescence anisotropy at 23 ± 2 °C in

0.020 M MES-NaOH buffer containing NaCl (0.010 M, 0.025 M, or

0.050 M) or in 0.10 M MES-NaOH buffer, pH 6.0, containing NaCl

(0.10 M). Each data point is the average of 6 – 8 measurements, with the

standard deviation for each point indicated by the bars. The curves are best fits

to eq 2.5.
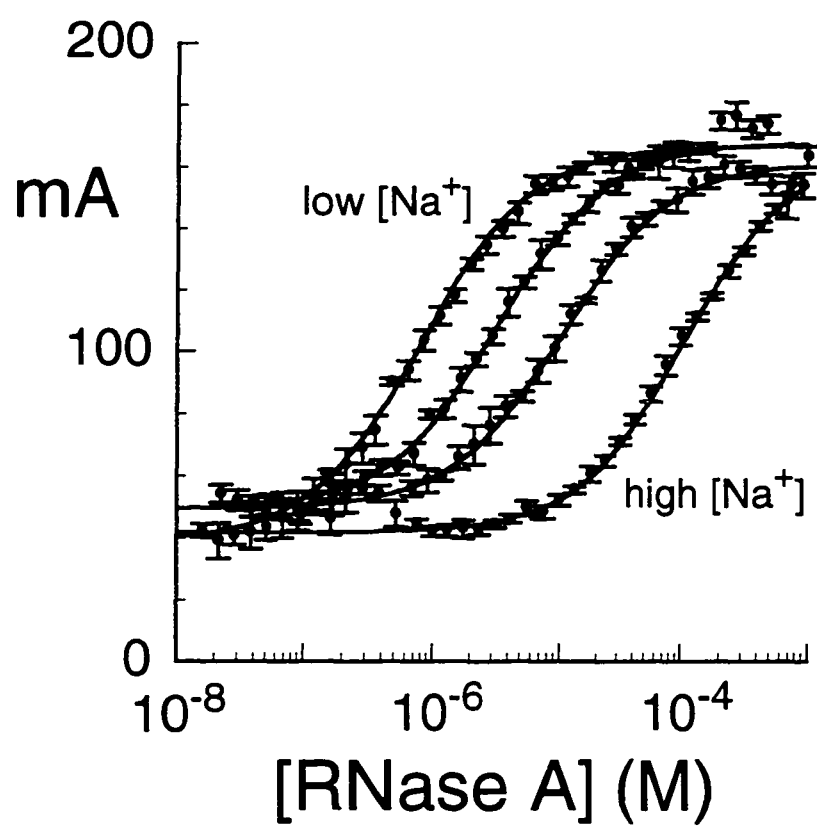
Figure 2.6 Transformed data for binding of fluorescein~d(AUAA) to wild-type RNase A

(●), K66A RNase A (■), K7A/R10A RNase A (▲), and K7A/R10A/K66A

RNase A (◆) at four [Na⁺]. Binding was measured by fluorescence anisotropy

at 23 ± 2 °C in 0.020 M MES-NaOH buffer, pH 6.0, containing NaCl

[0.010 M, 0.025 M, or 0.050 M (0.040 M for K7A/R10A/K66A RNase A)]

or in 0.10 M MES-NaOH buffer, pH 6.0, containing NaCl (0.10 M). The

slopes of the lines are 2.3 ± 0.1 (wild-type RNase A), 1.8 ± 0.1

(K66A RNase A), 1.4 ± 0.1 (K7A/R10A RNase A), and 0.9 ± 0.2

(K7A/R10A/K66A RNase A).
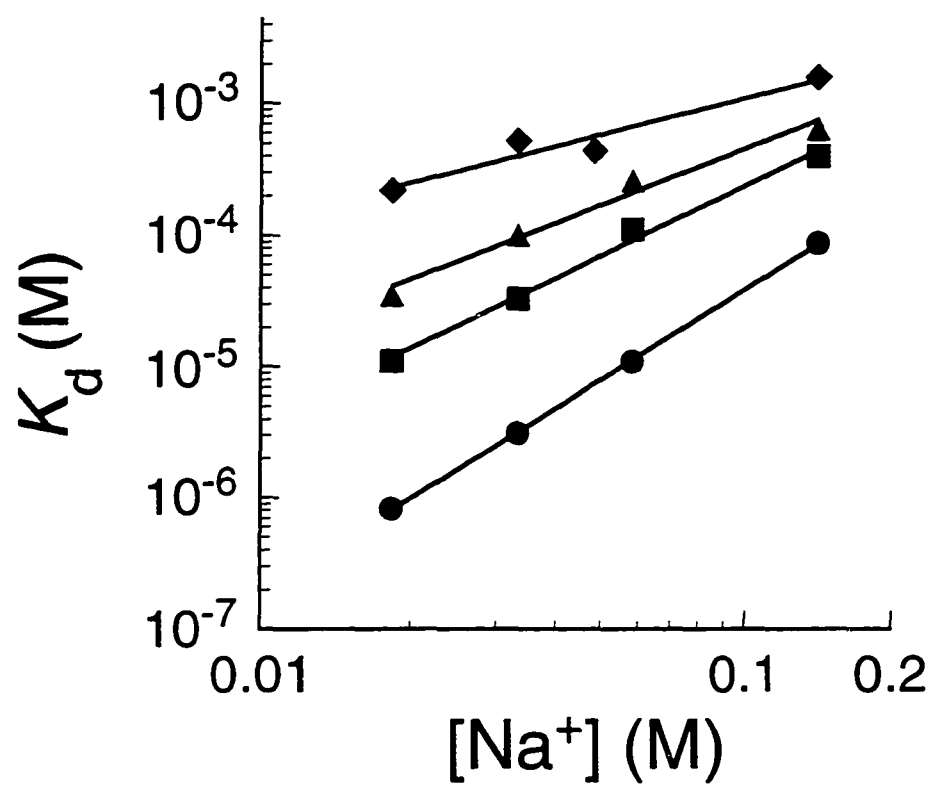
Figure 2.7 Transformed data for binding of fluorescein~d(AUAA) to wild-type RNase A

in the presence of different anions. Binding was assayed by fluorescence

anisotropy in the presence of NaCl (●) and NaF (○). Binding was measured at

23 ± 2 °C in 0.020 M MES-NaOH buffer containing NaCl or NaF (0.010 M,

0.025 M, or 0.050 M) or in 0.10 M MES-NaOH buffer, pH 6.0, containing

NaCl or NaF (0.10 M). The slopes of the lines are 2.3 ± 0.1 (NaCl) and

2.0 ± 0.2 (NaF).
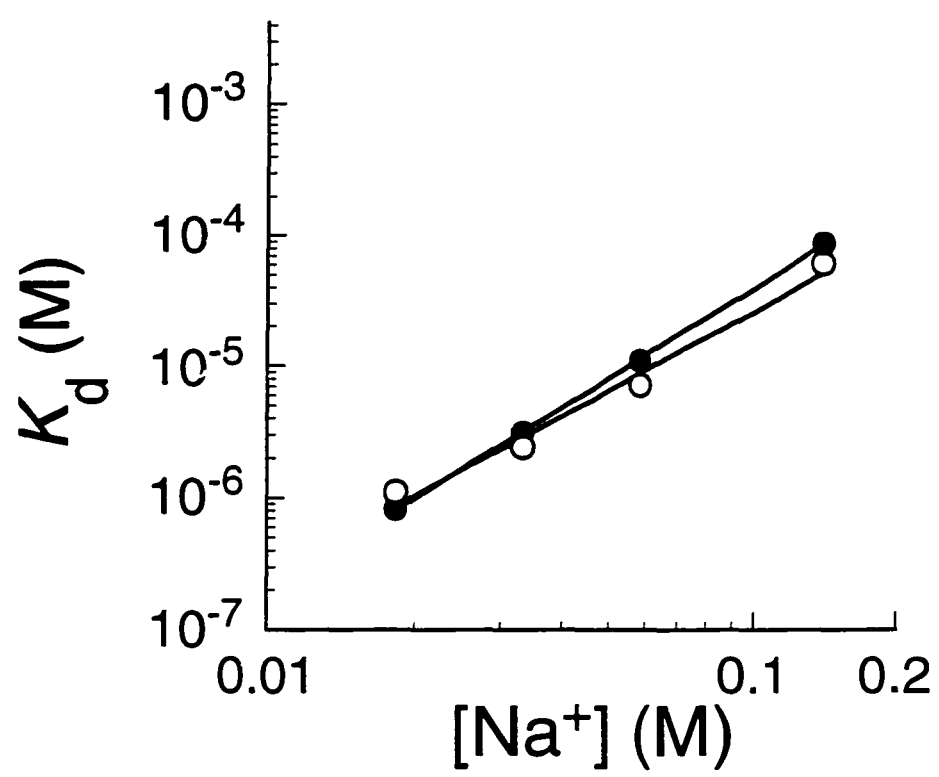
Chapter Three

Coulombic Effects of Remote Subsites
on the Active Site of Ribonuclease A

3.1 ABSTRACT: The active-site cleft of bovine pancreatic ribonuclease A (RNase A) is lined with cationic residues that interact with a bound nucleic acid. Those residues interacting with the phosphoryl groups comprise the P0, P1, and P2 subsites, with the scissile $P–O_{5'}$ bond residing in the P1 subsite. Coulombic interactions between the P0 and P2 subsites and phosphoryl groups of the substrate had been characterized previously. Here, the interactions between these subsites and the active-site residues His12 and His119 are described in detail. A protein variant in which the cationic residues in these subsites (Lys66 in the P0 subsite and Lys7 and Arg10 in the P2 subsite) were replaced with alanine was crystallized, both free and with a bound nucleotide [uridine 3'-phosphate (3'-UMP)]. Structures of K7A/R10A/K66A RNase A and the K7A/R10A/K66A RNase A•3'-UMP complex were determined by X-ray diffraction analysis to resolutions of 2.0 Å and 2.1 Å, respectively. There is little observable change between these structures and that of wild-type RNase A, either free or with bound 3'-cytidine monophosphate. K7A/R10A/K66A RNase A was evaluated for its ability to cleave UpA, a dinucleotide substrate that does not span the P0 or the P2 subsites. In comparison to the wild-type enzyme, the value of k_{cat} was decreased by 5-fold, and that of k_{cat}/K_m was decreased 10-fold, suggesting that these remote subsites interact with the active site. These interactions were characterized by determining the pK_a values of His12 and His119 at 0.018 M Na^+ and 0.142 M Na^+, both in wild-type RNase A and the K7A/R10A/K66A variant. The side chains of Lys7, Arg10, and Lys66 depress the pK_a values of these histidine residues, and this depression is sensitive to the salt concentration. In addition, the P0 and P2 subsites influence the interaction of His12 and His119 with each other, as demonstrated by changes in the cooperativity that gives rise to microscopic pK_a values. Finally, the affinity of 3'-UMP for wild-type RNase A and the K7A/R10A/K66A variant at 0.018 M Na^+ and 0.142 M Na^+ was determined by isothermal titration calorimetry. The variant protein binds to the 3'-UMP with 5-fold weaker affinity at 0.018 M Na^+ and 3-fold weaker affinity at 0.142 M Na^+ than does

wild-type RNase A. Together these data demonstrate that long-range Coulombic interactions are an important feature in catalysis by RNase A.

3.2 Introduction

Enzymes employ a variety of devices to effect catalysis (Gutfreund & Knowles, 1967; Jencks, 1987), with Coulombic forces[2] being one of the most important. The side chains of four (or five, if histidine is included) of the twenty amino acids bear a charge under physiological conditions. Coulombic forces can create environments that increase association rates of a substrate for an enzyme (Sharp *et al.*, 1987), contribute to the stabilization of the catalytic transition state (Jackson & Fersht, 1993), or affect the ionization of active-site residues (Russell *et al.*, 1987).

Short-range Coulombic interactions, such as those between neighboring residues, have long been known to contribute to enzymatic catalysis. For example, acetoacetate decarboxylase catalyzes the decarboxylation of acetoacetate to yield acetone and carbon dioxide. The reaction proceeds via a Schiff base intermediate with the active-site residue Lys115. To form the Schiff base, N_ζ of Lys115 must be in its unprotonated form (Kokesh & Westheimer, 1971), which is a minor form of a typical lysine residue [pK_a 10.4; (Fersht, 1985)] near neutral pH. The pK_a value of Lys115 is perturbed by more than four units (to 6.0) (Frey *et al.*, 1971; Schmidt & Westheimer, 1971) by its spatial proximity to N_ζ of Lys116 (Highbarger *et al.*, 1996). Thus, a Coulombic interaction between Lys115 and Lys116 obviates the need for general base catalysis.

---

[2] We prefer to use the term *Coulombic* rather than *electrostatic* to describe the force between two point charges. We consider "electrostatic" to be a general term that encompasses Coulombic forces, hydrogen bonds, and dipole – dipole interactions. "Coulombic" is thus more specific, referring only to interactions that obey Coulomb's law: $F = \dfrac{q_1 q_2}{4\pi\varepsilon r^2}$.

Only recently have the effects of distant, or long-range, Coulombic forces been explored. Long-range refers to interactions between residues that do not make direct contact due to distance constraints. For example, Jackson and Fersht altered charged residues 13 – 15 Å from the active site of subtilisin BPN′ and found that these alterations affected the binding of a transition state analog to the active site (Jackson & Fersht, 1993). One of the variants bound to the analog with 0.6 kcal/mol less free energy than did the wild-type enzyme. These results suggest that long-range Coulombic forces are important for transition state stabilization. In addition, these results suggest that long-range Coulombic forces could play a significant role in catalysis by many enzymes.

Bovine pancreatic ribonuclease A (RNase A; EC 3.1.27.5), the fourth protein and third enzyme for which a crystal structure had been solved, has been an excellent model system for studying protein structure – function relationships. RNase A is an endoribonuclease that cleaves and hydrolyzes RNA in two distinct steps (Figure 3.1). In the first step, the imidazole side chain of His12 acts as a base to abstract a proton from the 2′-hydroxyl of a substrate, thereby facilitating its nucleophilic attack on the phosphorus atom. The imidizolium side chain of His119 acts as an acid to protonate the 5′-oxygen, facilitating its displacement (Findlay *et al.*, 1961; Thompson & Raines, 1994). Both products are then released to solvent. The slow hydrolysis of the 2′,3′-cyclic phosphodiester occurs in a separate step that resembles the reverse of transphosphorylation (Cuchillo *et al.*, 1993; Thompson *et al.*, 1994).

His12 and His119 are the acid and base, respectively, in the transphosphorylation reaction catalyzed by RNase A. These assignments were deduced from chemical modification studies, pH–rate profiles (del Rosario & Hammes, 1969; Eftink & Biltonen, 1983), X-ray diffraction analyses (Avey *et al.*, 1967; Kartha *et al.*, 1967), and site-directed mutagenesis experiments (Crestfield *et al.*, 1962; Pincus *et al.*, 1975; Lennette & Plapp, 1979; Thompson & Raines, 1994). The pK_a values of these histidine residues have been investigated in detail using

^{1}H NMR spectroscopy (Meadows *et al.*, 1969; Rüterjans & Witzel, 1969; Cohen *et al.*, 1973; Haar *et al.*, 1974; Markley, 1975; Markley, 1975; Markley, 1975; Markley & Finkenstadt, 1975).

We are interested in the effect of long-range Coulombic forces on the active-site environment of RNase A. Here, we describe the role of three cationic residues in effecting this environment. In Chapter Two, we evaluated the role of RNase A residues Lys7, Arg10, and Lys66 in the binding of polymeric substrates. Coulombic interactions between the cationic side chains of these residues and the anionic phosphoryl groups of RNA contribute significantly to catalysis. Here, we have used X-ray diffraction analyses to determine the structure of K7A/R10A/K66A RNase A, both with and without bound uridine 3′-phosphate (3′-UMP). After demonstrating the similarity of these structures to that of wild-type RNase A, with and without bound cytidine 3′-phosphate (3′-CMP), we used steady-state kinetics, ^{1}H NMR spectroscopy, and isothermal titration calorimetry to show that the importance of these residues *extends beyond* their roles in RNA binding. Indeed, Lys7, Arg10, and Lys66 are important not only for creating a cationic environment that attracts polyanionic RNA but also for depressing the pK_a values of active-site residues His12 and His119. Together, these results suggest the importance of long-range Coulombic interactions in the catalysis of RNA cleavage by RNase A.

3.3 EXPERIMENTAL PROCEDURES

Materials. Wild-type and K7A/R10A/K66A RNase A were produced in *Escherichia coli* strain BL21(DE3) as described in Chapter Two. 2-(N-Morpholino)ethanesulfonic acid (MES), obtained as the free acid, was from ICN Biomedicals (Aurora, OH). Uridylyl (3′→5′)

adenosine (UpA), synthesized by the methods of Ogilvie (1978) and Beaucage and Caruthers (1981), was a generous gift of J. E. Thompson. 3′-UMP was from Sigma (St. Louis, MO). Deuterium oxide (D_2O; 99%) was from Aldrich Chemical (Milwaukee, WI). Deuterium chloride solution (DCl; 35% v/v in D_2O) and sodium deuteroxide solution (NaOD; 40% v/v in D_2O) were from Isotech (Miamisburg, OH). Sodium 2,2-dimethyl-2-silapentane-5-sulfonate (DSS) was from Cambridge Isotope Laboratories (Andover, MA). Sigmacote was from Sigma. All other chemicals and reagents were of commercial grade or better, and were used without further purification.

General Methods. Ultraviolet and visible absorbance measurements were made with a Cary Model 3 spectrophotometer equipped with a Cary temperature controller from Varian (Sugar Land, TX). RNase A concentrations were determined by assuming that $\varepsilon^{0.1\%} = 0.72$ at 277.5 nm (Sela *et al.*, 1957). 3′-UMP concentration was determined by assuming that $\varepsilon_{260} = 10000$ $M^{-1}cm^{-1}$ at pH 7.0 (Beaven *et al.*, 1955). pH was measured with a Beckman pH meter fitted with a Corning electrode, calibrated at room temperature with standard buffers from Fisher (Chicago, IL). Buffer solutions were prepared from the free acid of MES. The [Na^+] in these solutions was determined using the Henderson-Hasselbalch equation and assuming a pK_a value of 6.15 for MES at 25 °C (Scopes, 1994).

Structural Analyses. Investigation of protein structures was performed on a Personal Iris 4D/TG workstation from Silicon Graphics (Mountain View, CA) using the program MIDAS (Ferrin *et al.*, 1988). The Brookhaven Protein Data Bank (pdb) entry 1rph (Zegers *et al.*, 1994) was used to determine distances in native RNase A between Lys7, Arg10, or Lys66 and the nearest active-site histidine residue (His12 or His119). This structure was also used to create electrostatic molecular surface maps of RNase A using the program GRASP (Nicholls *et al.*, 1991). The electrostatic surfaces are based on the charges of RNase A residues at pH 6.0.

Isoelectric Focusing. The isoelectric point (pI) of K7A/R10A/K66A RNase A was determined using a Model 111 Mini IEF Cell from Bio-Rad (Hercules, CA) and a polyacrylamide (5% w/v) gel with Pharmolytes ampholytes (3% w/v; pI range 8–10.5) from Pharmacia (Piscataway, NJ). Focusing was carried out in a stepped fashion (100 V for 15 min, 200 V for 15 min, 450 V for 60 min) in a sealed environment flushed continuously with nitrogen. In addition, strips of Whatman paper soaked in NaOH (1 M) were placed on the bottom of the focusing apparatus to scavenge CO_2 and thereby reduce pH drift caused by CO_2 absorption by the ampholytes (Righetti *et al.*, 1990). The pI of K7A/R10A/K66A RNase A was determined by comparing its migration to that of the ampholytes. Strips from both sides of the polyacrylamide gel were cut into 0.5 cm pieces and placed in 1.6 mL microcentrifuge tubes filled with 0.5 mL H_2O to remove the ampholytes. After 20 min of shaking, the tubes were spun to pellet gel solids. The pH of the eluate was checked and a plot of pH vs distance was constructed (Righetti, 1984). The migration distance of K7A/R10A/K66A RNase A was measured in order to determine its pI. Similarly, the migration distance of a chymotrypsin standard [pI = 8.8; (Ui, 1971)] was measured to validate this technique for determining pI values.

Crystallization. Protein crystals were prepared by vapor diffusion using the hanging drop method. Lyophilized K7A/R10A/K66A RNase A was dissolved in unbuffered water to a concentration of 60 mg/mL. Drops consisting of protein solution (1.5 μL), water (1.5 μL), and reservoir solution (3.0 μL) were suspended from coverslips coated with Sigmacote (to prevent protein from adhering to the coverslip surface) over 0.5 mL of reservoir solution [0.1 M sodium acetate buffer, pH 4.5, containing 36% (w/v) polyethylene glycol 4000]. Trigonal crystals of K7A/R10A/K66A RNase A appeared within three days of incubation at 20 °C, and grew to a final size of 0.4 mm × 0.4 mm × 0.5 mm.

Crystals of K7A/R10A/K66A RNase A containing bound 3′-UMP were prepared by soaking native crystals for two days, at 20 °C, in mother liquor to which 3′-UMP was added at a final concentration of 5 mM.

X-Ray Diffraction Data Collection. The crystals of K7A/R10A/K66A RNase A were of space group P3$_2$21, with a = 68.15 Å, c = 65.51 Å, $\alpha = \beta = 90°$, and $\gamma = 120°$. Minor changes in cell constants were observed for crystals soaked with 3′-UMP, with a = 69.62 Å and c = 66.98 Å. All X-ray data were collected with a Siemens HI-STAR detector mounted on a Rigaku rotating anode operating at 50 kV, 90 mA, and a 300 μm focal spot. The X-ray beam was collimated by double focusing mirrors. The crystal to detector distance was 12.0 cm. Data were obtained in 512 × 512 pixel format, processed with the program XDS (Kabsch, 1988; Kabsch, 1988), and scaled using the program XSCALIBRE (G. E. Wesenberg and I. Rayment, unpublished results). Frames of data (900 × 0.15° = 135°) were collected from single crystals using a single φ-scan for both K7A/R10A/K66A RNase A and the K7A/R10A/K66A RNase A•3′-UMP complex. Reflections with I/σ < 0.33 were rejected. The crystals were cooled in a 0.5 °C air stream, resulting in negligible crystal decay for the entire data collection. Full crystallographic details are listed in Table 3.1.

Refinement of the K7A/R10A/K66A RNase A Structure. The starting model consisted of residues 1 – 124 of D121A RNase A (Schultz *et al.*, 1998) that was stripped of all solvent molecules. The model was subjected to 10 cycles of least-squares refinement using TNT (Tronrud *et al.*, 1987) and gave an initial *R*-factor of 0.217. Positive and negative $F_o - F_c$ showed clearly that residues 7, 10, and 66 had indeed been replaced with alanine. Manual adjustments to the model were performed in FRODO (Jones, 1985). After several cycles of manual adjustments and least-squares refinement, water molecules were added to the model. The peak searching algorithm in TNT was used to place ordered water molecules. Water

molecules were retained if they had at least 1σ of $2F_o - F_c$ density, 3σ of $F_o - F_c$ density, and were within hydrogen bonding distance of the protein or other water molecules.

Refinement of the Structure of the K7A/R10A/K66A RNase A•3′-UMP Complex. The starting model consisted of residues 1 – 124 of K7A/R10A/K66A RNase A that was stripped of all solvent molecules. The model was subjected to 10 cycles of least-squares refinement using TNT (Tronrud *et al.*, 1987) and gave an initial *R*-factor of 0.232. A positive $F_o - F_c$ map contoured at 3σ showed clearly the position of 3′-UMP in the active site. Non-active-site water molecules were added at this point using the crystalline structure of K7A/R10A/K66A RNase A as a guide, and the model was subjected to cycles of manual adjustment and least-squares refinement. Then, the 3′-UMP was built into the $F_o - F_c$ density and refined using geometric restraints provided by TNT. The solvent-accessible surface area buried upon K7A/R10A/K66A RNase A binding to 3′-UMP was determined using the program GRASP (Nicholls *et al.*, 1991). A 1.4 Å spherical probe, which mimics a water molecule, was rolled over the van der Waals surface of K7A/R10A/K66A RNase A and 3′-UMP, and of the K7A/R10A/K66A RNase A•3′-UMP complex. The solvent-accessible surface area buried during complex formation was calculated from these values.

Comparison of Variant Structures to that of Wild-Type RNase A. The K7A/R10A/K66A RNase A structure is compared here to that of wild-type RNase A that was likewise crystallized from high salt in the P3$_2$21 space group [pdb entry 1rph; (Zegers *et al.*, 1994)]. This wild-type RNase A structure was solved to a resolution of 2.2 Å. The structure of the 3′-UMP•K7A/R10A/K66A RNase A complex is compared here to that of the 3′-CMP•wild-type RNase A structure of the same space group that was prepared by soaking native crystals in a solution of 3′-CMP [pdb entry 1rpf; (Zegers *et al.*, 1994)]. This structure was solved to a resolution of 2.2 Å. RMS deviations were determined from a least-squares superposition of the two structures being compared with the program MIDAS (Ferrin *et al.*, 1988).

Steady-State Kinetic Analysis. Spectrophotometric assays were used to determine the steady-state kinetic parameters for the cleavage of UpA. The cleavage of UpA was monitored by following a decrease in absorbance at 286 nm as the products of the reaction, U>p and adenosine, were formed. The $\Delta\epsilon$ for this reaction is -620 $M^{-1}cm^{-1}$ at 286 nm (Thompson, 1995). Assays were performed at 25 °C in 0.10 M MES-NaOH buffer, pH 6.0, containing NaCl (0.10 M). The values of k_{cat}, K_m, and k_{cat}/K_m were determined from initial velocity data with the program HYPERO (Cleland, 1979).

NMR Spectroscopy. ^1H NMR spectroscopy was used to determine the pK_a values of three of the four histidine residues in wild-type RNase A and K7A/R10A/K66A RNase A at two [Na^+]. Prior to performing pH titrations of these proteins, exchangeable hydrogens were replaced with deuterium atoms. To exchange deuterium for hydrogen, protein (20 mg) that had been dialyzed exhaustively against water and lyophilized was dissolved in D_2O (1 mL), lyophilized, dissolved again in D_2O (1 mL), and lyophilized again. The pH*, which was a direct pH reading and not corrected for the deuterium isotope effect, was adjusted to 3.0 with DCl and the solution was heated to 60 °C for 1 h to exchange amide protons (Markley, 1975). Half of this solution was then removed and adjusted to pH* 9.0 with NaOD. To remove salt introduced during sample preparation, the solution was diluted 10-fold by the addition of D_2O and concentrated by centrifugation filtration using a Centriprep-10 from Amicon (Beverly, MA) that had been pre-rinsed with D_2O. Two additional 5-fold dilutions and concentrations by centrifugation filtration were performed, effectively reducing the salt concentration by approximately 250-fold. The final concentration step was repeated until the sample volume was < 0.5 mL. The solution analyzed by ^1H NMR spectroscopy contained protein (0.56 mM), NaCl (0.018 or 0.142 mM), and DSS (0.5 mM). During the experiment, pH* was adjusted using the protein solutions. The pH* 9 protein solution was added to the low pH* solution to raise the pH* and the pH* 3 solution was added to the high pH* solution to lower the pH*,

until the two solutions approached the midpoint of the titration, pH* 6.0. Using this technique, it was possible to perform each titration at a constant salt concentration and protein concentration.

Proton NMR spectra were acquired in 1D mode on a Bruker DMX 500 MHz NMR spectrometer at 25 °C using 16K data points and an acquisition time of 1.5 s, with 64, 128, or 256 scans following four dummy scans. Chemical shifts of the histidine C-2 protons, based on the assignments of Markley (Markley, 1975), are reported relative to DSS. Data were fitted using the program MATHEMATICA 3.0 (Wolfram Research; Champaign, IL). Data for His105 were fitted to eq 3.1, which describes the pH titration of a group with one pK_a. Data for His119, which has two microscopic pK_a's, were fitted to eq 3.2. Data for His12, which has an acidic inflection in the pH* titration in addition to two microscopic pK_a's, were fitted to eq 3.3. Data for His12 and His119 were fitted simultaneously because the difference in the microscopic pK_a's for each residue must be identical.

$$\delta_{obs} = \delta_{AH+} \times \delta_A \left[\frac{\left(10^{pK_a} + 10^{pH*}\right)}{\left(\delta_{AH+} \times 10^{pH*} + \delta_A \times 10^{pK_a}\right)} \right] \qquad (3.1)$$

$$\delta_{obs} = \delta_A \times \delta_{AH+} \times \frac{1 + \left[\frac{\left(10^{-pK_1^{119}} \times 10^{-pH*} + 10^{-pK_2^{119}} \times 10^{-pK_1^{12}}\right) \times 10^{pH*}}{\left(10^{-pH*} + 10^{-pK_1^{12}}\right)} \right]}{\delta_A + \left[\frac{\left(10^{-pK_1^{119}} \times 10^{-pH*} + 10^{-pK_2^{119}} \times 10^{-pK_1^{12}}\right) \times \delta_{AH+} \times 10^{pH*}}{\left(10^{-pH} + 10^{-pK_1^{12}}\right)} \right]} \qquad (3.2)$$

$$\delta_{obs} = \frac{\dfrac{\delta_A \times \delta_{AH+} \times \left[1 + \left(10^{-pK_1^{12}} \times 10^{-pH^*} + 10^{-pK_1^{12}} \times 10^{-pK_2^{119}}\right) \times 10^{pH^*}\right]}{\left(10^{-pH^*} \times 10^{-pK_2^{119}}\right)}}{\delta_A + \dfrac{\left[\left(10^{-pK_1^{12}} \times 10^{-pH^*} + 10^{-pK_1^{12}} \times 10^{-pK_2^{119}}\right) \times \delta_{AH+} \times 10^{pH^*}\right]}{\left(10^{-pH^*} + 10^{-pK_1^{119}}\right)}}$$
$$- \left[\delta_A \times 10^{-pH^*} \times \frac{\left(\delta_0 - \delta_{0H+}\right)}{\left(10^{-pK_0} \times \delta_{0H+} + 10^{-pH^*} \times \delta_0\right)}\right] \tag{3.3}$$

In eq 3.2 and 3.3, pK_1 is the microscopic pK_a of one active-site histidine residue when the other active-site histidine residue is protonated and pK_2 is the pK_a of this histidine when the other histidine residue is deprotonated. In eq 3.3, pK_0 is the pK_a for the acidic inflection in the His12 titration curve. Equations 3.1 – 3.3 are analogous to those used by Schechter and co-workers (Shrager *et al.*, 1972) and Raines and co-workers (Chivers *et al.*, 1997).

Isothermal Titration Calorimetry. The binding affinities of 3'-UMP for wild-type and K7A/R10A/K66A RNase A were determined by using a Micro Calorimetry System isothermal titration calorimeter from MicroCal (Northampton, MA). All buffer and protein samples were degassed by vacuum prior to use. For the experiment at 0.142 M Na$^+$, RNase A was in the reaction cell at an initial concentration of 0.4 mM. For the experiment at 0.018 M Na$^+$, RNase A was in the reaction cell at an initial concentration of 0.12 mM. Following thermal equilibration of the system, there was a delay of 600 s before the first injection. Successive injections (48) of 3'-UMP (5 µL of a 9.2 mM or 3.0 mM solution) were made into the cell at 240-s intervals, and heats of binding were measured after each injection. Binding at the higher sodium concentration was measured at 25 °C in 0.10 M MES-NaOH buffer, pH 6.0, containing NaCl (0.10 M final [Na$^+$]). The lower salt concentration experiments were performed in 0.020 M MES-NaOH buffer, pH 6.0, containing NaCl (0.010 M final [Na$^+$]). The reference cell, acting only as a thermal reference to the sample cell, was filled with water.

The least-squared estimates of binding parameters n, ΔH°, and K_a were determined from the raw data using the program ORIGIN (MicroCal Software; Northampton, MA). Values of ΔG° and $T\Delta S^\circ$ were determined from values of ΔH° and K_a by using eq 3.4:

$$\Delta G^\circ = -RT \ln K_a = \Delta H^\circ - T\Delta S^\circ \tag{3.4}$$

The first data point in the sequence was omitted during data processing due to error in the accurate delivery of a particular volume of sample during the first injection.

3.4 RESULTS

Isoelectric Point of K7A/R10A/K66A RNase A. The pI of K7A/R10A/K66A RNase A was determined by isoelectric focusing to be 8.3 (data not shown). As expected for a protein variant with several cationic residues replaced with neutral residues, this value is lower than that for the wild-type protein, which has pI 9.3 (Ui, 1971). In addition to determining this value, the presence of a single band in the lane corresponding to K7A/R10A/K66A RNase A testifies to its purity.

Crystalline Structure. The statistics for X-ray diffraction analyses of K7A/R10A/K66A RNase A (with and without bound 3′-UMP) are listed in Table 3.1. The final model for K7A/R10A/K66A RNase A contains the complete protein (residues 1 – 124), 84 water molecules, and an acetate ion. The R-factor for all data in the range 30 Å – 2.0 Å is 0.174. The RMS deviations for target geometries are 0.010 Å for bond lengths and 2.2° for bond angles. Average B-factors for the main chain and side chains are 37.8 Å^2 and 42.6 Å^2, respectively.

Atomic coordinates for K7A/R10A/K66A RNase A have been deposited in the pdb with accession code 3rsk.

The final model for the K7A/R10A/K66A RNase A•3′-UMP complex contains the complete protein (residues 1 – 124), 3′-UMP, and 94 water molecules. The R-factor for all data in the range 30 Å to 2.1 Å is 0.168. The RMS deviations for target geometries are 0.011 Å for bond lengths and 2.2° for bond angles. Average B-factors for the main chain, side chains, and 3′-UMP are 36.7 Å^2, 40.5 Å^2, and 40.0 Å^2, respectively. Atomic coordinates for the K7A/R10A/K66A RNase A•3′-UMP complex have been deposited in the pdb with accession code 4rsk.

The structures of residues 2 – 10 and the active site of K7A/R10A/K66A RNase A, superimposed on the wild-type RNase A structure [pdb entry 1rph; (Zegers *et al.*, 1994)], are shown in Figures 3.2 and 3.3. Shown in Figure 3.4 is the structure of the active site of K7A/R10A/K66A RNase A with bound 3′-UMP, superimposed on the same region of the wild-type RNase A•3′-CMP complex [pdb entry 1rpf; (Zegers *et al.*, 1994)].

Steady-State Kinetic Parameters. Replacing Lys7, Arg10, and Lys66 with alanine has an effect on the values of k_{cat}, K_m, and k_{cat}/K_m for cleavage of UpA (Table 3.2). The k_{cat} for UpA cleavage by K7A/R10A/K66A RNase A is 5-fold less than that of the wild-type enzyme and the K_m is increased by twofold. Accordingly, the k_{cat}/K_m is reduced 10-fold relative to that of wild-type RNase A.

Histidine pK_a Values. The pK_a values for His12, His119, and His105 of RNase A can be determined by analyzing the shift of the imidazolyl C-2 proton upon changing pH* (Markley, 1975). The other histidine residue in RNase A, His48, is inaccessible to solvent and its titration curve shows anomalous behavior with pH*, preventing a determination of its pK_a value (Markley, 1975). Shown in Figure 3.5 is the pH* titration of wild-type and K7A/R10A/K66A RNase A at 0.142 M Na$^+$ and 0.018 M Na$^+$. His105 is solvent exposed and

its titration curve can be fitted to a model with a single pK_a. In contrast, His12 and His119 interact with each other, necessitating the use of a model that includes microscopic pK_a's. These microscopic pK_a's account for the effect of the protonation state of one histidine residue on the protonation state of the other histidine residue (Markley & Finkenstadt, 1975). In addition, His12 shows an inflection in the acidic region of its pH* titration, necessitating the use of a third pK_a to fit the data accurately. This inflection is due to the titration of a nearby carboxyl group, which perturbs the chemical shift of the C-2 proton of His12 (Karpeisky & Yakovlev, 1981). This third pK_a value is the least precise of the pK_a values determined due to the lack of data below pH* 3.

The pK_a values of His12, His119, and His105 and the chemical shifts of the protonated and unprotonated forms of these histidine residues in wild-type and K7A/R10A/K66A RNase A at 0.142 M Na$^+$ and 0.018 M Na$^+$ are listed in Table 3.3. The pK_a values for His105 in all four pH* titrations are similar, whereas the pK_a values for His12 and His119 differ dramatically in the four pH* titrations. For the wild-type protein, reducing the sodium concentration in the solution results in a large decrease in the pK_a values for both His12 and His119. The pK_a values for His12 are decreased by 0.60 units (pK_1) and 0.53 units (pK_2) upon reducing the sodium concentration, and the pK_a values for His119 are decreased by 0.51 units (pK_1) and 0.42 units (pK_2) upon reducing the sodium concentration. The pK_a values for K7A/R10A/K66A RNase A are also decreased upon reducing the sodium concentration, but to a lesser extent. The pK_a values for His12 are decreased by 0.55 units (pK_1) and 0.37 units (pK_2), and the pK_a values for His119 are decreased by 0.41 units (pK_1) and 0.20 units (pK_2) upon reducing the sodium concentration.

A comparison of the His12 and His119 pK_a values in the wild-type and K7A/R10A/K66A proteins, at either salt concentration examined, shows that the cationic side chains of residues 7, 10, and 66 contribute to a depression in these values. When these side chains are removed, the pK_a values of His12 and His119 are increased. These increases are more dramatic at the

lower sodium concentration examined than at the higher sodium concentration examined. At 0.018 M Na$^+$, the pK_a values of His12 are increased by 0.33 units (pK_1) and 0.75 units (pK_2), and the pK_a values for His119 are increased 0.35 units (pK_1) and 0.79 units (pK_2) upon removing the side chains of residues 7, 10, and 66. At 0.142 M Na$^+$, the pK_a values of His12 are increased 0.28 units (pK_1) and 0.59 units (pK_2), and the pK_a values of His119 are increased 0.25 units (pK_1) and 0.57 units (pK_2) upon removing the side chains of residues 7, 10, and 66.

RNase A Binding to 3′-UMP. Shown in Figure 3.6 are representative data for the calorimetric titrations of wild-type RNase A and the K7A/R10A/K66A variant with 3′-UMP. The thermodynamic parameters derived for these experiments, which were performed at 0.018 M Na$^+$ and 0.142 M Na$^+$, are reported in Table 3.4. These conditions are similar to those used in the NMR experiments described above. Replacing Lys7, Arg10, and Lys66, which are all remote to the enzymic active site, with alanine residues results in a decrease in binding affinity for 3′-UMP at both the lower and higher sodium concentration examined. The affinity for 3′-UMP is tighter for both proteins under the lower sodium concentration condition than under the higher sodium concentration condition. The value of K_d for 3′-UMP binding to wild-type RNase A is 9.7 μM at 0.018 M Na$^+$. The value for K_d increases by 5-fold to a value of 53.8 μM at 0.142 M Na$^+$. The value of K_d for binding to the K7A/R10A/K66A variant is 47.4 μM at 0.018 M Na$^+$ and increases by 3-fold to a value of 153.6 μM at 0.142 M Na$^+$.

The binding stoichiometries, *n*, are nearly 1.0 for all four binding experiments, suggesting that a single 3′-UMP ligand binds to each protein molecule. The enthalpies for binding vary slightly, with the enthalpies for binding to the wild-type protein being more exothermic than those for binding to the variant protein. These $\Delta H°$ values are −13.8 kcal/mol and −11.8 kcal/mol for binding to the wild-type protein at the lower and higher sodium concentration conditions, respectively. The $\Delta H°$ values for binding to the K7A/R10A/K66A

variant are −10.1 kcal/mol and −9.4 kcal/mol at the lower and higher sodium concentration conditions, respectively. The entropies for binding of 3′-UMP to RNase A appear to depend more on the protein than on the solution condition. The $T\Delta S^\circ$ values for binding to the wild-type protein are −6.8 kcal/mol and −5.8 kcal/mol at the lower and higher sodium concentration, respectively. The $T\Delta S^\circ$ value for binding to the variant protein is −4.1 kcal/mol at both solution conditions examined.

3.5 DISCUSSION

RNase A is a cationic protein under physiological conditions [pI = 9.3; (Ui, 1971)]. Its active-site cleft is lined with basic amino acid residues that interact with the RNA substrate during catalysis. The interactions of several of these basic residues with the RNA substrate had been characterized previously. For example, the residues known to interact with the phosphoryl groups on RNA have been characterized as belonging to one of several phosphoryl group binding pockets, named the P0, P1, and P2 subsites (Figure 3.7). The active-site residues His12, His119, and Lys41 comprise the P1 subsite. Lys66 comprises the P0 subsite, and Lys7 and Arg10 comprise the P2 subsite. Chemical modification and mutagenesis experiments have been used to characterize these binding pockets (Nogués *et al.*, 1995; Raines, 1998). In addition, the salt concentration-dependence of binding of a ssDNA oligomer to wild-type RNase A and the K66A, K7A/R10A, and K7A/R10A/K66A variants demonstrated that significant Coulombic interactions exist between the side chains of Lys7, Arg10, and Lys66 and the phosphoryl groups of the bound nucleic acid (Chapter Two).

Enzymic residues can be involved in substrate binding and substrate cleavage. Distinguishing between these two functions can be problematic. Although the P0 and P2

subsites of RNase A have been characterized extensively in terms of their involvement in substrate binding, their roles in catalysis have been described only briefly. Cuchillo and co-workers noted an effect on both K_m and k_{cat} for cleavage of CpA and poly(C), and hydrolysis of C>p when Lys7 and Arg10 were replaced with glutamine residues (Boix *et al.*, 1994). The reductions in k_{cat} upon removing the positive charges in the P2 subsite were not expected, especially for CpA and C>p, which do not interact directly with this subsite. Our results for the cleavage of UpA by variants at positions 7, 10, and 66 are in accord with those of Cuchillo and co-workers. As listed in Table 3.2, the catalysis of UpA cleavage is compromised by replacement of these residues with alanine. Molecular dynamics calculations indicate that Lys7 is displaced toward CpA or the transition state analog uridine 2',3'-cyclic vanadate upon binding, relative to its position in the free enzyme (Brünger *et al.*, 1985). These calculations led Cuchillo and co-workers to suggest that the role of Lys7 during catalysis is to stabilize the transition state through a network of intervening water molecules (Boix *et al.*, 1994). A role for Arg10 and Lys66 during catalysis had not been described previously.

The results of our ^{1}H NMR spectroscopy and calorimetry experiments suggest two roles for Lys7, Arg10, and Lys66. First, the side chains of Lys7, Arg10, and Lys66 enhance the cationic nature of the positively-charged binding cleft, attracting the anionic RNA substrate to the enzymic active site. Second, the side chains of Lys7, Arg10, and Lys66 depress the pK_a values of the active-site histidine residues. The impaired catalysis by RNase A variants with altered P0 and P2 subsites is explained by a failure to fulfill this second role. Before defining the roles of the Lys7, Arg10, and Lys66 side chains in affecting the active-site environment of RNase A, the structure of the K7A/R10A/K66A variant, both with and without bound 3'-UMP, will be described in detail.

Crystalline Structures. RNase A was one of the first enzymes whose structure was determined by X-ray diffraction analysis (Kartha *et al.*, 1967). In total, over 70 sets of three-

dimensional coordinates (from both X-ray diffraction analysis and ^{1}H NMR spectroscopy) related to RNase A have been deposited in the pdb (Raines, 1998), including structures of RNase A with bound oligonucleotides, dinucleotides, and mononucleotides (Gilliland, 1997; González et al., 1997). Recently, we reported the first crystalline structures of active-site [D121A RNase A (pdb entry 3rsd) and D121N RNase A (pdb entry 4rsd); (Schultz et al., 1998)] and other variants [P93G RNase A (pdb entry 3rsp); (Schultz et al., 1998)] of RNase A. The crystalline structure of K7A/R10A/K66A RNase A reported here is the first for a distal subsite variant. We also report the first crystalline structure of an RNase A variant with a bound ligand, 3′-UMP. These structures show that replacing Lys7, Arg10, and Lys66 with an alanine residue does not affect the overall structure of RNase A, either with or without bound 3′-UMP. In addition, the similarity of the K7A/R10A/K66A RNase A crystalline structures to the three-dimensional structure of the wild-type protein with and without bound 3′-CMP supports our hypothesis that residues Lys7, Arg10, and Lys66 affect the active-site environment of RNase A via long-range Coulombic interactions, and not by perturbing the three-dimensional structure of the enzyme.

The structure of the K7A/R10A/K66A variant of RNase A was solved in the trigonal space group $P3_221$ and contains an acetate ion in the active site. The main-chain atoms of K7A/R10A/K66A RNase A have an average RMS deviation of 0.36 Å from those of wild-type RNase A [pdb entry 1rph; (Zegers et al., 1994)]. The structure of the K7A/R10A/K66A RNase A•3′-UMP complex was also solved in the trigonal space group $P3_221$ and contains a single 3′-UMP ligand bound in the active site. The main chain atoms of K7A/R10A/K66A RNase A in the K7A/R10A/K66A RNase A•3′-UMP complex have an average RMS deviation of 0.48 Å from those of the wild-type RNase A•3′-CMP complex [pdb entry 1rpf; (Zegers et al., 1994)].

P0 and P2 Subsites. There is little observable change in the main-chain atoms of residues 7, 10, and 66 upon replacement with alanine. As shown in Figures 3.2 and 3.4, the K7A/R10A/K66A RNase A structure contains two water molecules in the position occupied by Arg10 in the wild-type protein structure and a single water molecule in the position occupied by Lys66 in that structure. No ordered water molecules in the place of Lys7 are apparent.

Active Site. In the structure of K7A/R10A/K66A RNase A, we find little change in the positions of the main-chain and side-chain atoms of residues residing in the P1 or B1 (pyrimidine binding) subsites (Figure 3.7). The position of His12 in the K7A/R10A/K66A RNase A structure has not changed from that in the wild-type structure. The side chain of His119 in RNase A has been shown to occupy two distinct positions, denoted as A and B, which are related by a 100° rotation about the C_α–C_β bond and a 180° rotation about the C_β–C_γ bond (Borkakoti *et al.*, 1982; Borkakoti, 1983). The position of the His119 side chain has been shown to be dependent on the pH and ionic strength of the crystallization solution (Fedorov *et al.*, 1996). In the wild-type structure used for comparison here, the His119 side chain occupies both positions A and B. In the K7A/R10A/K66A RNase A structure, the side chain of His119 occupies only position A, with a χ_1 angle of 165° (the χ_1 angle in the 1rph structure is also 165°). Although the χ_1 angles for His119 are similar in the variant and wild-type proteins, a superposition of the two structures shows that the His119 side chain position in K7A/R10A/K66A RNase A is altered slightly with respect to His119 in the wild-type structure. This small alteration is presumably due to the presence of an acetate ion, rather than a sulfate ion, bound in the active site. A sulfate ion is larger than is an acetate ion [thermochemical radius of 248 pm vs 148 pm; (Huheey, 1983)] and occupies a tetrahedral, rather than planar, geometry. In the wild-type structure, the oxygen atoms of the bound sulfate bridge the $N_{\epsilon 2}$ atom of His12 and the $N_{\delta 1}$ atom of His119. Similarly, the oxygen atoms of the bound acetate also bridge the $N_{\epsilon 2}$ atom of His12 and the $N_{\delta 1}$ atom of His119 in the

K7A/R10A/K66A RNase A structure. In addition, there is a water molecule in the K7A/R10A/K66A RNase A structure occupying the space taken by the B position of the His119 side chain in the wild-type structure. The positions of the other active-site residues, Lys41, Gln11, and Asp121 in the P1 subsite and Thr45 and the Phe120 main-chain atoms in the B1 subsite, are virtually unchanged between the wild-type and variant crystalline structures.

S-Peptide. In the presence of the protease subtilisin, RNase A is cleaved preferentially between residues 20 and 21 to form S-peptide (residues 1–20) and S-protein (residues 21–124) (Richards & Vithayathil, 1959). When these two fragments are recombined to form the noncovalent complex RNase S, enzymatic activity is indistinguishable from that of RNase A. Residues 1–15 of S-peptide (S15) are sufficient for binding S-protein and effecting catalysis (Hofmann *et al.*, 1966). Residues 2–13 of S-peptide form a stable α-helix when bound to S-protein and in isolation, maintains considerable helicity (10-50%) in water (Osterhout *et al.*, 1989; Finkelstein *et al.*, 1991). This α-helical structure is necessary for stabilizing intermediates in the folding of RNase S (Kato & Anfinsen, 1969; Labhardt & Baldwin, 1979; Brems & Baldwin, 1984) and proper alignment of the catalytically important residue His12 in RNase A or RNase S. S-peptide [and also C-peptide, residues 1–13 of RNase A, terminating in homoserine lactone; (Gross & Witkop, 1962)] is frequently used as a model system for studying α -helices; several such studies have focused on the determinants of α-helix formation. A salt bridge between Glu2 and Arg10 plays a fundamental role in the folding of isolated S-peptide (Rico *et al.*, 1984; Fairman *et al.*, 1990). Replacement of Glu2 with alanine in C-peptide results in a peptide with no measurable helix formation (Shoemaker *et al.*, 1985).

The structure of the N-terminal residues in K7A/R10A/K66A RNase A is similar to that in the wild-type protein. Lys1 is disordered, but residues 2–15 of the variant protein structure are superimposable on the wild-type protein structure. The average RMS deviation for residues 2–15 of K7A/R10A/K66A RNase A is 0.23 Å from those residues in the wild-type structure. As

shown in Figure 3.2 (Kraulis, 1991), K7A/R10A/K66A RNase A has two water molecules in the position occupied by Arg10 in the wild-type structure. Neither of these water molecules are within hydrogen bonding distance of Glu2 (one water molecule is 4.9 Å away from $O_{\varepsilon1}$ of Glu2 and the other is 5.5 Å away from this atom). Although the $Glu2^-\cdots Arg10^+$ salt bridge is important for α-helix formation in isolated S-peptide, the structure reported herein with alanine at position 10 suggests that this salt bridge is not necessary for α-helix formation in the context of the entire protein.

3'-UMP. The structure of the K7A/R10A/K66A RNase A•3'-UMP complex determined here is similar to that of the wild-type RNase A•3'-CMP complex determined previously (Zegers *et al.*, 1994). Still, there are some minor changes between these two complexes due to structural differences between uridine and cytidine. The relevant intermolecular interactions are listed in Table 3.5 (Ferrin *et al.*, 1988). Briefly, 3'-UMP makes contact with the B1 subsite, the P1 subsite, and bound water molecules (Figure 3.4), burying 515 $Å^2$ of solvent-accessible surface area of the protein upon binding. In the B1 subsite, a hydrogen bond mediates the nucleotide specificity of RNase A (delCardayré & Raines, 1995). In accord with the crystalline complex of RNase A with uridine 2',3'-cyclic vanadate (Wlodawer *et al.*, 1983), hydrogen bonds are formed between the N3 and O2 atoms of bound uridine and the $O_{\gamma1}$ and main chain N atoms of Thr45, respectively, and between the $O_{\gamma1}$ atom of Thr45 and the $O_{\delta1}$ atom of Asp83. In addition, a bound water molecule donates a hydrogen bond to the O4 atom of uridine.

The active-site residues in the K7A/R10A/K66A RNase A•3'-UMP complex are unchanged from those in the wild-type RNase A•3'-CMP complex. The side chains of His12 in the two structures are superimposable, as are those of His119. Both the $N_{\varepsilon2}$ atom of His12 and the $N_{\delta1}$ atom of His119 donate hydrogen bonds to O atoms of the bound phosphoryl

group. In addition, His119 donates a hydrogen bond to a bound water molecule, which is not seen in the wild-type RNase A•3′-CMP crystalline structure. In both the wild-type and variant crystalline structures with bound nucleotide, His119 is in the B position. The χ_1 angle for the His119 side chain in the variant structure is –64°, compared to –69° in the wild-type structure. Further, N_ζ of Lys41 donates hydrogen bonds to three atoms: the 2′-hydroxyl of the bound nucleotide, $O_{\epsilon 1}$ of Gln11, and $O_{\delta 1}$ of Asn44. The structural similarities between the wild-type and variant free proteins and protein•nucleotide complexes justify our explaining the roles of Lys7, Arg10, and Lys66 in terms of function rather than structure.

His12 and His119 in RNase A. The titration behaviors of His12 and His119 in RNase A are well-documented. [For a review, see: (Antosiewicz *et al.*, 1996).] The pK_a values of these residues (and His105) in free RNase A and RNase A with a bound nucleotide have been determined in a variety of different solution conditions, including various NaCl concentrations (< 0.1 M – 0.4 M) and in the absence and presence of inorganic phosphate. We are interested in the role of Coulombic interactions in RNase A, and such interactions are masked by concentrated solutions of electrolytes (Russell & Fersht, 1987). Thus, we performed our experiments both in a solution of much lower salt concentration (0.018 M) than had been reported previously and in a solution of salt concentration (0.142 M) similar to that used in our laboratory for RNase A activity assays (delCardayré *et al.*, 1995).

pH* Titrations – Methodology. The most common method for performing pH titrations involves the addition of acid or base to the sample to change the pH. At high salt concentrations, the change in salt concentration upon adding acid or base is negligible. But at low salt concentrations (such as 0.018 M Na^+), the addition of enough NaOD to change the pH* from 3 to 9 would alter dramatically the salt concentration of the solution. Had we used this method, we would have performed a pH titration *and* an ionic strength titration. Our method, which involves mixing two solutions that differ only in pH*, changes only the pH* of

the protein solution during the experiment. His105 serves as a useful control for testing the validity of this method. This residue is solvent-exposed and is not known to interact with neighboring residues through Coulombic interactions. Its pK_a value should therefore report on the ability of the acidic and basic protein solutions to meet at the appropriate midpoint of the titration curve. Indeed, the pK_a value of His105 is in gratifying agreement (within 0.12 pK_a units) in wild-type RNase A and the K7A/R10A/K66A variant at both solution conditions examined (Table 3.3), and is also similar to that reported previously (Markley, 1975). This agreement indicates that our method for varying pH* gives valid results.

Salt Concentration-Dependence of His12 and His119 pK_a Values. If the protonation states of His12 and His119 are influenced by their environment through Coulombic interactions, then their pK_a values should be sensitive to the salt concentration. Rüterjans and Witzel (1969) have shown that the pK_a values of these residues are influenced by the solution salt concentration, and more so than is the pK_a values of imidazole or a free histidine residue. We also find a strong dependence of the His12 and His119 pK_a values on the salt concentration. Unfortunately, a direct comparison of our results to those of Rüterjans and Witzel is not possible because their titrations involved adding base to their RNase A solutions and their data were not fitted to equations describing microscopic pK_a values.[3]

Interaction between His12 and His119. Microscopic pK_a's arise from Coulombic interactions that create either positive or negative cooperativity. In RNase A, the histidine residues interact with positive cooperativity—deprotonation of one histidine residue stabilizes the protonated state of the other histidine residue. As shown in Scheme 3.1, microscopic pK_a

---

[3] Microscopic pK_a values for His12 and His119 in RNase A were described six years subsequent to the publication of the work of Rüterjans and Witzel (Markley & Finkenstadt, 1975).

values are related by a thermodynamic box, wherein a complete titration by the path **I → II →**

IV is identical to that by the path **I → III → IV** (Chivers *et al.*, 1997).

Scheme 3.1:

$$
\begin{array}{ccc}
 & \begin{array}{c}\text{12 His}\\\text{119 HisH}^+\end{array} & \\
K_1^{12}\quad\quad\quad \text{II} & \quad cK_1^{119}=K_2^{119} \\
\begin{array}{c}\text{12 HisH}^+\\\text{119 HisH}^+\end{array} & & \begin{array}{c}\text{12 His}\\\text{119 His}\end{array}\\
\text{I}\quad\quad\quad\quad\quad\quad\quad\quad \text{IV} \\
K_1^{119}\quad\quad\quad cK_1^{12}=K_2^{12} \\
 & \begin{array}{c}\text{12 HisH}^+\\\text{119 His}\end{array} & \\
 & \text{III} &
\end{array}
$$
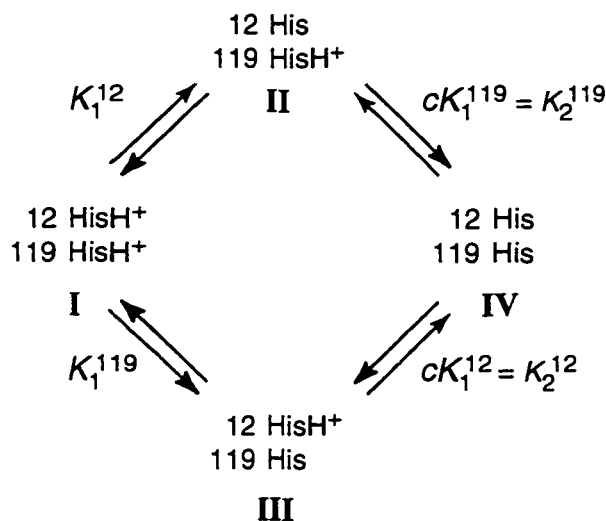
These four distinct titrations are related by eq 3.5:

$$ pK_1^{12} + p(cK_1^{119}) = pK_1^{119} + p(cK_1^{12}) \tag{3.5} $$

Equation 3.5 and the values of pK_1 for His12 and His119 (Table 3.3) can be used to determine the value of c, which provides a measure of the strength of the interaction between His12 and His119. A c value of 1 indicates that no interaction exists between residues and the system need not be described by microscopic pK_a values. In contrast, a c value $<<$ 1 indicates strong cooperativity between titratable residues (Wyman & Gill, 1990).

The degree of cooperativity between His12 and His119 in RNase A is affected more by the replacement of Lys7, Arg10, and Lys66 with alanine residues than by an increase in sodium concentration. As listed in Table 3.6, the deprotonation of His12 and His119 is more

cooperative in K7A/R10A/K66A RNase A than in wild-type RNase A. Wild-type RNase A is more cationic than is K7A/R10A/K66A RNase A (pI = 9.3 vs 8.3; Figures 3.8B and 3.8C). In both proteins, a state in which both histidine residues are protonated is disfavored. But once one histidine is deprotonated, the second histidine is less driven to become deprotonated in the variant protein than in the wild-type protein. This change in cooperativity of the His12 and His119 protonation states upon the removal of three cationic side chains may result from a change in the dielectric constant close to the surface of RNase A. From the Kirkwood-Westheimer equation (Edsall *et al.*, 1958), one can predict the relationship between ΔpK (= $pK_2 - pK_1$) and the dielectric constant ε, as shown in eq 3.6:

$$r = \frac{q^2}{2.303\varepsilon kT(\Delta pK)}$$

(3.6)

where r is the distance between the two titratable groups, q is the proton charge, k is Boltzmann's constant, and T is the absolute temperature. Because the distance between His12 and His119 is the same in wild-type RNase A and K7A/R10A/K66A RNase A (vide infra) and q, k, and T are constant in both proteins, ΔpK is inversely proportional to the dielectric constant ε. Hence, the larger cooperativity (*i.e.*, smaller c value) observed for the deprotonation of His12 and His119 in the variant protein may be due to a decrease in the dielectric constant of the active-site cleft upon removing the cationic side chains of residues 7, 10, and 66. These results are consistent with the general finding that neutral systems have a lower dielectric constant than do charged systems (Creighton, 1993).

Why does replacing Lys7, Arg10, and Lys66 with alanine residues have a much larger effect on the cooperativity of the protonation states of His12 and His119 than does an increase in [Na$^+$]? To answer this question, we must relate the positions of these three point charges,

relative to the active-site histidine residues, to that of a single point charge that interacts with His12 and His119 equivalently. We call the distance between this single point charge and the active-site histidine residues the "reduced radius," or "ρ." The value of ρ can be calculated using eq 3.7 and the distances (r) between pairs of residues.

$$\rho = \sqrt{\frac{1}{\sum_{i=1}^{n}\left(\frac{1}{r_i}\right)^2}} \tag{3.7}$$

This equation is derived from basic mechanics (A. H. Fisher, personal communication), where an electrostatic force F is proportional to the inverse of r^2 (*i.e.*, $F \propto 1/r^2$). The value of ρ is always smaller than any of the distances r, hence the name *reduced* radius. A similar concept is used in quantum and solid-state physics to describe the oscillation between two objects (Resnick & Halliday, 1966; Levine, 1983). The movement of the two objects relative to each other is equivalent to the movement of a single object with reduced mass μ relative to a fixed point.

The atomic coordinates for the wild-type RNase A crystalline structure [pdb entry 1rph; (Zegers *et al.*, 1994)] were used to determine the distances between N_ζ of Lys7, the midpoint of the line segment connecting $N_{\eta 1}$ and $N_{\eta 2}$ of Arg10, or N_ζ of Lys66 and the midpoint of the line segment connecting $N_{\epsilon 2}$ of His12 and $N_{\delta 1}$ of His119. These distances are shown in Figure 3.9. From eq 3.7 and these values ($r_1 = 7.6$ Å, $r_2 = 11$ Å, and $r_3 = 14$ Å), we calculate that $\rho = 5.7$ Å. Thus, by this analysis the three point charges of Lys7, Arg10, and Lys66 are equivalent to a single point charge 5.7 Å from His12 and His119. Interestingly, this value of ρ is only slightly smaller than is the distance from N_ζ of Lys41 to the midpoint of the line segment connecting $N_{\epsilon 2}$ His12 and $N_{\delta 1}$ His119, which is 6.0 Å (Figure 3.9). Lys41 is an

intimate member of the RNase A active site whose role is to donate a hydrogen bond to the transition state during catalysis (Messmore *et al.*, 1995). This residue influences dramatically the pK_a values of the active-site histidine residues (J. M. Messmore, B. M. Fisher, and R. T. Raines, unpublished results). Replacement of Lys41 with alanine yields a *c* value of 0.19 for the interaction of Lys41 with His12 and His119 (Table 3.6). In contrast to the residue – residue distances, using a semi-quantitative analysis[4] we calculate that sodium atoms are separated by 45 Å in a 0.018 M Na$^+$ solution and by 23 Å in a 0.142 M Na$^+$ solution. These two distances represent averages. Of course, sodium ions are not spaced homogeneously in a solution containing protein; the ionic distribution in the bulk solution differs from that near the protein surface. Nonetheless, the effective molarity of the positive charges of Lys7, Arg10, and Lys66, or of Lys41, is much higher than the [Na$^+$] used in our experiments. Indeed, it would take a solution of ~ 8 M NaCl to approach a separation distance of 6.0 Å for each sodium atom. Given this value, it is not surprising that raising the salt concentration in our solutions by only 0.124 M had little effect on the cooperativity of His12 and His119. In both wild-type RNase A and the K7A/R10A/K66A variant, raising the salt concentration increased the *c* value by only 0.09 (Table 3.6).

Implications for Catalysis. Enzymatic catalysis is most efficient when the pK_a of the reactive group matches the pH of the solution (Jencks, 1987). Bases with pK_a values below the solution pH will have a high concentration of unprotonated (*i.e.*, reactive) species, but the reactivity of these species will be low. In contrast, bases with pK_a values above the solution pH will be highly reactive, but the concentration of unprotonated species will be low. A compromise between reactivity and concentration of reactive species is therefore necessary for

---

[4] The average interatomic distance (*r*) can be calculated using Avogadro's number to convert molarity to atom density. Then, $r = \dfrac{1}{\sqrt[3]{\text{atom density}}}$.

optimal catalytic rates. Indeed, many enzymic active sites contain histidine residues because the pK_a value of its imidazolium side chain [6.3 in a polypeptide; (Tanford, 1962)] is close to the pH at which most enzymes act.

RNase A catalyzes the cleavage and hydrolysis of RNA by general acid/base catalysis, as shown in Figures 3.1A and 3.1B. A pH-rate profile for the cleavage of UpA by wild-type RNase A shows that the pH optimum for this reaction is close to 6.0 (Richards & Wyckoff, 1971; Thompson, 1995). The microscopic pK_a values of His12 and His119 in wild-type RNase A are close to this value (Table 3.3). In contrast, the average of the microscopic pK_a values for His12 and His119 in K7A/R10A/K66A RNase A is 6.5 (at 0.142 M Na^+). Thus, one of the functions of the Lys7, Arg10, and Lys66 side chains is to depress the pK_a values of the active-site histidine residues, and the cleavage of UpA by K7A/R10A/K66A RNase A at pH 6.0 is impaired by a failure to fulfill this role.

The biological function typically ascribed to bovine RNase A is to digest RNA produced by stomach microflora (Barnard, 1969). Nonetheless, the homology of RNase A to cytotoxic ribonucleases (Beintema, 1987; Beintema *et al.*, 1988) suggests that its true physiological role may be more complex. Ribonucleases are cytotoxic because the degradation of cellular RNA renders indecipherable its encoded information (Raines, 1998). RNase A is a better catalyst of transphosphorylation (Figure 3.1A) than hydrolysis (Figure 3.1B). Accordingly, RNA polymers are likely to be the natural susbtrates for RNase A. In Chapter Two, we described the role of the Lys7, Arg10, and Lys66 side chains in binding and cleaving polymeric substrates. Significant Coulombic interactions exist between these cationic side chains and the anionic phosphoryl groups of the substrates. When an RNA strand is bound to RNase A, both the cationic charges in the P0 and P2 subsites and the anionic phosphoryl groups bound in these subsites may form long-range Coulombic interactions with the active-site histidine residues. These repulsive forces and attractive forces should counterbalance, thereby masking the charges on the Lys7, Arg10, and Lys66 side chains with respect to the active-site histidine

residues. The result of this effect would be diminished depression of the His12 and His119 pK_a values when an RNA polymer is bound. The transphosphorylation of dinucleotides and hydrolysis of nucleoside 2′,3′-cyclic phosphates should be affected differently by the P0 and P2 subsites than is the transphosphorylation of polymeric substrates. Indeed, the optimal pH for the transphosphorylation of UpA and hydrolysis of U>p is close to 6.0 (Richards & Wyckoff, 1971; Thompson, 1995) whereas the optimal pH for the transphosphorylation of longer substrates [i.e., (Up)$_4$U>p] is shifted upward by ~1 pH unit (Irie et al., 1984).

RNase A•3′-UMP Complex Formation. Binding of nucleotides to RNase A has been studied as a function of both pH and ionic strength. (Bolen et al., 1971; Flogel et al., 1975; Flogel & Biltonen, 1975; Flogel & Biltonen, 1975). Moreover, the reliability of computer-assisted titration calorimetry for characterizing biological binding reactions was demonstrated by using the binding of 2′-CMP to RNase A as a model (Wiseman et al., 1989). It is the dianionic form of 3′-CMP (and presumably 3′-UMP) that binds to RNase A. This ligand binds to RNase A when both active-site histidine residues are protonated or unprotonated, however there is a 4.3×10^3-fold preference for complex formation with the doubly protonated form of the enzyme (Eftink et al., 1983). At physiological pH, His12 and His119 in RNase A are not fully protonated, prompting a description of complex formation that involves protonation of these residues (Flogel et al., 1975; Flogel & Biltonen, 1975; Flogel & Biltonen, 1975; Karpeisky & Yakovlev, 1981). This type of mechanism, called "proton linkage" because proton binding is linked to ligand binding, is common in protein binding reactions. [For examples, see: (Mauk et al., 1991; Raman et al., 1995).] The increase in the pK_a values of His12 and His119 upon binding 3′-UMP or 3′-CMP (Meadows et al., 1969; Haar et al., 1974) is consistent with a proton linkage mechanism for RNase A•nucleotide complex formation.

The positive charges of the Lys7, Arg10, and Lys66 side chains all reside more than 8.2 Å from either active-site histidine residue [pdb entry 1rph; (Zegers et al., 1994)]. Yet, the binding

of 3′-UMP, a nucleotide bound to the RNase A active site but not the P0 or P2 subsites, is weakened dramatically upon replacement of these residues with alanine (Table 3.4). The relative free energies for the protein – 3′-UMP interaction are shown in Figure 3.10.

On the right side of Figure 3.10, we depict a constant free energy for the protein•3′-UMP complexes at low-salt (0.018 M Na⁺) and high-salt (0.142 M Na⁺) solution conditions. This depiction is based on the work of Eftink and Biltonen (1983), who examined the hydrolysis of cytidine cyclic 2′,3′-phosphate in detail and concluded that when a substrate is bound to the active site of an enzyme, it is relatively impervious to the ionic strength or dielectric constant of the surrounding solution. In the RNase A•3′-UMP complex, the cationic P0 and P2 subsites can interact via long-range Coulombic interactions with both the cationic histidine residues and the anionic nucleotide. These repulsive forces and attractive forces should be of nearly equal, but opposite, magnitude, negating the effect of these subsites. Likewise, salt effects on the free energy of the protein•3′-UMP complexes should be minimal. Thus, we depict all of the protein•3′-UMP complexes at the same free energy.

On the left side of Figure 3.10, we depict the free proteins at varying energy levels. The four free energy levels were derived from the binding data listed in Table 3.4. These levels are consistent with the "entatic" state of each protein in a particular solution condition. Enzymatic catalysis was once described as resulting from the destabilization of the free enzyme (Vallee & Williams, 1968; Williams, 1971) rather than the stabilization of the transition state that occurs along the reaction pathway. In each of these scenarios, enzymes lower the activation barrier of the reaction, but by different means. In the former scenario, enzymic active sites are viewed as tense or entatic—poised for catalysis even in the absence of substrate. More entatic enzymes are better catalysts. Although the latter description of enzymatic catalysis is now accepted more widely (Jencks, 1987), the former description provides a reasonable framework with which to describe our binding data.

Wild-type RNase A in a low-salt solution has a highly cationic active-site cleft. This protein and this solution condition yield the most entatic state examined here. As listed in Table 3.3 and described above, the pK_a values of His12 and His119 are most depressed in the wild-type protein at low salt because charge repulsion in the active site is greatest. By comparison, K7A/R10A/K66A RNase A in a high-salt solution has a much less cationic active site. The pK_a values of His12 and His119 in this variant (at high salt) is most similar to that of an imidazolium side chain in a polypeptide. Wild-type RNase A at high salt and K7A/R10A/K66A RNase A at low salt have intermediate entasis.

Thermodynamic Basis for Complex Formation. A detailed description of RNase A•3′-CMP complex formation by Biltonen and co-workers has yielded much information about the thermodynamic basis for the binding of nucleotides to RNase A (Flogel *et al.*, 1975; Flogel & Biltonen, 1975; Flogel & Biltonen, 1975). Their work and ours are consistent with the following picture. The enthalpic component of the binding free energy is derived primarily from favorable van der Waals interactions and hydrogen bonds between the base of the bound nucleotide and the B1 subsite of RNase A and from the protonation of His12 and His119. As mentioned above, the dianionic nucleotide has a large preference for binding RNase A when both His12 and His119 are in their protonated states. Although the protonation of histidine residues is favored enthalpically [$\Delta H^{\circ}_{protonation}$ = −6.3 kcal/mol for a histidine residue (Shiao & Sturtevant, 1976)], such protonation is disfavored entropically. The magnitude of the enthalpic component of the binding free energy is pH-dependent, being larger at low pH. The entropic contribution to the binding free energy is a compilation of both favorable and unfavorable terms. Attractive Coulombic interactions between the protonated histidine residues in the active site and the bound nucleotide is entropically favorable because of the release of ions or water molecules bound to the enzymic active site. Yet, restricting the

conformational freedom of the nucleotide about the glycosidic bond upon binding is entropically unfavorable.

Conclusions. ^{1}H NMR spectroscopy and isothermal titration calorimetry coupled with X-ray diffraction analyses of K7A/R10A/K66A RNase A and the K7A/R10A/K66A RNase A•3'-UMP complex has enabled us to study the effect of the Lys7, Arg10, and Lys66 side chains on the active site of RNase A. The increased pK_a values of His12 and His119 upon replacing Lys7, Arg10, and Lys66 with alanine residues and the subsequent effects on the kinetics of UpA cleavage and the thermodynamics of 3'-UMP binding suggests that Lys7, Arg10, and Lys66 affect the enzymic active site through long-range Coulombic interactions. We conclude that long-range Coulombic interactions, such as those observed in RNase A, may be a common feature of enzymatic catalysis.

3.6 ACKNOWLEDGEMENT

Table 3.1: X-Ray Diffraction Analysis Statistics

Crystal Data	K7A/R10A/K66A RNase A	K7A/R10A/K66A RNase A + 3′-UMP
Space group	P3$_2$21	P3$_2$21
Cell dimensions (Å)	a = 68.15 ± 0.01	a = 69.62 ± 0.01
	b = 68.15 ± 0.01	b = 69.62 ± 0.01
	c = 65.51 ± 0.02	c = 66.98 ± 0.02
Protein molecules/unit cell	6	6
Crystallization conditions	PEG 4000 (36% w/v), sodium acetate buffer, pH 4.5	PEG 4000 (36% w/v), sodium acetate buffer, pH 4.5
Data collection statistics		
Resolution (Å)	2.0	2.1
No. of measured reflections	33804	33552
No. of unique reflections	14929	14210
Average redundancy	2.3	2.4
Average I/σ	20.1	19.8
Completeness (30 − 2.0 Å) (%)	91	88
Completeness high resolution shell (%)	(2.1 − 2.0 Å) 84	(2.2 − 2.1 Å) 88
R_{sym}[a]	0.029	0.026
R_{sym} high resolution shell	(2.1 − 2.0 Å) 0.171	(2.2 − 2.1 Å) 0.122
Final refinement statistics		
RNase A atoms	937	941
3′-UMP atoms	—	21
Solvent atoms	84	94
R-factor[b]	(30 − 2.0 Å) 0.174	(30 − 2.1 Å) 0.168
RMS deviation from ideal geometry		
Bond distances (Å)	0.010	0.011
Bond angles (°)	2.2	2.2
Average B-factors (Å^2)		
Main-chain atoms	37.8	36.7
Side-chain + solvent atoms	42.6	40.5
3′-UMP	—	40.0

[a] $R_{sym} = \sum_{hkl} |I - <I>| / \sum_{hkl} I$, where I = observed intensity and $<I>$ = average intensity obtained from multiple observations of symmetry related reflections.

[b] $R = \sum_{hkl} |F_o - F_c| / \sum_{hkl} |F_o|$, where F_o and F_c are the observed and calculated structure factors, respectively.

Table 3.2: Steady-State Kinetic Parameters for the Cleavage of UpA by Wild-Type RNase A and K7A/R10A/K66A RNase A[a]

RNase A	k_{cat} (s⁻¹)	K_m (mM)	k_{cat}/K_m (10⁶ M⁻¹s⁻¹)
Wild-Type	347 ± 40	0.20 ± 0.06	1.7 ± 0.3
K7A/R10A/K66A	70 ± 9	0.39 ± 0.10	0.18 ± 0.03

[a] Data were obtained at 25 °C in 0.10 M MES-NaOH buffer, pH 6.0, containing NaCl (0.10 M).

Table 3.3: Microscopic pK_a Values and Chemical Shifts from the Analysis of the pH Dependence of the Chemical Shifts of the $^1H_{\epsilon 1}$ Nuclei of His12, His119, and His105 in Wild-Type RNase A and K7A/R10A/K66A RNase A[a]

Residue		Wild-Type RNase A		K7A/R10A/K66A RNase A	
		0.018 M	0.142 M	0.018 M	0.142 M
His12[b]	pK_0	4 ± 1	4.0 ± 0.8	4 ± 1	4.3 ± 0.4
	pK_1	5.3 ± 0.3	5.87 ± 0.05	5.6 ± 0.1	6.15 ± 0.07
	pK_2	5.67 ± 0.09	6.18 ± 0.04	6.4 ± 0.1	6.78 ± 0.08
	δ_{0H+}[c]	9.1 ± 0.3	9.01 ± 0.06	9.1 ± 0.2	9.07 ± 0.05
	δ_{AH+}	8.8 ± 0.3	8.87 ± 0.04	8.8 ± 0.1	8.77 ± 0.06
	δ_A	7.65 ± 0.01	7.65 ± 0.01	7.67 ± 0.03	7.67 ± 0.03
His119[b]	pK_1	5.5 ± 0.2	6.03 ± 0.05	5.9 ± 0.1	6.28 ± 0.04
	pK_2	5.92 ± 0.06	6.34 ± 0.04	6.71 ± 0.07	6.91 ± 0.06
	δ_{AH+}	8.80 ± 0.02	8.80 ± 0.02	8.78 ± 0.03	8.78 ± 0.01
	δ_A	7.74 ± 0.02	7.75 ± 0.02	7.73 ± 0.03	7.72 ± 0.02
His105	pK_a	6.70 ± 0.02	6.82 ± 0.03	6.80 ± 0.02	6.81 ± 0.01
	δ_{AH+}	8.74 ± 0.01	8.74 ± 0.01	8.75 ± 0.01	8.75 ± 0.00
	δ_A	7.69 ± 0.01	7.68 ± 0.01	7.72 ± 0.01	7.70 ± 0.01

[a] Data were obtained on a Bruker DMX 500 MHz NMR spectrometer at 25 °C. Solutions contained protein (0.56 mM), NaCl (0.018 M or 0.142 M), and DSS (0.5 mM). Values were determined by fitting the experimental data to eq 3.1 for His105, eq 3.2 for His119, and eq 3.3 for His12. Errors were determined by a nonlinear least squares fit of the data to eqs 3.1 – 3.3. Chemical shift values are in parts per million.

[b] Microscopic pK_a values are reported for His12 and His119.

[c] The value for δ_0 was defined to be 8.86 (Quirk, 1996).

Table 3.4: Thermodynamic Parameters for the Binding of 3′-UMP to Wild-Type RNase A and

K7A/R10A/K66A RNase A[a]

RNase A	[Na⁺] (M)	n	K_d (10^{-6} M)	$\Delta G°$ (kcal/mol)	$\Delta H°$ (kcal/mol)	$T\Delta S°$ (kcal/mol)
Wild-Type	0.018[b]	0.931 ± 0.005	9.7 ± 0.3	−7.0 ± 0.1	−13.8 ± 0.1	−6.8 ± 0.1
Wild-Type	0.142[c]	0.949 ± 0.005	54 ± 1	−6.0 ± 0.1	−11.8 ± 0.1	−5.8 ± 0.1
K7A/R10A/K66A	0.018	1.00 ± 0.02	47 ± 2	−6.1 ± 0.1	−10.1 ± 0.3	−4.1 ± 0.3
K7A/R10A/K66A	0.142	0.958 ±0.006	154 ± 2	−5.3 ± 0.1	−9.4 ± 0.1	−4.1 ± 0.1

[a] Data were obtained at 25 °C by isothermal titration calorimetry.

[b] Data at 0.018 M Na⁺ were obtained in 0.020 M MES-NaOH buffer, pH 6.0, containing NaCl (0.010 M).

[c] Data at 0.142 M Na⁺ were obtained in 0.10 M MES-NaOH buffer, pH 6.0, containing NaCl (0.10 M).

Table 3.5: Hydrogen Bonds in the Active Sites of the Wild-Type RNase A•3′-CMP and K7A/R10A/K66A RNase A•3′-UMP Complexes

Hydrogen Bond Donor	Hydrogen Bond Acceptor	K7A/R10A/K66A RNase A•3′-UMP[a]	Wild-Type RNase A•3′-CMP[b]
Thr45 $O_{\gamma 1}$	N3	n.a.[c]	2.9 Å
N3	Thr45 $O_{\gamma 1}$	2.8 Å	n.a.
Thr45 N	O2	2.8 Å	2.7 Å
Thr45 $O_{\gamma 1}$	Asp83 $O_{\delta 1}$	3.0 Å	n.a.
Water (206)	O4	2.9 Å	n.a.
His12 $N_{\epsilon 2}$	O2P	3.0 Å	2.7 Å
His12 $N_{\epsilon 2}$	O2′	3.5 Å	2.9 Å
His119 $N_{\delta 1}$	O3P	2.7 Å	3.2 Å
His119 $N_{\delta 1}$	O1P	3.5 Å	3.1 Å
His119 $N_{\epsilon 2}$	Water (249)	3.2 Å	n.a.
Lys41 N_{ζ}	O2′	2.7 Å	2.7 Å
Lys41 N_{ζ}	Asn44 $O_{\delta 1}$	3.0 Å	2.7 Å
Lys41 N_{ζ}	Gln11 $O_{\epsilon 1}$	2.9 Å	3.1 Å
Phe120 N	O1P	2.8 Å	2.7 Å

[a] Distances were determined by using the three-dimensional structure reported herein (pdb entry 4rsk) and the program MIDAS (Ferrin *et al.*, 1988).

[b] Data taken from (Zegers *et al.*, 1994).

[c] Not applicable.

Table 3.6: Cooperativity Values (c) from the Analysis of the Microscopic pK_a Values for Wild-Type RNase A and K7A/R10A/K66A RNase A[a]

	[Na$^+$]	
RNase A	0.018 M	0.142 M
Wild-Type	0.40	0.49
K7A/R10A/K66A	0.14	0.23
K41A	0.19[b]	nd[c]

[a] These values were determined from the microscopic pK_a values of His12 and His119, where $p(K_2) = p(cK_1)$.

[b] Data from J. M. Messmore, B. M. Fisher, and R. T. Raines (unpublished results).

[c] Not determined.

Figure 3.1   Mechanism of the transphosphorylation (A) and hydrolysis (B) reactions

catalyzed by RNase A. B is His12; A is His119; py is a pyrimidine base

(Findlay *et al.*, 1961; Thompson *et al.*, 1994).

This figure is the same as Figure 1.3.

A

B
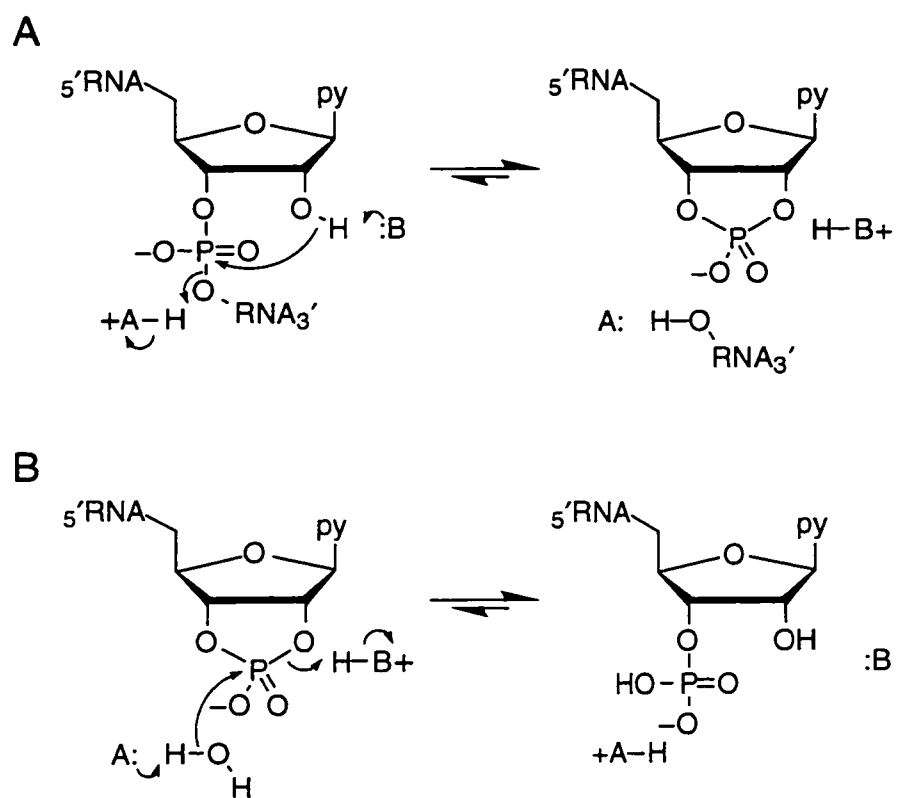
Figure 3.2   Stereoview of the least-squares superposition of residues 2 – 10 of

K7A/R10A/K66A RNase A and of wild-type RNase A [pdb entry 1rph; (Zegers

et al., 1994)]. Residues of the variant protein (thick red lines) are overlayed on

those of the wild-type protein (thin purple lines). Salt bridges between Glu2 and

Arg10 of the wild-type protein are indicated by dashed lines. Water molecules

are also indicated (red spheres). This figure was created with the program

MOLSCRIPT (Kraulis, 1991).
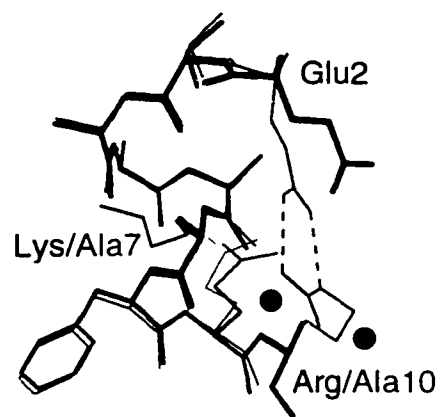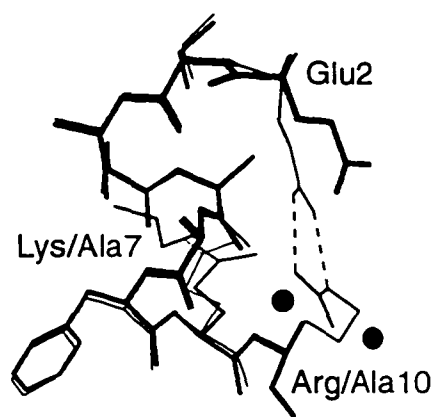
Figure 3.3   Stereoview of the least-squares superposition of the active sites of crystalline

K7A/R10A/K66A RNase A and wild-type RNase A [pdb entry 1rph; (Zegers

et al., 1994)]. The variant protein (thick red lines) has an acetate ion in its active

site. The wild-type protein (thin purple lines) has a sulfate ion in its active site.

Water molecules are depicted for the variant (red spheres) and wild-type (purple

spheres) enzymes. This figure was created with the program MOLSCRIPT

(Kraulis, 1991).

Figure 3.4   Stereoview of the least-squares superposition of the active sites of the

K7A/R10A/K66A RNase A•3'-UMP complex (thick red lines) and the

wild-type RNase A•3'-CMP complex [(thin purple lines); pdb entry 1rpf;

(Zegers *et al.*, 1994)]. Water molecules are depicted for the variant (red

spheres) and wild-type (purple spheres) proteins. This figure was created with

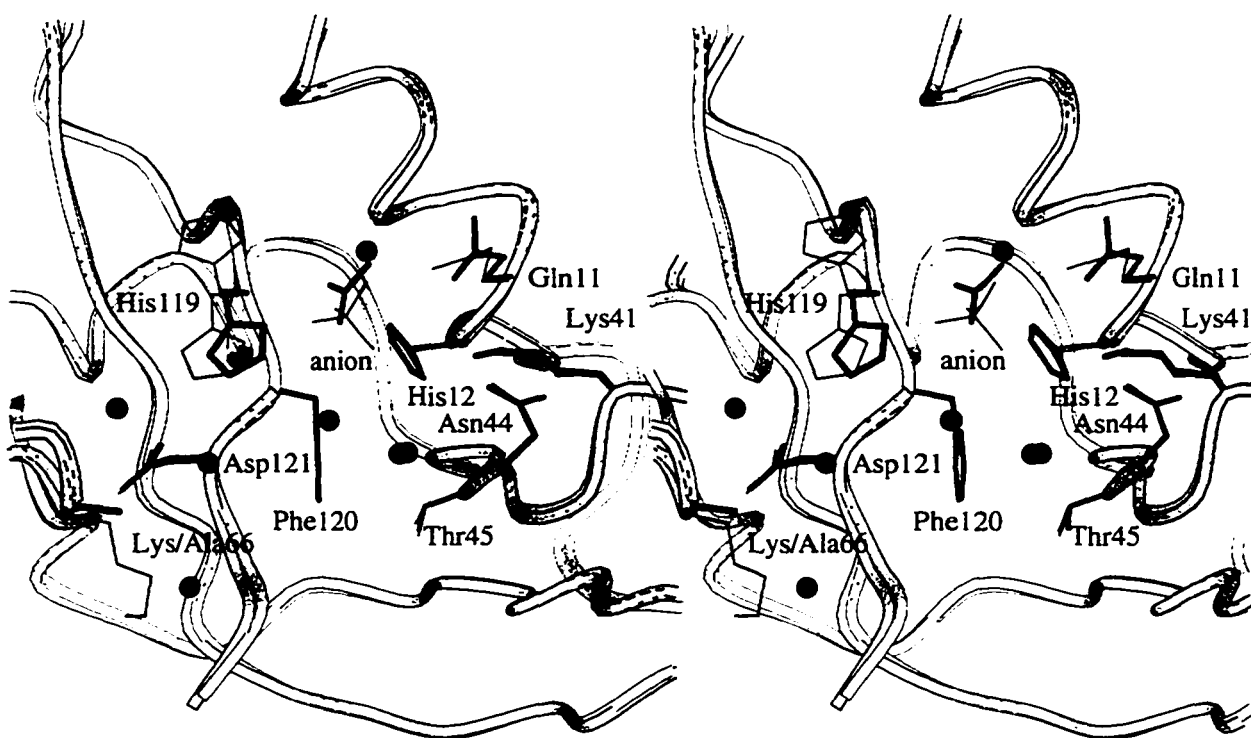the program MOLSCRIPT (Kraulis, 1991).
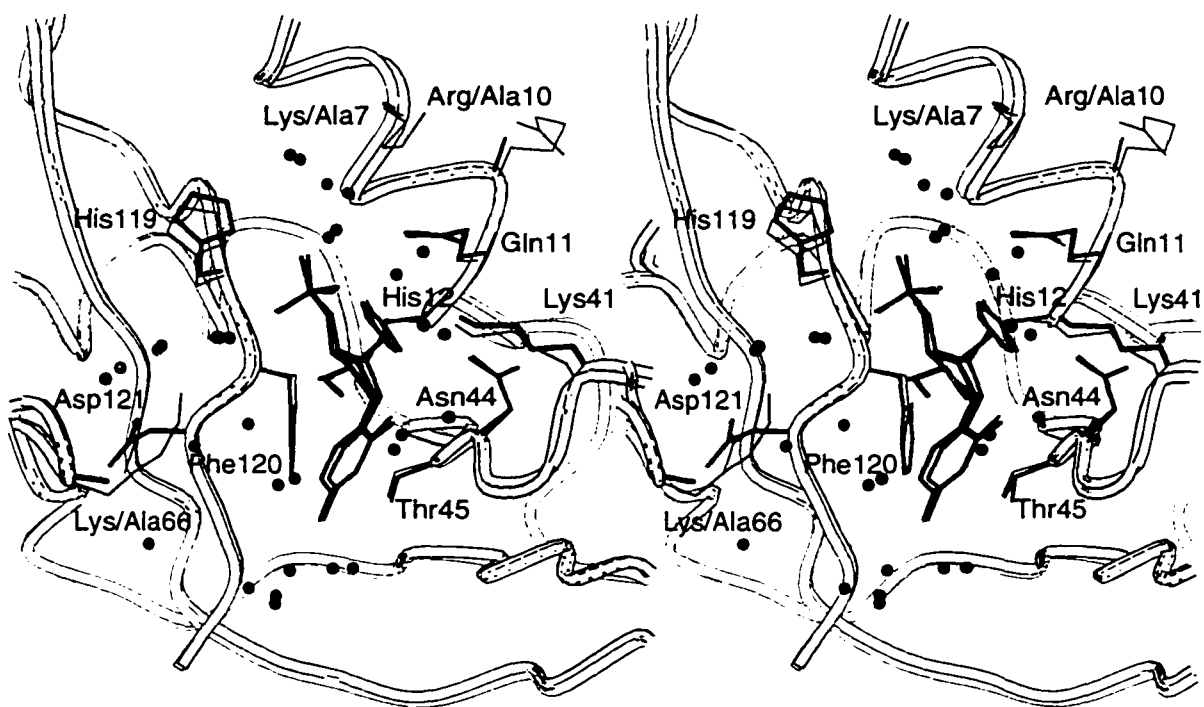
Figure 3.5   The pH dependence of the histidine $^1\text{H}^{\epsilon 1}$ signals of wild-type RNase A and

K7A/R10A/K66A RNase A in D_2O. (A) Wild-type RNase A at

0.018 M Na^+. (B) Wild-type RNase A at 0.142 M Na^+. (C) K7A/R10A/K66A

RNase A at 0.018 M Na^+. (D) K7A/R10A/K66A RNase A at 0.142 M Na^+.

Chemical shifts are shown for all four histidine residues: His12 (●), His119

(O), His105 (■), and His48 (×). Titrations were carried out at 25 °C. The pK_a

values determined from fitting the data to eq 3.1 – 3.3 are listed in Table 3.3.
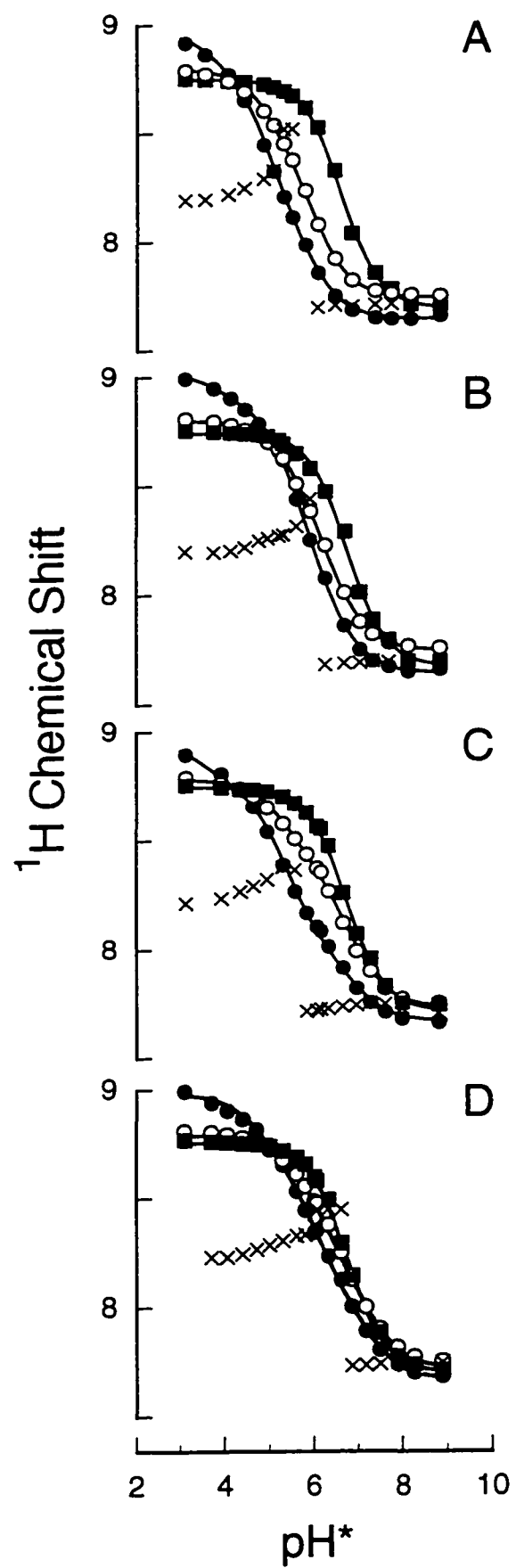
Figure 3.6   Thermograms for the binding of 3'-UMP to wild-type RNase A (A) and

K7A/R10A/K66A RNase A (B) at 0.142 M Na^+. The upper graphs show the

heat released by the protein solutions upon injection of 3'-UMP. The lower

graphs are plots of heat released upon binding versus the molar ratio of 3'-UMP

to RNase A. Binding was measured by isothermal titration calorimetry at 25 °C

in 0.10 M MES-NaOH buffer, pH 6.0, containing NaCl (0.10 M).

A
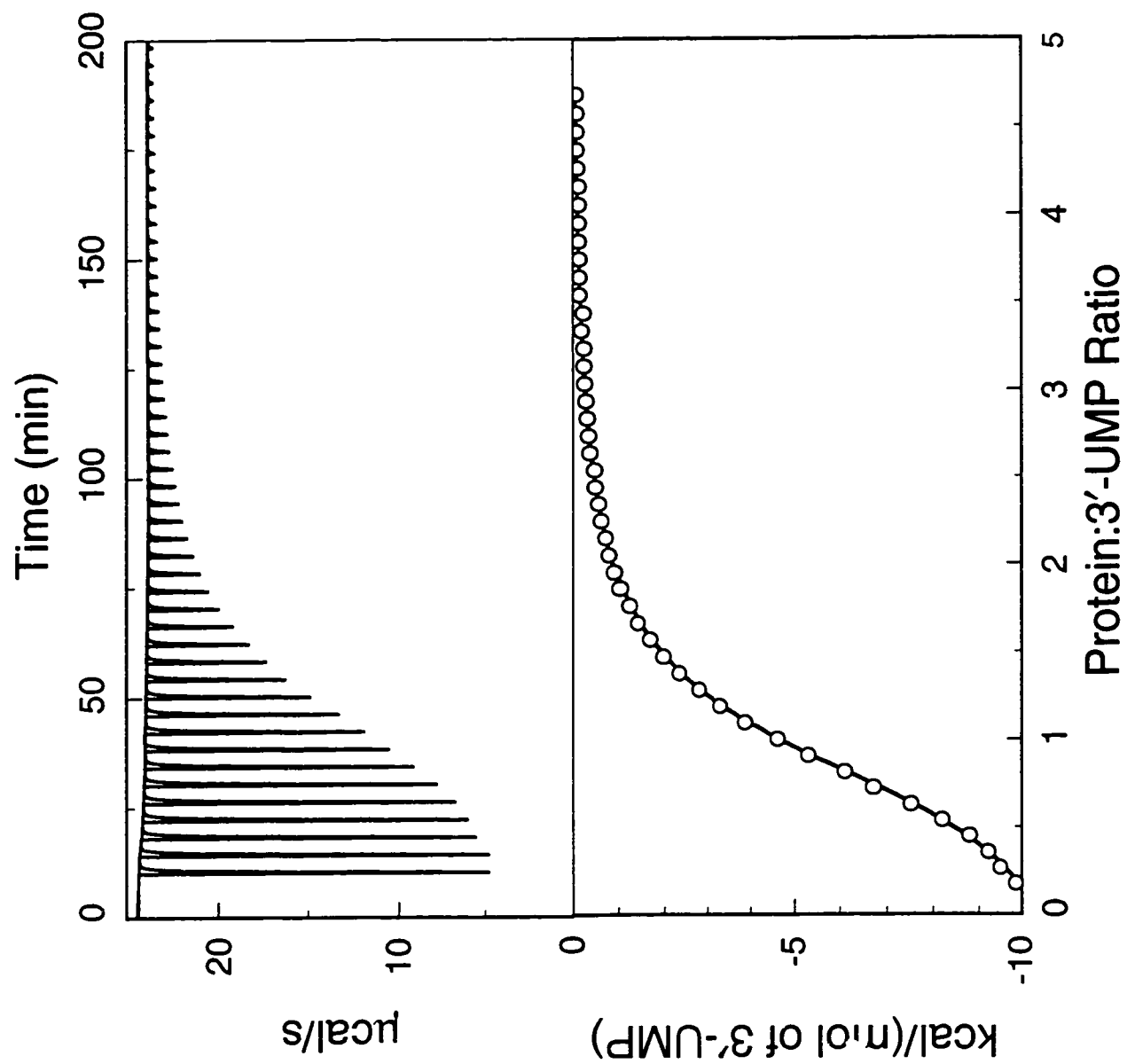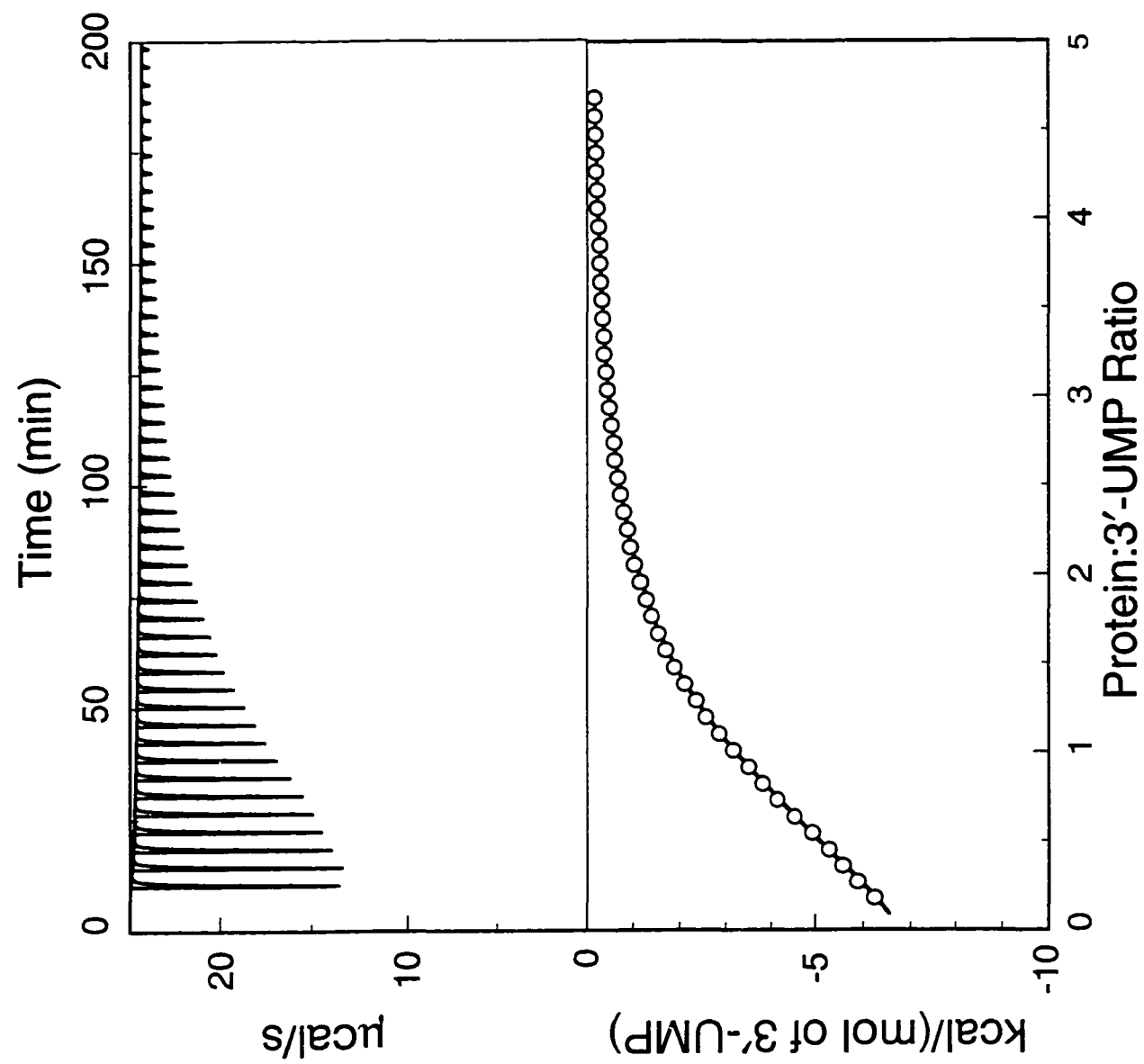
Figure 3.7   Schematic representation of the binding of an RNA fragment to RNase A. The

scissile bond is indicated. B and P refer to base and phosphoryl group binding

subsites, respectively. In each subsite, the amino acid residues that are known or

presumed to be involved in the interaction with RNA are indicated (Raines,

1998).

This figure is the same as Figure 2.2.
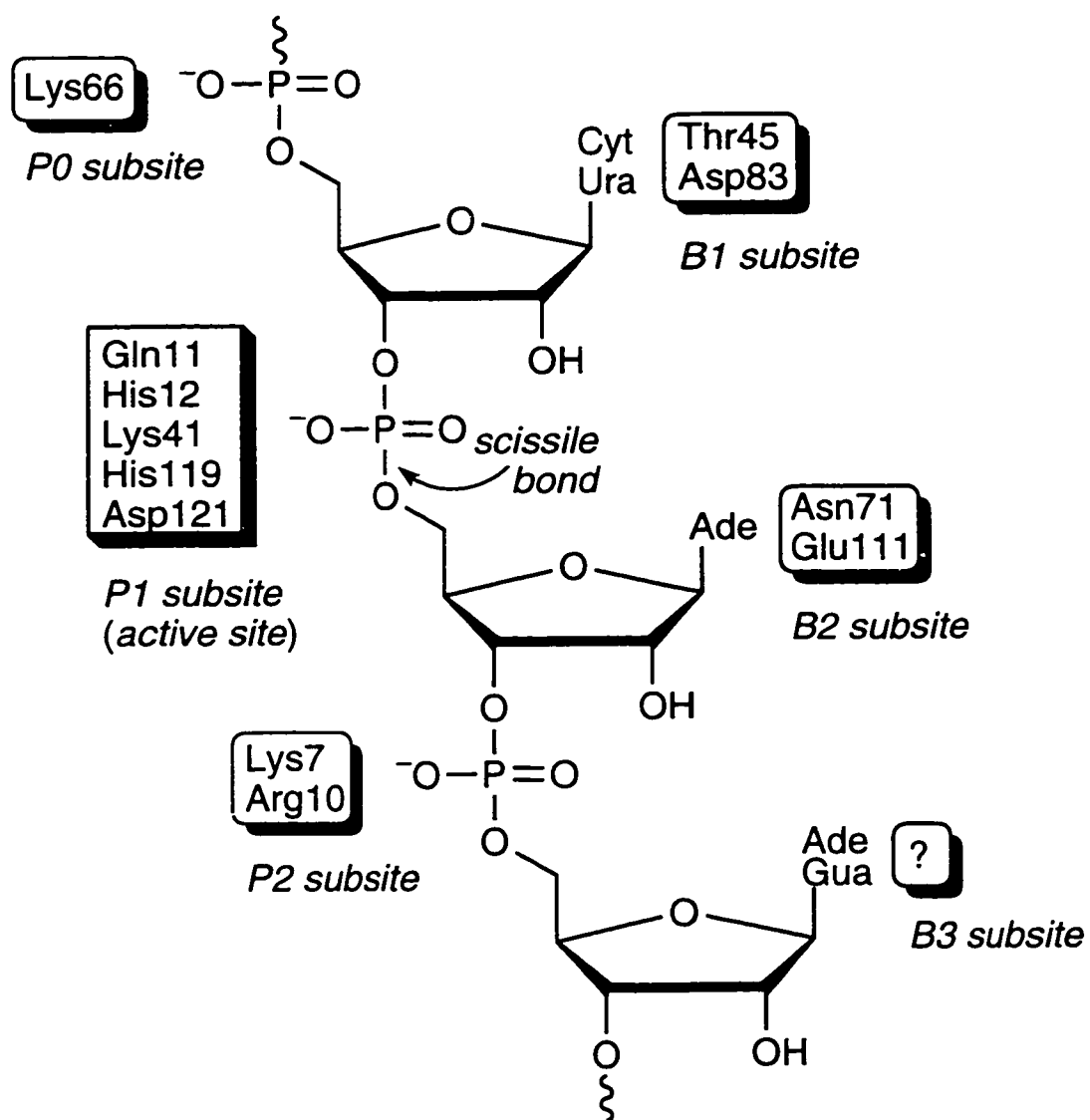
Figure 3.8   Ribbon diagram of wild-type RNase A (A) and electrostatic potential maps of

the surface of wild-type RNase A (B) and K7A/R10A/K66A RNase A (C)

positioned in the same orientation. Blue denotes regions of positive charge and

red denotes regions of negative charge. Charges were calculated for RNase A at

pH 6.0 and 0.142 M Na$^+$, using the pK_a values determined for the active-site

histidine residues using ^{1}H NMR spectroscopy (Table 3.3). The ribbon diagram

was created using the program MOLSCRIPT (Kraulis, 1991). Electrostatic

potential maps were created with the program GRASP (Nicholls *et al.*, 1991)

and atomic coordinates for wild-type RNase A [pdb entry 1rph; (Zegers *et al.*,

1994)] and K7A/R10A/K66A RNase A.
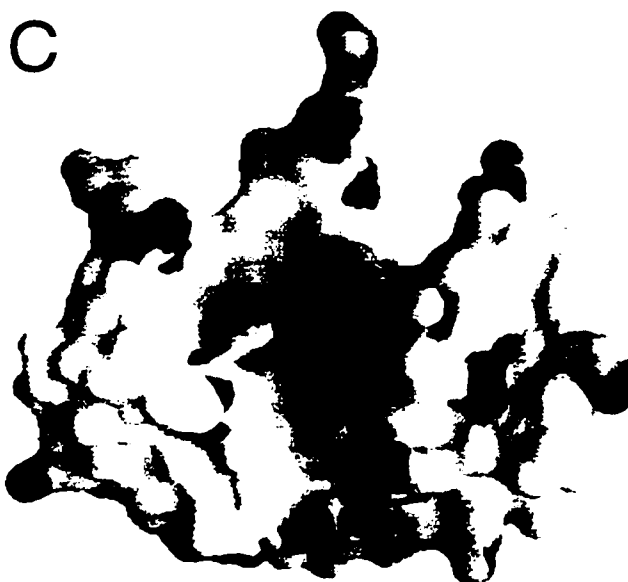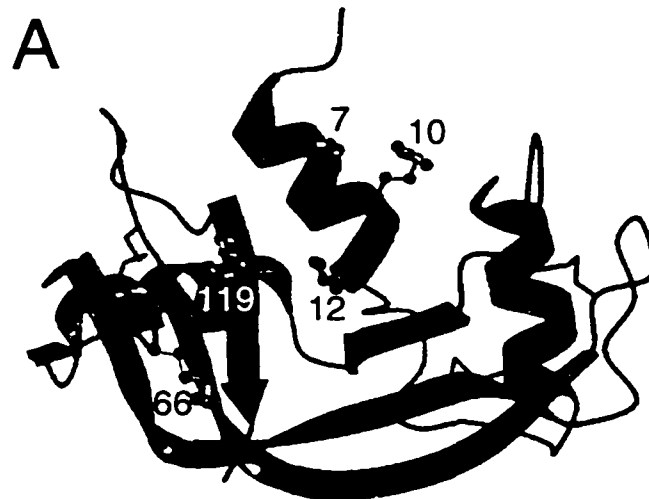
Figure 3.9   Structure of His12, His119, and Lys41 and the P0 and P2 subsites of wild-type

RNase A. The midpoint of the line segment connecting $N_{\delta1}$ of His119 and $N_{\epsilon2}$

of His12 is indicated by a plus sign, and the distances from this point to N_ζ of

Lys7, the midpoint of the line segment connecting $N_{\eta1}$ and $N_{\eta2}$ of Arg10, N_ζ of

Lys66, and N_ζ of Lys41 are shown. Distances were determined by using the

atomic coordinates for wild-type RNase A [pdb entry 1rph; (Zegers *et al.*,

1994)] and the program MIDAS (Ferrin *et al.*, 1988). The reduced radius of

Lys7, Arg10, and Lys66 to the midpoint of line segment connecting $N_{\delta1}$ of

His119 and $N_{\epsilon2}$ of His12 was calculated with eq 3.7 to be $\rho = 5.7$ Å.
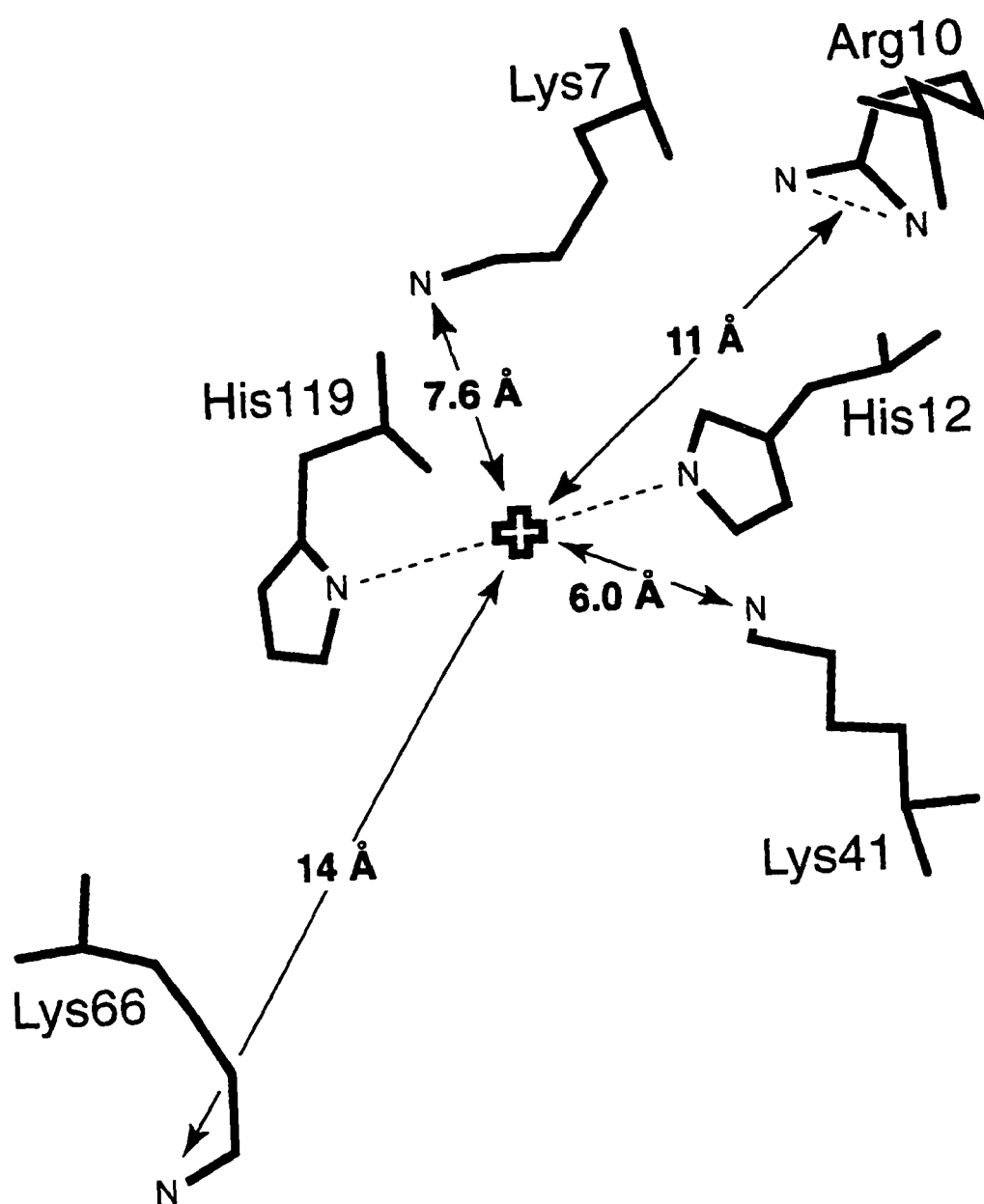
Figure 3.10   Free energy profile for the binding of wild-type RNase A and K7A/R10A/K66A

RNase A to uridine 3′-phosphate at low and high salt concentrations. Free

energies were calculated for complex formation at 25 °C and a standard state of

1 M with the equation $\Delta G° = -RT\ln K_a$, where K_a for RNase A•3′-UMP

complex formation was determined by isothermal titration calorimetry. Solid

lines (—) are for experiments at 0.018 M Na⁺; dashed lines (---) are for

experiments at 0.142 M Na⁺. The closed plus sign (+) represents the positive

charges in the P0 and P2 subsites in wild-type RNase A and the circles (O)

represent the neutral residues in these subsites in K7A/R10A/K66A RNase A.

The open plus sign (+) represents the positive charges on His12 and His119 in

the active site. The minus sign (–) represents the anionic nucleotide 3′-UMP.
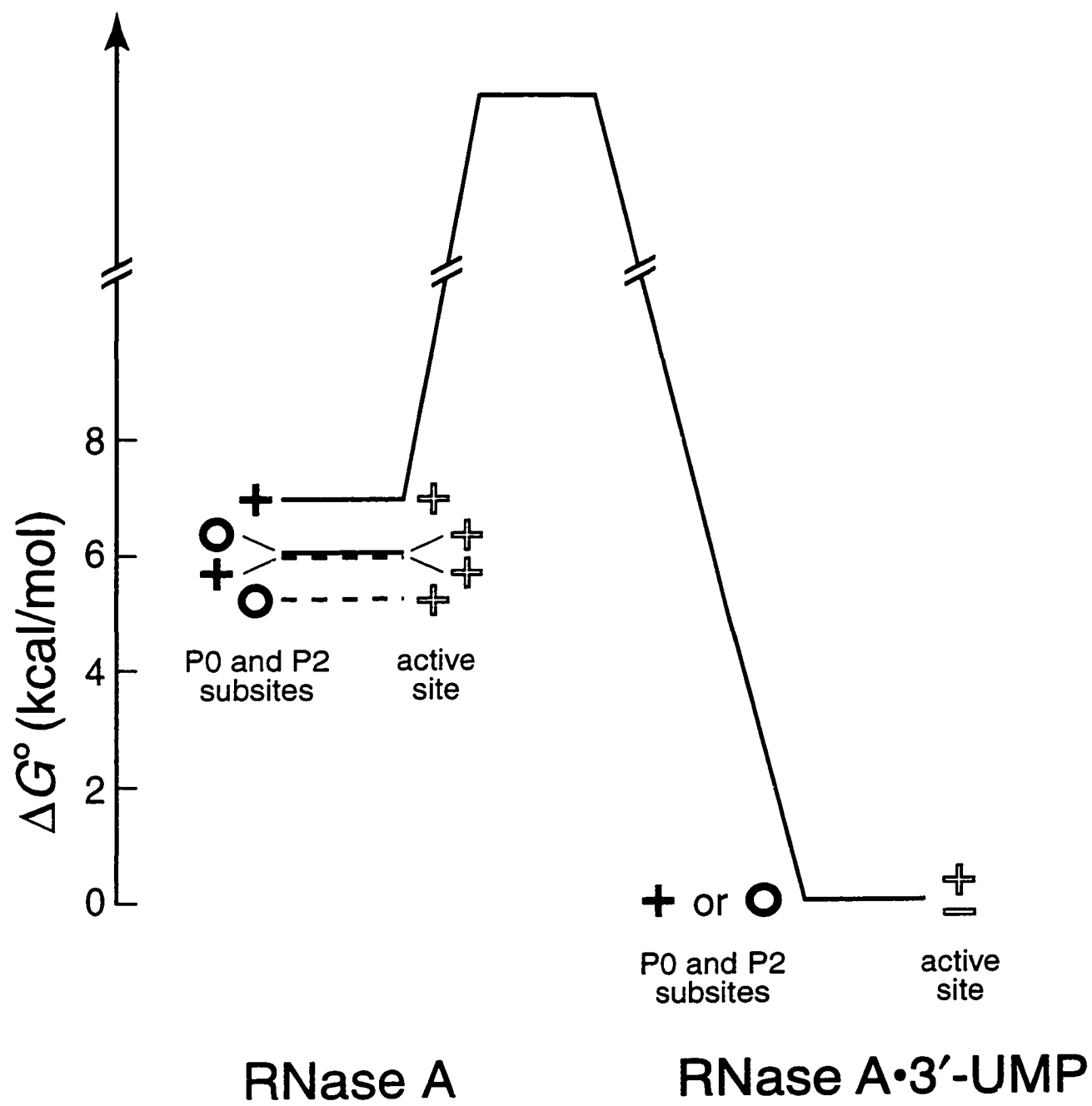
Chapter Four

A New Remote Subsite in Ribonuclease A

This chapter is in preparation for submission to *J. Biol. Chem.* as a communication:

Fisher, B. M., Grilley, J. E., and Raines, R. T. A new remote subsite in ribonuclease A.

4.1 ABSTRACT: The interactions between bovine pancreatic ribonuclease A (RNase A) and its RNA substrate extend beyond the scissile bond. Enzymic subsites interact with the bases and the phosphoryl groups of the bound substrate. We evaluated three cationic residues that reside nearest to subsites characterized previously, Arg39, Arg85 and Lys104, for their abilities to interact with a bound nucleic acid. Each residue was replaced with alanine, and the resulting enzymes were assayed as catalysts of poly(cytidylic acid) [poly(C)] cleavage. The values of K_m and k_{cat}/K_m for poly(C) cleavage were affected dramatically by replacement of Arg85, but not Arg39 or Lys104, with alanine. The K_m value for poly(C) cleavage by R85A RNase A was 15-fold higher than that of wild-type RNase A and the k_{cat}/K_m value was 10-fold lower. Results from binding assays with oligonucleotides of varying length were in accord with those from kinetic assays. Wild-type RNase A and R85A RNase A bind a trinucleotide with similar affinity (23 μM), but bind a tetranucleotide with different affinities (3 μM and 9.6 μM, respectively). Together, these data suggest that the side chain of Arg85 interacts specifically with a bound nucleic acid. We therefore propose that Arg85 comprises a new distal subsite in RNase A, the P(-1) subsite.

4.2 INTRODUCTION

Enzymes confer large rate enhancements over the corresponding uncatalyzed reactions. These rate enhancements can be as high as 10^{17}, as demonstrated for the decarboxylation of orotic acid by ornithine monophosphate decarboxylase (Radzicka & Wolfenden, 1995) or the cleavage of the phosphorus–oxygen bond in a nucleic acid by staphylococcal nuclease (Wolfenden *et al.*, 1998). The efficiency of enzymatic catalysts is a source of continued interest and inspiration as scientists strive to design new catalysts.

A distinguishing characteristic of enzymes is that they bind their substrates specifically with binding energies that are very large (Fersht, 1985; Jencks, 1987). Large binding energies are necessary to compensate for the loss of translational and rotational entropy, and for any destabilization of the substrate required to reach the transition state (Page, 1977; Jencks, 1981). Multiple, distinct contacts between an enzyme and substrate may provide much of this required binding energy.

Many enzymes that cleave polymeric substrates have subsites that interact with individual groups on the substrate. These subsites may enhance binding energy and substrate specificity simultaneously. For example, individual members of the serine protease family differ in their substrate specificity according to the enzymic residue residing in the S1′ subsite (Kurth *et al.*, 1997). Other proteases, including retroviral proteases (Dunn *et al.*, 1994) and elastases (Thompson, 1974), lysozymes (Kuhara *et al.*, 1982; Malcolm *et al.*, 1989), and nucleases (Chuang *et al.*, 1994; Steyaert, 1997) also have multiple subsites that enhance binding of both the ground state and transition state during catalysis.

Bovine pancreatic ribonuclease A (RNase A; EC 3.1.27.5) is a classic model for revealing the physical, chemical, and biological properties of enzymes. [For reviews, see: (Richards & Wyckoff, 1971; Eftink & Biltonen, 1987; Raines, 1998).] A monomeric

polypeptide of molecular mass 13.7 kDa, RNase A is an endoribonuclease that catalyzes RNA cleavage on the 3' side of pyrimidine residues. Despite over 60 years of study devoted to RNase A, the number of enzymic sites that interact with a polymeric RNA substrate cannot be stated with certainty.

RNase A binds to an RNA substrate binds RNase A in a cleft. The cleft contains both side chains that interact specifically with bases (B1, B2, and B3), and cationic sites (P0, P1, and P2) that interact with phosphoryl groups. The specificity of RNase A for cleavage after pyrimidine bases is in part due to exclusion of larger purine bases from the B1 subsite (delCardayré & Raines, 1994). The B2 and B3 subsites preferentially bind purine bases. His12, His119, and Lys41, which together comprise the P1 subsite, are the residues most central to the catalytic function of the enzyme (Nogués et al., 1995). The amino acid residues that comprise the P0 (Lys66) and P2 (Lys7 and Arg10) subsites increase the affinity with which the substrate binds to the enzyme, participating indirectly in the cleavage and hydrolysis reactions [Chapters Two and Three; (Boix et al., 1994)].

Several lines of evidence suggest the existence of additional RNase A binding sites beyond those characterized previously. Three-dimensional structures derived from X-ray diffraction analyses reveal a line of cationic residues stretching well-beyond the active site (McPherson et al., 1986). In addition, cation titration suggests that RNase A can occlude eleven nucleotides of a single-stranded nucleic acid (Jensen & von Hippel, 1976) and that binding involves seven Coulombic interactions (Record et al., 1976).

In this study, we probed for additional RNase A subsites that interact with the bound nucleic acid. Specifically, we examined the roles of Arg39, Arg85, and Lys104 in substrate binding. The importance of these cationic residues was investigated by replacing each with alanine. The kinetic parameters for the cleavage of poly(cytidylic acid) [poly(C)] by each RNase A variant were determined and the values were compared to those of the wild-type

enzyme. Based on the altered kinetic parameters for poly(C) cleavage by R85A RNase A, we investigated directly the role of Arg85 in substrate binding using fluorescence anisotropy assays. DNA acts as a useful model for studying RNase A•RNA complex formation because RNase A binds to single-stranded DNA, but does not cleave this nucleic acid (Walz, 1971). By comparing the affinity of a trinucleotide versus a tetranucleotide for wild-type RNase A and R85A RNase A, we demonstrate directly that Arg85 interacts with a 5′-phosphonucleoside on the bound nucleic acid. Therefore, Arg85 defines the enzymic P(-1) subsite.

4.3 EXPERIMENTAL PROCEDURES

Materials. Escherichia coli strain BL21(DE3) (F⁻ ompT r_B-m_B-) was from Novagen (Madison, WI). *E. coli* strain CJ236 was from Bio-Rad (Richmond, CA). *E. coli* strain DH5α was from Gibco BRL (Grand Island, NY). All enzymes for the manipulation of recombinant DNA were from either Promega (Madison, WI) or New England Biolabs (Beverly, MA). Purified, de-salted oligonucleotides for site-directed mutagenesis were obtained from Integrated DNA Technologies (Coralville, IA). DNA was sequenced with an ABI 373 Automated Sequencer using an ABI PRISM Dye Terminator Cycle Sequencing Ready Reaction Kit, AmpliTaq DNA polymerase, FS (Foster City, CA), and a PTC-100 Programmable Thermo Controller from MJ Research (Watertown, MA). Bacto tryptone, Bacto peptone, and Bacto agar were from Difco (Detroit, MI). Bacterial terrific broth [TB; (Tartof, 1992)] contained (in 1 L) Bacto tryptone (12 g), Bacto yeast extract (24 g), glycerol (4 mL), KH_2PO_4 (2.31 g), and K_2HPO_4 (12.54 g). All media were prepared in distilled, deionized water and autoclaved. Isopropyl-1-thio-β-D-galactopyranoside (IPTG) was from Gold Biotechnology (St. Louis, MO). Poly(C) was from Midland Certified Reagent (Midland, TX) and was precipitated from

aqueous ethanol (70% v/v) before use. Gel-purified oligonucleotides used for fluorescence anisotropy experiments were obtained from Promega. 2-(N-Morpholino)ethanesulfonic acid (MES), obtained as the free acid, was from ICN Biomedicals (Aurora, OH). Sigmacote was from Sigma (St. Louis, MO). All other chemicals and reagents were of commercial grade or better and used without further purification.

General Methods. Ultraviolet and visible absorbance measurements were made with a Cary Model 3 spectrophotometer equipped with a Cary temperature controller from Varian (Sugar Land, TX). RNase A concentrations were determined by assuming that $\varepsilon^{0.1\%} = 0.72$ at 277.5 nm (Sela *et al.*, 1957). pH was measured with a Beckman pH meter fitted with a Corning electrode, calibrated at room temperature with standard buffers from Fisher (Chicago, IL).

Site-Directed Mutagenesis. pBXR is a plasmid that directs the expression of wild-type RNase A in *E. coli* (delCardayré *et al.*, 1995). Oligonucleotide-mediated site-directed mutagenesis (Kunkel *et al.*, 1987) was performed on single-stranded pBXR isolated from *E. coli* strain CJ236. To produce the DNA coding for R39A RNase A, the CGA codon for Arg39 was replaced with the GCA codon for alanine (reverse complement in bold) using the oligonucleotide JG1: CACTGGCTT<u>**GCATGC**</u>TTTGGTCAGG, which also incorporates a translationally silent *Sph*I site (underlined). The R85A variant was produced by replacing the CGT codon for Arg85 with the GCG codon for alanine (reverse complement in bold) using the oligonucleotide JG4: GGGGTACTTGGA<u>**GGATCC**</u>GGTCTCCGCGCAGTCGGTG, which also incorporates a translationally silent *Bam*H1 site (underlined). The K104A variant was produced by replacing the AAA codon for Lys104 with the GCC codon for alanine (reverse complement in bold) using the oligonucleotide JG3: GTTTCCCTC<u>**GCATGC**</u>CACATTGATGTG**GGC**ATTCGCCTG, which also incorporates a translationally silent *Sph*I site (underlined). Mutagenesis reactions were transformed into

competent DH5α cells, and plasmid DNA from the isolated transformants was analyzed by sequencing.

Protein Production and Purification. Wild-type RNase A and the R39A, R85A, and K104A variants were produced in *E. coli* strain BL21(DE3) as described in Chapter Two. Briefly, fermenter-scale growths (12 L) of *E. coli* strain BL21(DE3) carrying the plasmids encoding the wild-type or variant proteins were grown in TB to late log phase (OD = 2.0 at 600 nm), and protein production was induced by the addition of IPTG (to 0.5 mM). After 3 h of growth, cells were harvested by centrifugation and broken by passage three times through a French pressure cell. Proteins were solubilized from inclusion bodies, denatured and reduced with DTT, folded (and oxidized) *in vitro*, concentrated by ultrafiltration, and purified by loading on a Pharmacia FPLC HiLoad™ 26/60 Superdex 75 gel filtration column. Fractions corresponding to monomeric protein were pooled and loaded onto an FPLC mono-S cation exchange column. Protein fractions were pooled and characterized. Peak symmetry on chromatography elution profiles, SDS-polyacrylamide gel electrophoresis, and A_{280}/A_{260} ratios greater than 1.8 indicated that the proteins were > 99% pure. Purified proteins were dialyzed exhaustively against H_2O to remove buffer salts, lyophilized, and stored at −70 °C.

Thermal Denaturation. The stabilities of the wild-type and variant proteins were determined by thermal denaturation studies as described elsewhere (Eberhardt *et al.*, 1996). Briefly, the six tyrosine residues of RNase A become solvent exposed upon protein denaturation, thereby decreasing the molar absorptivity at 287 nm. The thermal stability (as indicated by T_m, the midpoint of the thermal denaturation curve) of RNase A can be assessed by monitoring the change in absorbance at 287 nm with temperature, and fitting the data to a two-state model for denaturation (Pace *et al.*, 1989; delCardayré *et al.*, 1994; Eberhardt *et al.*, 1996).

Steady-State Kinetic Analysis. Spectrophotometric assays were used to determine the steady-state kinetic parameters for the cleavage of poly(C). The cleavage of poly(C) was monitored by following a change in ultraviolet hyperchromicity of cytidine. The $\Delta\varepsilon$ for this reaction, calculated from the difference in molar absorptivity of the polymeric substrate and the mononucleotide cyclic phosphate product, is 2380 $M^{-1}cm^{-1}$ at 250 nm (delCardayré & Raines, 1994). Assays were performed at 25 °C in 0.10 M MES-NaOH buffer, pH 6.0, containing NaCl (0.10 M). The values of k_{cat}, K_m, and k_{cat}/K_m were determined from initial velocity data using the program HYPERO (Cleland, 1979).

Fluorescence Anisotropy. Fluorescence anisotropy assays can be used to quantitate the binding affinity between two molecules. These assays are based on the increase in the rotational correlation time of a fluorophore upon binding of a fluorophore-labeled oligonucleotide to a protein (LeTilly & Royer, 1993). The protein•oligonucleotide complex, due to its increased molecular volume, tumbles more slowly than does the free, labeled oligonucleotide. The ensuing reduction in the rotational correlation time of the fluorophore causes an increase in anisotropy, allowing binding to be monitored in solution (Wittmayer & Raines, 1996).

We used fluorescence anisotropy to assay the binding of Fl~d(AUAA) and Fl~d(UAA) to wild-type RNase A and the R85A variant. Fluorescein, incorporated during the final coupling step of DNA synthesis, was attached to the 5′ end of the oligonucleotides via a six-carbon spacer. The fluorescein-labeled oligonucleotides were obtained in purified, desalted form from Promega. The oligonucleotide concentrations were determined by assuming that $\varepsilon = 52650$ $M^{-1}cm^{-1}$ at 260 nm for Fl~d(AUAA) and $\varepsilon = 40,400$ $M^{-1}cm^{-1}$ at 260 nm for Fl~d(UAA) (Wallace & Miyada, 1987 626).

Fluorescence anisotropy was measured at room temperature (23 ± 2 °C) on a Beacon Fluorescence Polarization System (Panvera; Madison, WI). Purified oligonucleotides were

dissolved in 0.020 M MES-NaOH buffer, pH 6.0, containing NaCl (0.025 M), to a final

concentration of 2.5 nM. Pure, lyophilized RNase A was dissolved in 1 – 1.5 mL of buffer to

a final concentration of 0.5 mM. The protein solution was divided in half, and each half was

brought to a volume of 1 mL by the addition of either oligonucleotide solution (to 2.5 nM) or

buffer (to make a blank). Silinized glass tubes were used to minimize protein adhesion to the

glass. A blank was necessary to subtract out large background fluorescence intensity from the

concentrated protein solution. Measurements (6 – 8) were taken for each protein concentration,

with each sample measurement preceded by a blank. The sample tube was diluted serially by

removing 0.25 mL of sample and replacing it with 0.25 mL of the oligonucleotide solution to

maintain a constant oligonucleotide concentration. The blank was diluted correspondingly,

except using buffer rather than oligonucleotide solution. The dilutions and data collection were

repeated until the anisotropy value approached that for the free oligomer, typically 30 dilutions.

RNase A concentrations were extrapolated from protein concentrations measured from aliquots

of tubes 1, 4, and 7. DELTA GRAPH 4.0 (DeltaPoint; Monterey, CA) was used to fit the data

to eq 4.1 (Attie & Raines, 1995) by non-linear least squares analysis, which was weighted by

the standard deviation of each reading.

$$A = \frac{\Delta A \cdot [\text{RNase A}]}{K_d + [\text{RNase A}]} + A_{min} \tag{4.1}$$

In eq 4.1, A is the average of the measured fluorescence anisotropy at each protein

concentration, A_{min} is the anisotropy of the unbound oligonucleotide, and ΔA is the anisotropy

at oligonucleotide saturation minus A_{min}. [RNase A] is protein concentration, and K_d is the

equilibrium dissociation constant.

4.4 RESULTS

Rationale for Investigation of the Roles of Arg39, Arg85, and Lys104 in Substrate Binding. An electrostatic surface potential map created from a wild-type RNase A crystalline structure [Brookhaven Protein Data Bank (pdb) entry 1rph; (Zegers *et al.*, 1994)] highlights the cationic cleft in the enzyme that interacts with a bound nucleic acid (Figure 4.1). The active site of the enzyme, comprised of His12, His119, and Lys41 (the P1 subsite) is located in the center of the cleft. The cationic residues that reside closest to the active site are Lys7 and Arg10 (the P2 subsite) to one side and Lys66 (the P0 subsite) to the other side, all three of which have been characterized in detail (Chapters Two and Three). Arg85 and Lys104 are the next closest cationic residues to Lys66, and Arg39 is the closest cationic residue to Lys7 and Arg10. Hence, the roles of these residues were evaluated through site-directed mutagenesis. We substituted an alanine residue for Arg39, Arg85, and Lys104, and assayed the resulting three variant proteins for their abilities to interact with a bound nucleic acid.

Catalysis of Poly(C) Cleavage by RNase A Variants. Steady-state kinetic parameters for the cleavage of poly(C) by wild-type RNase A and the R39A, R85A, and K104A variants are listed in Table 4.1. Also listed in this table are the values of T_m determined for the three variant proteins. These values, which are all similar to that of the wild-type protein, suggest that the tertiary structures of the variant proteins do not differ markedly from that of the wild-type protein. Further, these values indicate that the kinetic parameters determined at 25 °C are indeed those of the native proteins.

Of the three residues investigated in this study, Arg85 has the most dramatic effect on the kinetic parameters for the cleavage of poly(C). The k_{cat} value is similar to that of the wild-type enzyme; however, the K_m value differs dramatically. The K_m value for poly(C) cleavage

by R85A RNase A is > 15-fold higher than that for the wild-type enzyme. The value of k_{cat}/K_m for poly(C) cleavage by R85A RNase A is 10-fold lower than that for the wild-type enzyme.

Replacing Arg39 or Lys104 with alanine has little change on the kinetic parameters for the cleavage of poly(C). The k_{cat}, K_m, and k_{cat}/K_m values for poly(C) cleavage by R39A RNase A are indistinguishable from those of wild-type RNase A. The k_{cat} and K_m values for poly(C) cleavage by K104A RNase A are both twofold lower than those for the wild-type enzyme, and the k_{cat}/K_m value is similar.

Oligonucleotide Binding to Wild-Type RNase A and the R85A Variant. Single-stranded DNA is a useful model to investigate binding (without turnover) to RNase A because it lacks the 2′-hydroxyl group necessary for cleavage by the enzyme (Walz, 1971). The specific interaction between Arg85 and bound DNA was evaluated by fluorescence anisotropy assays. These assays employed two fluorescein-labeled DNA oligonucleotides that differ by only a single 5′-phosphoryl group and adenosine nucleoside. These ligands, Fl~d(UAA) and Fl~d(AUAA), were modeled after d(ATAAG), which forms a complex with known three-dimensional structure (Fontecilla-Camps *et al.*, 1994). The single uridine in these ligands, which binds to RNase A specifically in the B1 subsite, presumably prevents fluorescein from interacting with the enzyme.

The affinity of Fl~d(AUAA) for wild-type RNase A is salt-concentration dependent, with higher affinity at low salt concentrations and lower affinity at high salt concentrations (Chapter Two). Therefore, the binding assays were performed in a solution of lower ionic strength than were the poly(C) cleavage assays to maximize any difference in K_d values.

Binding of Fl~d(UAA) and Fl~d(AUAA) to wild-type RNase A is shown in Figure 4.2A. Binding of Fl~d(UAA) and Fl~d(AUAA) to R85A RNase A is shown in Figure 4.2B. Although the anisotropy values of the bound (A_{max}) and unbound oligomer (A_{min}) varied slightly between experiments, the total change in anisotropy (ΔA) remained constant for

all experiments. This value ($\Delta A = 120$ mA) is consistent with that seen previously for the binding of Fl~d(AUAA) (Chapter Two) and Fl~d(UAA) to wild-type RNase A (Kelemen & Raines, 1997).

As listed in Table 4.2, Fl~d(AUAA) binds to wild-type RNase A to form a complex with a K_d value of 3.0 μM. This value is 8-fold lower than that for the complex of Fl~d(UAA) and wild-type RNase A. This result suggests that there are specific interactions between RNase A and the 5′-phosphoryl group or adenosine on the bound nucleic acid. Fl~d(AUAA) binds to the R85A variant to form a complex with a K_d value of 9.6 μM. This value is 2.4-fold lower than the wild-type RNase A•Fl~d(UAA) complex, again suggesting that RNase A interacts specifically with the 5′-phosphoadenosine. Fl~d(UAA) binds to wild-type RNase A and the R85A variant with similar affinity.

4.5 DISCUSSION

The active site and several base-binding and phosphoryl group-binding subsites of RNase A have been well characterized [(Nogués *et al.*, 1995); Chapters Two and Three]. The primary goal of this work is to identify additional subsites in RNase A that interact with the RNA substrate during catalysis. Using both kinetic and thermodynamic approaches, we show that the side chain of Arg85 interacts with the phosphonucleoside 5′ to the phosphoryl group residing in the P0 subsite. In addition, our work suggests that Arg39 and Lys104 do not, at least individually, comprise subsites.

X-Ray diffraction analyses, computer modeling, and RNase A superfamily homology provided the basis for investigation of the roles of Arg39, Arg85 and Lys104 in substrate

binding. These three residues are the next closest cationic residues to subsites characterized previously and all have been postulated as components of newly identified subsites.

Thirty years ago, Takahashi (1968) proposed roles for Arg39 and Arg85 based on decreased ribonuclease activity caused by covalent modification of these arginines. Subsequently, affinity labeling and computer modeling studies led Cuchillo and co-workers to predict that Lys104 comprises an additional phosphoryl group subsite on the 5′ side of the scissile bond (de Llorens *et al.*, 1989). After determining a high resolution structure of the crystalline RNase A•d(ATAAG) complex, Cuchillo and co-workers modified their hypothesis to include Arg85 as a subsite residue. However, since the oligonucleotide used in the crystalline complex lacked a 5′ phosphoryl group, interaction between the side chain of either Arg85 or Lys104 and this phosphoryl group could not be determined explicitly (Fontecilla-Camps *et al.*, 1994). In addition, assignment of enzymic residues interacting with the phosphoryl group 3′ to that in the P2 subsite was precluded due to a lack of electron density in that region of the crystalline complex. An electrostatic surface potential map of a native RNase A crystalline structure [Figure 4.1; pdb entry 1rph; (Zegers *et al.*, 1994)] concurs with the observations of Cuchillo and co-workers—the positions of the Arg39, Arg85 and Lys104 side chains make all three residues good candidates for additional enzymic subsites.

The Role of Arg39. Replacing Arg39 with alanine has little effect on the kinetic parameters for the cleavage of poly(C). As listed in Table 4.1, k_{cat}, K_m, and k_{cat}/K_m are effectively the same as the wild-type values. Despite the proximity of Arg39 to the P2 subsite and the positive charge on Arg39 that could interact with the phosphoryl group on RNA, these data suggest that this residue does not contribute to catalysis. In addition, arginine at position 39 is not highly conserved. Of the 41 known pancreatic ribonucleases of known sequence, only 29 of these ribonucleases have an arginine residue at this position (Beintema, 1987).

Arg39 may function in conjunction with other proximal cationic residues to form a subsite. For instance, Lys7 and Arg10 have been shown to comprise jointly the P2 subsite of RNase A. When either of these residues are replaced with glutamine, the other residue plays a compensatory role, resulting in little effect on the kinetic parameters for poly(C) cleavage. Upon replacement of both Lys7 and Arg10 with glutamine or alanine, substrate binding and cleavage are affected [(Boix *et al.*, 1994); Chapter Two]. Lys37 is the nearest cationic residue to Arg39. Perhaps Lys37 and Arg39 function together in a manner similar to the residues comprising the P2 subsite. Examination of the role of Lys37 awaits further study.

The Role of Lys104. The kinetic parameters for the cleavage of poly(C) are not affected dramatically by the replacement of Lys104 with alanine. Although the value of both k_{cat} and K_m for K104A RNase A are twofold lower than those of the wild-type enzyme, the change to the value of k_{cat}/K_m is not significant. These results suggest that Lys104 has little importance in the RNase A-catalyzed cleavage of RNA. The similarity in the kinetic parameters for poly(C) cleavage by K104A RNase A and the wild-type enzyme was unexpected. In contrast to Arg39, Lys104 is a highly conserved residue. The side chain of residue 104 is cationic in 39 of 40 pancreatic ribonucleases whose sequences have been determined, with all but four of these residues being lysine.

The Role of Arg85. Residue 85 is the most conserved residue of the three investigated in this study. An arginine is present at position 85 in 40 of 41 pancreatic ribonucleases (Beintema, 1987). The single exception is mouse pancreatic ribonuclease, which has a histidine at this position. Based on its conservation by evolution and its proximity to the active site, Arg85 appeared likely to play a role in substrate binding.

The impaired kinetic parameters for the cleavage of poly(C) by R85A RNase A suggest a significant role for residue 85. Although k_{cat} remains essentially the same as wild-type, the K_m and k_{cat}/K_m values for poly(C) cleavage differ dramatically (Table 4.1). Interestingly, the > 15-fold increase in the value of K_m is larger than that for K41A RNase A, which has the largest

K_m value observed previously for an RNase A variant (J. M. Messmore, personal communication). In addition, the value of k_{cat}/K_m for poly(C) cleavage by R85A RNase A is 10-fold lower than that of the wild-type enzyme. Thus, Arg85 is important for interaction with the RNA substrate, likely making a uniform contribution toward binding the ground state and the rate-limiting transition state.

Thermodynamic Studies Confirm Kinetic Results. The phosphoryl groups on a bound nucleic acid often form Coulombic interactions with cationic enzymic residues. The driving force for complex formation is the entropically-favorable release of cations from the nucleic acid upon binding (Record *et al.*, 1976). Theory predicts that a protein•nucleic acid complex will associate with decreased cation concentration. Indeed, the affinity of Fl~d(AUAA) for RNase A increases with decreasing sodium concentration (Chapter Two). The K_d values for Fl~d(AUAA) and Fl~d(UAA) binding to wild-type RNase A, at conditions similar to those used in the poly(C) cleavage assays [0.10 M MES-NaOH, pH 6.0, containing NaCl (0.10 M)], are 88 μM (Chapter Two) and 130 μM (Kelemen & Raines, 1997), respectively. These K_d values differ by only 1.5-fold. To enhance the differences in K_d values between binding of the two oligonucleotides to wild-type RNase A and the R85A variant, a low salt-concentration buffered solution was used in our binding experiments. Indeed, we observed an eight-fold difference in the affinities of Fl~d(AUAA) and Fl~d(UAA) for the wild-type protein (Table 4.2 and Figure 4.3).

Why is the affinity of R85A RNase A for Fl~d(AUAA) greater than that for Fl~d(UAA)? In the crystalline RNase A•d(ATAAG) complex, the side chain of Arg85 is directed toward the 5'-hydroxyl group of the ligand, and thus, the position that would be occupied by a phosphoryl group in a 5'-phosphorylated oligonucleotide such as the one used in our binding assays. Although this interaction is removed upon replacing Arg85 with alanine, another enzymic residue may interact with this group in the absence of the Arg85 side chain.

The side chain of Lys66, which comprises the adjacent P0 subsite, may form a Coulombic interaction with the 5′-phosphoryl group of the bound nucleic acid in the absence of Arg85. A more likely scenario is that an enzymic residue interacts with the 5′-adenosine of Fl~d(AUAA). Indeed, C_β and C_γ of Pro42 make van der Waals contact with the face of the 6-membered ring of the 5′-adenosine [pdb entry 1rcn; (Fontecilla-Camps *et al.*, 1994)]. These interactions would provide additional binding energy upon complex formation with the longer oligonucleotide.

Conclusion. Both kinetic and thermodynamic experiments suggest for the first time an important role for Arg85 in nucleic acid binding by RNase A. Based on the proximity of Arg85 to the P0 subsite, the dramatic change in the K_m value for poly(C) cleavage, and the differential binding affinities of Fl~d(AUAA) and Fl~d(UAA) for the wild-type protein and R85A variant, we conclude that the side chain of Arg85 constitutes a new enzymic subsite, which we call "P(-1)" (Figure 4.4).

4.6 ACKNOWLEDGEMENT

Table 4.1: Steady-State Kinetic Parameters for the Cleavage of Poly(C) by Wild-Type RNase A[a], R39A RNase A, R85 RNase A, and K104 RNase A[b]

RNase A (T_m; °C)[c]	k_{cat} (s^{-1})	K_m (mM)	k_{cat}/K_m (10^6 M^{-1} s^{-1})
Wild-Type (62)	507 ± 15	0.089 ± 0.009	5.7 ± 0.5
R39A (62)	541 ± 28	0.096 ± 0.002	5.7 ± 1.1
R85A (62)	659 ± 80	1.42 ± 0.30	0.46 ± 0.04
K104A (62)	281 ± 5	0.042 ± 0.004	6.4 ± 0.5

[a] Same data as that in Table 2.1 in this Dissertation.

[b] Data were obtained at 25 °C in 0.10 M MES-NaOH buffer, pH 6.0, containing NaCl (0.10 M).

[c] Values of T_m are reported ± 2 °C.

Table 4.2: Values of K_d (µM) for the Binding of Fluorescein-Labeled DNA Oligonucleotides to Wild-Type RNase A and the R85A Variant[a]

RNase A	Ligand	
	Fl~d(UAA)	Fl~d(AUAA)
Wild-Type	24	3.0
R85A	23	9.6

[a]Values were determined at 23 ± 2 °C in 0.020 M MES-NaOH buffer, pH 6.0, containing NaCl (0.025 M).

Figure 4.1   Electrostatic potential map of the surface of wild-type RNase A. In this map,

blue denotes regions of positive charge and red denotes regions of negative

charge. Charges were calculated for RNase A at pH 6.0 and 0.142 M Na$^+$,

assuming pK_a values for the histidine residues determined in Chapter Three.

This map was created using the program GRASP (Nicholls *et al.*, 1991) and the

structure of wild-type RNase A [pdb entry 1rph; (Zegers *et al.*, 1994)]. Lys66

(P0 subsite), active site (P1 subsite), Lys7 and Arg10 (the P2 subsite), and

Arg39, Arg85, and Lys104, the residues examined in this work, are indicated.

Lys7/Arg10

Arg39

active
site

Lys104

Lys66

Arg85
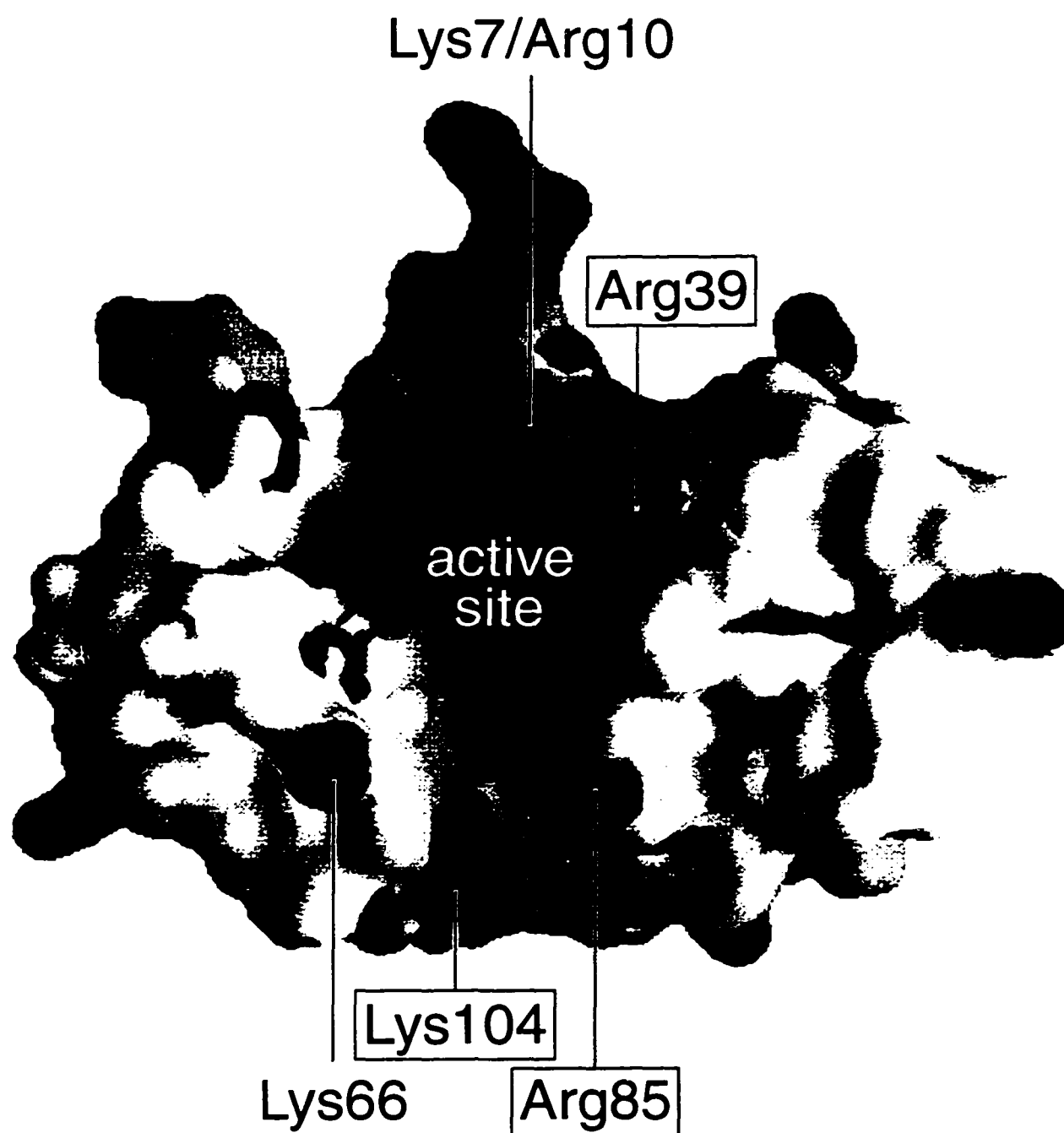
Figure 4.2   Binding of wild-type RNase A to Fl~d(AUAA) (●) and Fl~d(UAA) (○) (A) and

binding of R85A RNase A to Fl~d(AUAA) (■) and Fl~d(UAA) (□) (B).

Binding was assayed by fluorescence anisotropy in 0.020 M MES-NaOH

buffer, pH 6.0, containing NaCl (0.025 M), at 23 ± 2 °C. Each data point is the

average of 6 – 8 measurements, with the standard deviation for each point

indicated by the bars. The curves are best fits to eq 4.1.

A
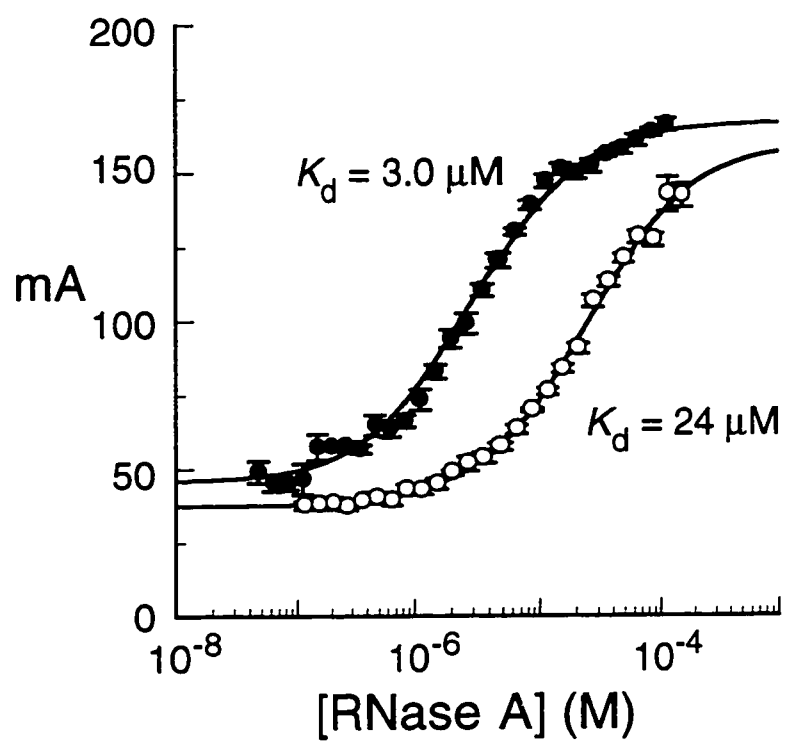
B
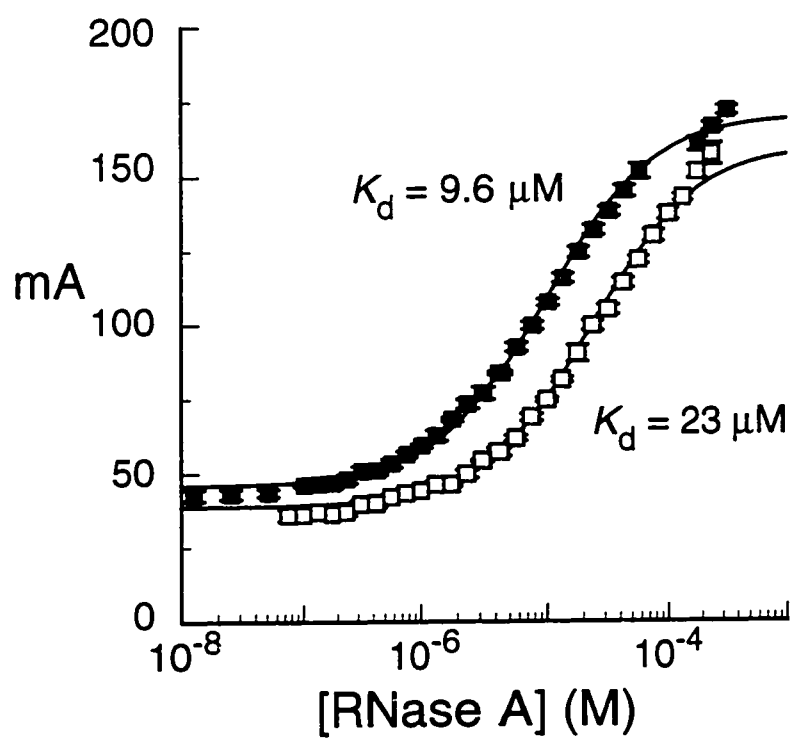
Figure 4.3   Effects of eliminating an RNase A – nucleic acid interaction by removal of an

enzymic subsite, a 5′-phosphonucleoside of the nucleic acid, or both. Values of

K_d for wild-type RNase A or R85A RNase A bound to fluorescein~d(AUAA)

and fluorescein~d(UAA) were determined using fluorescence anisotropy.

Binding was assayed at 23 ± 2 °C in 0.020 M MES-NaOH buffer, pH 6.0,

containing NaCl (0.025 M).

wt•AUAA
$K_d = 3.0$ M

remove $\textcircled{P}$

wt•UAA
$K_d = 24$ M

remove subsite

remove subsite

R85A•AUAA
$K_d = 9.6$ M

remove $\textcircled{P}$

R85A•UAA
$K_d = 23$ M
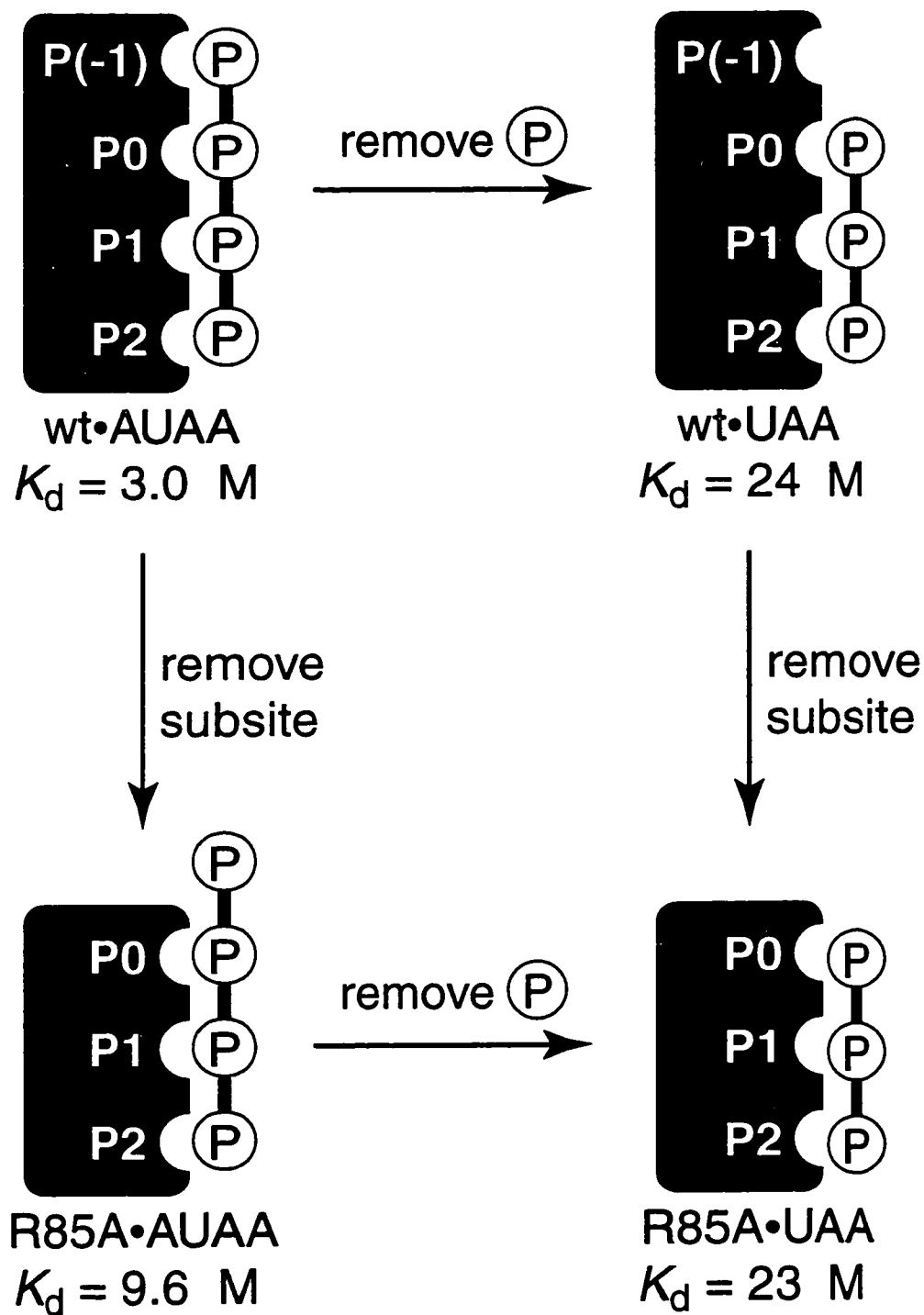
Figure 4.4   Schematic representation of the binding of an RNA fragment to RNase A. The

scissile bond is indicated. B and P refer to base and phosphoryl group binding

sites, respectively. The twelve indicated residues in boxes have been shown by

site-directed mutagenesis to make a contribution to substrate binding or turnover

(or both). Here, Arg85 [P(-1) subsite; red] was shown to interact with a

phosphoryl group of a bound nucleic acid.

Arg85

P(-1) subsite

Lys66

P0 subsite

Gln11
His12
Lys41
His119
Asp121

P1 subsite
(active site)

Lys7
Arg10

P2 subsite

Cyt
Ura

Thr45
Asp83

B1 subsite

scissile
bond

Ade

Asn71
Glu111

B2 subsite

Ade
Gua

?

B3 subsite

OH

OH

OH

OH

?
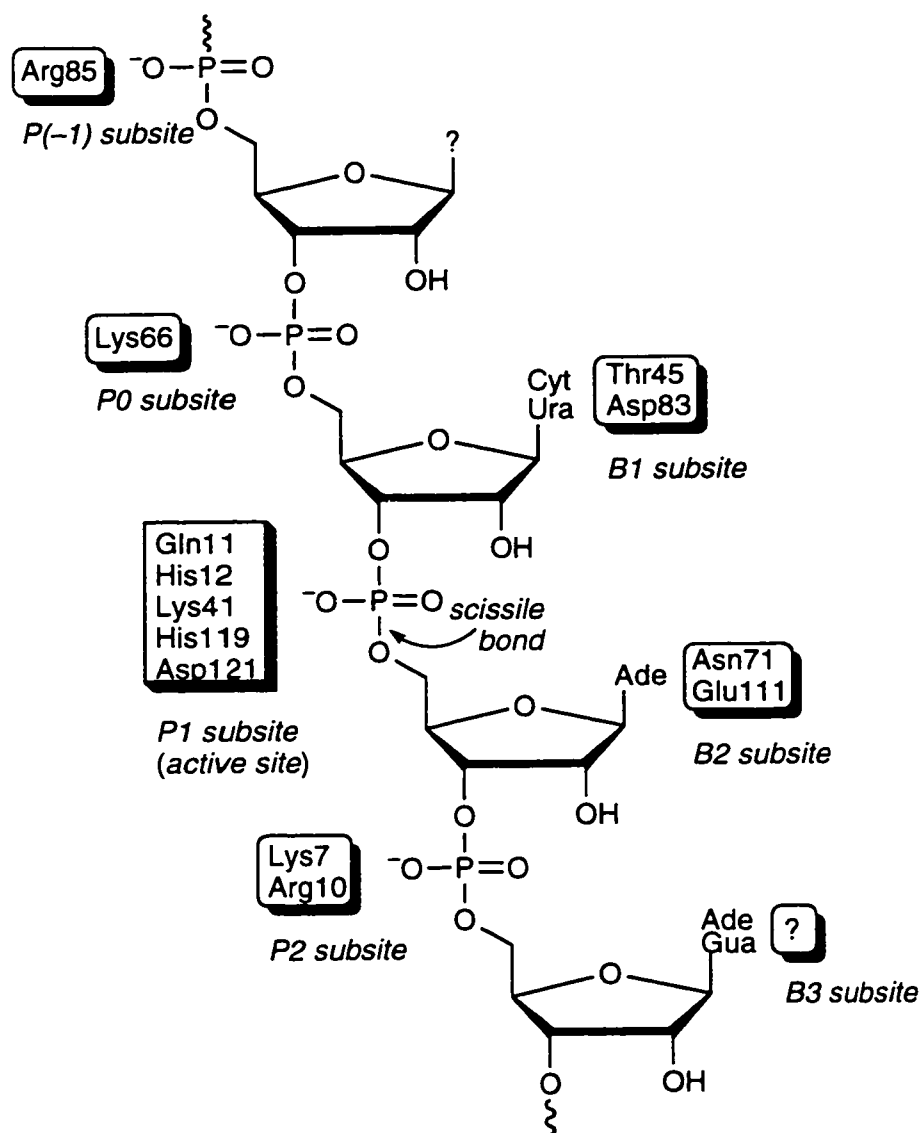
Chapter Five

References

Aguilar, C. F., Thomas, P. J., Mills, A., Moss, D. S. & Palmer, R. A. (1992). Newly observed binding mode in pancreatic ribonuclease. *J. Mol. Biol.* **224**, 265-267.

Anderson, C. F. & Record, M. T., Jr. (1995). Salt-nucleic acid interactions. *Annu. Rev. Phys. Chem.* **46**, 657-700.

Anfinsen, C. B. (1973). Principles that govern the folding of protein chains. *Science* **181**, 223-230.

Antosiewicz, J., McCammon, J. A. & Gilson, M. K. (1996). The determinants of pK_as in proteins. *Biochemistry* **35**, 7819-7833.

Attie, A. D. & Raines, R. T. (1995). Analysis of receptor-ligand interactions. *J. Chem. Educ.* **72**, 119-124.

Avey, H. P., Boles, M. O., Carlisle, C. H., Evans, S. A., Morris, S. J., Palmer, R. A., Woolhouse, B. A. & Shall, S. (1967). Structure of ribonuclease. *Nature* **213**, 557-562.

Barnard, E. A. (1969). Biological function of pancreatic ribonuclease. *Nature* **221**, 340-344.

Bartik, D., Redfield, C. & Dobson, C. M. (1994). Measurement of the individual pK_a values of acidic residues of hen and turkey lysozymes by two-dimensional ^{1}H NMR. *Biophys. J.* **66**, 1180-1184.

Beaucage, S. L. & Caruthers, M. H. (1981). Deoxynucleoside phosphoramidites—a new class of key intermediates for deoxypolynucleotide synthesis. *Tetrahedron Lett.* **22**, 1859-1862.

Beaven, G. H., Holiday, E. R. & Johnson, E. A. (1955). Optical properties of nucleic acids and their components. In *The Nucleic Acids, Chemistry and Biology* (E. Chargraff & J. N. Davidson, Ed.), pp. 493-553, Academic Press, New York.

Beintema, J. J. (1987). Structure, properties and molecular evolution of pancreatic-type ribonucleases. *Life Chem. Rep.* **4**, 333-389.

Beintema, J. J. (1989). Presence of a basic amino acid residue at either position 66 or 122 is a condition for enzymatic activity in the ribonuclease superfamily. *FEBS Letters* **254**, 1-4.

Beintema, J. J., Schüller, C., Irie, M. & Carsana, A. (1988). Molecular evolution of the ribonuclease superfamily. *Prog. Biophys. Molec. Biol.* **51**, 165-192.

Berkhout, B. & van Wamel, J. (1996). Accurate scanning of the *Bss*HII endonuclease in search for its DNA cleavage site. *J. Biol. Chem.* **271**, 1837-1840.

Birdsall, D. L. & McPherson, A. (1992). Crystal structure disposition of thymidylic acid tetramer in complex with ribonuclease A. *J. Biol. Chem.* **267**, 22230-22236.

Blackburn, P. & Moore, S. (1982). Pancreatic ribonuclease. *The Enzymes* **XV**, 317-433.

Blank, A., Sugiyama, R. H. & Dekker, C. A. (1982). Activity staining of nucleolytic enzymes after SDS-PAGE: Use of aqueous isopropanol to remove detergent from gels. *Anal. Biochem.* **120**, 267-275.

Blasie, C. A. & Berg, J. M. (1997). Electrostatic interactions across a β-sheet. *Biochemistry* **36**, 6218-6222.

Boix, E., Nogués, M. V., Schein, C. H., Benner, S. A. & Cuchillo, C. M. (1994). Reverse transphosphorylation by ribonuclease A needs an intact p_2-binding site. *J. Biol. Chem.* **269**, 2529-2534.

Bolen, D. W., Flögel, M. & Biltonen, R. (1971). Calorimetric studies of protein-inhibitor interaction. I. Binding of 3'-cytidine monophosphate to ribonuclease A at pH 5.5. *Biochemistry* **10**, 4136-4140.

Boqué, L., Gràcia Coll, M., Vilanova, M., Cuchillo, C. M. & Fita, I. (1994). Structure of ribonuclease A derivative II at 2.1-Å resolution. *J. Biol. Chem.* **269**, 19707-19712.

Borkakoti, N. (1983). The active site of ribonuclease A from the crystallographic studies of ribonuclease-A-inhibitor complexes. *Eur. J. Biochem.* **132**, 89-94.

Borkakoti, N., Moss, D. A. & Palmer, R. A. (1982). Ribonuclease-A: Least-squares refinement of structure at 1.45 Å resolution. *Acta Crystallogr., Sect B* **38**, 2210-2217.

Brems, D. N. & Baldwin, R. L. (1984). Amide proton exchange used to monitor the formation of a stable α-helix by residues 3 to 13 during folding of ribonuclease S. *J. Mol. Biol.* **80**, 1141-1156.

Brünger, A. T., Brooks, C. L., III & Karplus, M. (1985). Active site dynamics of ribonuclease. *Proc. Natl. Acad. Sci. U.S.A.* **82**, 8458-8462.

Bujalowski, W. & Lohman, T. M. (1986). Escherichia coli single-stranded binding protein forms multiple, distinct complexes with single-stranded DNA. *Biochemistry* **25**, 7799-7802.

Burley, S. K. & Petsko, G. A. (1988). Weakly polar interactions in proteins. *Adv. Prot. Chem.* **39**, 125-189.

Cantor, C. R. & Schimmel, P. R. (1980). *Biophysical Chemistry. Part 1: The Conformation of Biological Macromolecules*, W. H. Freeman and Company, New York.

Carter, P. J., Winter, G., Wilkinson, A. J. & Fersht, A. R. (1984). The use of double mutants to detect structural changes in the active site of the tyrosyl-tRNA synthetase (Bacillus stearothermophilus). *Cell* **38**, 835-840.

Cederholm, M. T., Stuckey, J. A., Doscher, M. S. & Lee, L. (1991). Histidine pK_a shifts acccompanying the inactivating Asp[121] → Asn substitution in a semisynthetic bovine pancreatic ribonuclease. *Proc. Natl. Acad. Sci., USA* **88**, 8116-8120.

Chivers, P. T., Prehoda, K. E., Volkman, B. F., Kim, B.-M., Markley, J. L. & Raines, R. T. (1997). Microscopic pK_a values of *Escherichia coli* thioredoxin. *Biochemistry* **36**, 14985-14991.

Chuang, W.-J., Gittis, A. G. & Mildvan, A. S. (1994). Magnetic resonance studies of the binding of oligonucleotide substrates to mutants of staphylococcal nuclease. *Proteins: Struct., Funct., and Genet.* **18**, 68-80.

Cleland, W. W. (1979). Statistical analysis of enzyme kinetic data. *Methods Enzymol.* **63**, 103-138.

Cohen, J. S., Griffen, J. H. & Schechter, A. N. (1973). Nuclear magnetic resonance titration curves of histidine ring protons. *J. Biol. Chem.* **248**, 4305-4310.

Coulomb, C. A. (1884). *Collection de Mémoires Relatifs a la Physique*, Gauthier-Villars, Paris.

Creighton, T. E. (1993). *Proteins: Structures and Molecular Properties*, W. H. Freeman and Company, New York.

Crestfield, A. M., Stein, W. H. & Moore, S. (1962). On the aggregation of bovine pancreatic ribonuclease. *Arch. Biochem. Biophys.* **Suppl. 1**, 217-222.

Cuchillo, C. M., Parés, X., Guasch, A., Barman, T., Travers, F. & Nogués, M. V. (1993). The role of 2′,3′-cyclic phosphodiesters in the bovine pancreatic ribonuclease A catalyzed cleavage of RNA: Intermediates or products? *FEBS Lett.* **333**, 207-210.

de Llorens, R., Arús, C., Parés, X. & Cuchillo, C. M. (1989). Chemical and computer graphics studies on the topography of the ribonuclease A active site cleft. A model of the enzyme-pentanucleotide substrate complex. *Protein Eng.* **2**, 417-429.

Debye, V. P. & Hückel, E. (1923). Zur theorie des elektrolyte. II. Das grenzgesetz für die elekrische leitfähigkeit. *Phys. Z.* **24**, 305-325.

deHaseth, P. L., Lohman, T. M. & Record, M. T., Jr. (1977). Nonspecific interaction of *lac* repressor with DNA: An association reaction driven by counterion release. *Biochemistry* **16**, 4783-4790.

del Rosario, E. J. & Hammes, G. G. (1969). Kinetic and equilibrium studies of the ribonuclease-catalyzed hydrolysis of uridine 2′,3′-cyclic phosphate. *Biochemistry* **8**, 1884-1889.

delCardayré, S. B. & Raines, R. T. (1994). Structural determinants of enzymatic processivity. *Biochemistry* **33**, 6031-6037.

delCardayré, S. B. & Raines, R. T. (1995). A residue to residue hydrogen bond mediates the nucleotide specificity of ribonuclease A. *J. Mol. Biol.* **252**, 328-336.

delCardayré, S. B., Ribó, M., Yokel, E. M., Quirk, D. J., Rutter, W. J. & Raines, R. T. (1995). Engineering ribonuclease A: Production, purification, and characterization of wild-type enzyme and mutants at Gln11. *Protein Eng.* **8**, 261-273.

delCardayré, S. B., Thompson, J. T. & Raines, R. T. (1994). Altering substrate specificity and detecting processivity in nucleases. In *Techniques in Protein Chemistry V* (J. W. Crabb, Ed.), pp. 313-320, Academic Press, San Diego, CA.

Doi, T., Recktenwald, A., Karaki, Y., Kikuchi, M., Morikawa, K., Ikehara, M., Inaoka, T., Hori, N. & Ohtsuka, E. (1992). Role of the basic amino acid cluster and Glu-23 in pyrimidine dimer glycosylase activity of T4 endonuclease V. *Proc. Natl. Acad. Sci. U.S.A.* **89**, 9420-9424.

Dunn, B. M., Gustchina, A., Wlodawer, A. & Kay, J. (1994). Subsite preferences of retroviral proteinases. *Meth. Enzymol.* **241**, 254-278.

Eberhardt, E. S., Wittmayer, P. K., Templer, B. M. & Raines, R. T. (1996). Contribution of a tyrosine side chain to ribonuclease A catalysis and stability. *Protein Sci.* **5**, 1697-1703.

Edsall, J. T., Martin, R. B. & Hollingworth, B. R. (1958). Ionization of individual groups in dibasic acids, with application to the amino and hydroxyl groups of tyrosine. *Proc. Natl. Acad. Sci., U.S.A.* **44**, 505-518.

Edsall, J. T. & Wyman, J. (1958). *Biophysical Chemistry*, Academic Press, New York.

Eftink, M. R., Anusiem, A. C. & Biltonen, R. L. (1983). Enthalpy-entropy compensation and heat capacity changes for protein–ligand interactions: General thermodynamic models and data for the binding of nucleotides to ribonuclease A. *Biochemistry* **22**, 3884-3896.

Eftink, M. R. & Biltonen, R. L. (1983). Energetics of ribonuclease A catalysis. 1. pH, ionic strength, and solvent isotope dependence of the hydrolysis of cytidine cyclic 2′,3′-phosphate. *Biochemistry* **22**, 5123-5134.

Eftink, M. R. & Biltonen, R. L. (1987). Pancreatic ribonuclease A: The most studied endoribonuclease. In *Hydrolytic Enzymes* (A. Neuberger & K. Brocklehurst, Ed.), pp. 333-375, Elsevier, New York.

Fairman, R., Shoemaker, K. R., York, E. J., Stewart, J. M. & Baldwin, R. L. (1990). The Glu 2⁻ ⋯ Arg 10⁺ side-chain interaction in the C-peptide helix of ribonuclease A. *Biophys. Chem.* **37**, 107-119.

Fedorov, A. A., Joseph-McCarthy, D., Fedorov, E., Sirakova, D., Graf, I. & Almo, S. C. (1996). Ionic interactions in crystalline bovine pancreatic ribonuclease A. *Biochemistry* **35**, 15962-15979.

Ferrin, T. E., Huang, C. C., Jarvis, L. E. & Langridge, R. (1988). The MIDAS display system. *J. Mol. Graphics* **6**, 13-27.

Fersht, A. (1985). *Enzyme Structure and Mechanism*, W.H. Freeman, New York.

Findlay, D., Herries, D. G., Mathias, A. P., Rabin, B. R. & Ross, C. A. (1961). The active site and mechanism of action of bovine pancreatic ribonuclease. *Nature* **190**, 781-784.

Finkelstein, A. V., Badretdinov, A. Y. & Ptitsyn, O. B. (1991). Physical reasons for secondary structural stability: α-Helices in short peptides. *Proteins: Struct., Funct., and Genet.* **10**, 287-299.

Flogel, M., Albert, A. & Biltonen, R. L. (1975). The magnitude of electrostatic interactions in inhibitor binding and during catalysis by ribonuclease A. *Biochemistry* **14**, 2616-2621.

Flogel, M. & Biltonen, R. L. (1975). Calorimetric and potentiometric characterization of the ionization behavior of ribonuclease A and its complex with 3'-cytosine monophosphate. *Biochemistry* **14**, 2603-2609.

Flogel, M. & Biltonen, R. L. (1975). The pH dependence of the thermodynamics of the interaction of 3'-cytidine monophosphate with ribonuclease A. *Biochemistry* **14**, 2610-2615.

Fontecilla-Camps, J. C., de Llorens, R., le Du, M. H. & Cuchillo, C. M. (1994). Crystal structure of ribonuclease A•d(ApTpApApG) complex. *J. Biol. Chem.* **269**, 21526-21531.

Frankel, A. D. (1992). Peptide models of the Tat-TAR protein–RNA interaction. *Protein Sci.* **1**, 1539-1542.

Frankel, A. D. (1994). Using peptides to study RNA–protein recognition. In *RNA–Protein Interactions* (K. Nagai & I. W. Mattaj, Ed.), pp. 221-247, Oxford University Press, Oxford.

Frey, P. A., Kokesh, F. C. & Westheimer, F. H. (1971). A reporter group at the active site of acetoacetate decarboxylase. I. Ionization constant of the nitrophenol. *J. Am. Chem. Soc.* **93**, 7266-7269.

Getzoff, E. D., Cabelli, D. E., Fisher, C. L., Parge, H. E., Silvia Viezzcli, M., Banci, L. & Hallewell, R. A. (1992). Faster superoxide dismutase mutants designed by enhancing electrostatic guidance. *Nature* **358**, 347-351.

Getzoff, E. D., Tainer, J. A., Weiner, P. K., Kollman, P. A., Richardson, J. S. & Richardson, D. C. (1983). Electrostatic recognition between superoxide and copper, zinc superoxide dismutase. *Nature* **306**, 287-290.

Gilliland, G. L. (1997). Crystallographic studies of ribonuclease complexes. In *Ribonucleases: Structures and Functions* (G. D'Alessio & J. F. Riordan, Ed.), pp. 306-341, Academic Press, New York.

Gillmor, C. S. (1971). *Coulomb and the Evolution of Physics and Engineering in Eighteenth-Century France*, Princeton University Press, Princeton, NJ.

Gilson, M. K. & Honig, B. H. (1988). Energetics of charge-charge interactions in proteins. *Proteins: Struct., Funct., Genet.* **3**, 32-52.

Gilson, M. K., Rashin, A., Fine, R. & Honig, B. (1985). On the calculation of electrostatic interactions in proteins. *J. Mol. Biol.* **183**, 503-516.

González, C., Santoro, J. & Rico, M. (1997). NMR solution structures of ribonuclease A and its complexes with mono- and dinucleotides. In *Ribonucleases: Structures and Functions* (G. D'Alessio & J. F. Riordan, Ed.), pp. 343-381, Academic Press, New York.

Gross, E. & Witkop, B. (1962). Nonenzymatic cleavage of peptide bonds: The methionine residues in bovine pancreatic ribonuclease. *J. Biol. Chem.* **237**, 1856-1860.

Gutfreund, H. & Knowles, J. R. (1967). The foundations of enzyme action. *Essays Biochem.* **3**, 25-72.

Ha, J.-H., Capp, M. W., Hohenwalter, M. D., Baskerville, M. & Record, M. T., Jr. (1992). Thermodynamic stoichiometries of participation of water, cations and anions in specific and non-specific binding of *lac* repressor to DNA. *J. Mol. Biol.* **228**, 252-264.

Haar, W., Maurer, W. & Rüterjans, H. (1974). Proton-magnetic-resonance studies of complexes of pancreatic ribonuclease A with pyrimidine and purine nucleotides. *Eur. J. Biochem.* **44**, 201-211.

Hermans, J. J. & Scheraga, H. A. (1961). Structural studies of ribonuclease. V. Reversible change of configuration. *J. Am. Chem. Soc.* **83**, 3283-3292.

Heyduk, T. & Lee, J. C. (1990). Application of fluorescence energy transfer and polarization to monitor *Escherichia coli* cAMP receptor protein and *lac* promoter interaction. *Proc. Natl. Acad. Sci. U.S.A.* **87**, 1744-1748.

Heyduk, T., Lee, J. C., Ebright, Y. W., Blatter, E. E., Zhou, Y. & Ebright, R. H. (1993). CAP interacts with RNA polymerase in solution in the absence of promoter DNA. *Nature* **364**, 548-549.

Heyduk, T., Ma, Y., Tang, H. & Ebright, R. H. (1996). Fluorescence anisotropy: Rapid, quantitative assay for protein–DNA and protein–protein interaction. *Methods Enzymol.* **274**, 492-503.

Highbarger, L. A., Gerlt, J. A. & Kenyon, G. L. (1996). Mechanism of the reaction catalyzed by acetoacetate decarboxylase. Importance of lysine 116 in determining the pK_a of active-site lysine 115. *Biochemistry* **35**, 41-46.

Hofmann, K., Finn, F. M., Limetti, M., Montibeller, J. & Zanetti, G. (1966). Studies on polypeptides. XXXIV. Enzymic properties of partially synthetic de(16-20)- and de(15-20)-ribonuclease S'. *J. Am. Chem. Soc.* **88**, 3633-3636.

Horowitz, A. & Fersht, A. (1990). Strategy for the analysis of co-operativity of intramolecular interactions in peptides and proteins. *J. Mol. Biol.* **214**, 613-617.

Horowitz, A., Serrano, L., Avron, B., Bycroft, M. & Fersht, A. R. (1990). Strength and co-operativity of contributions of surface salt bridges to protein stability. *J. Mol. Biol.* **216**, 1031-1044.

Huheey, J. E. (1983). *Inorganic Chemistry: Principles of Structure and Reactivity*, Harper Collins, New York.

Inoue, M., Yamada, H., Yasukochi, T., Kuroki, R., Miki, T., Horiuchi, T. & Imoto, T. (1992). Multiple role of hydrophobicity of tryptophan-108 in chicken lysozyme: Structural stability, saccharide ability, and abnormal pK_a of glutamic acid-35. *Biochemistry* **31**, 5545-5553.

Irie, M., Mikami, F., Monma, K., Ohgi, K., Watanabe, H., Yamaguchi, R. & Nagase, H. (1984). Kinetic studies on the cleavage of oligouridylic acids and poly U by bovine pancreatic ribonuclease A. *J. Biochem.* **96**, 89-96.

Irie, M., Watanabe, H., Ohgi, K., Tobe, M., Matsumura, G., Arata, Y., Hirose, T. & Inayama, S. (1984). Some evidence suggesting the existence of P2 and B3 sites in the active site of bovine pancreatic ribonuclease A. *J. Biochem.* **95**, 751-759.

Jackson, S. E. & Fersht, A. R. (1993). Contribution of long-range electrostatic interactions to the stabilization of the catalytic transition state of the serine protease subtilisin BPN'. *Biochemistry* **32**, 13909-13916.

Jeltsch, A., Alves, J., Wolfes, H., Maass, G. & Pingoud, A. (1994). Pausing of the restriction endonuclease *Eco*RI during linear diffusion on DNA. *Biochemistry* **33**, 10215-10219.

Jencks, W. J. (1981). On the attribution and additivity of binding energies. *Proc. Natl. Acad. Sci U.S.A.* **78**, 4046-4050.

Jencks, W. P. (1987). *Catalysis in Chemistry and Enzymology*, Dover, Mineola, NY.

Jensen, D. E. & von Hippel, P. H. (1976). DNA "melting" proteins. I. Effects of bovine pancreatic ribonuclease binding on the conformation and stability of DNA. *J. Biol. Chem.* **251**, 7198-7214.

Jones, T. A. (1985). Diffraction methods for biological macromolecules. Interactive computer graphics: FRODO. *Methods Enzymol.* **115**, 157-171.

Kabsch, W. (1988). Automatic indexing of rotation diffraction patterns. *J. Appl. Crystallogr.* **21**, 67-71.

Kabsch, W. (1988). Evaluation of single-crystal X-ray diffraction data from a position-sensitive detector. *J. Appl. Crystallogr.* **21**, 916-924.

Karpeisky, M. Y. & Yakovlev, G. I. (1981). Topochemical principles of the substrate specificity of nucleases. *Sov. Sci. Rev., Sect. D* **2**, 145-257.

Kartha, G., Bello, J. & Harker, D. (1967). Tertiary structure of ribonuclease. *Nature* **213**, 862-865.

Kato, I. & Anfinsen, C. B. (1969). On the stabilization of ribonuclease S-protein by ribonuclease S-peptide. *J. Biol. Chem.* **244**, 1004-1007.

Katoh, H., Yoshinaga, M., Yanagita, T., Ohgi, K., Irie, M., Beintema, J. J. & Meinsma, D. (1986). Kinetic studies on turtle pancreatic ribonuclease: A comparative study of the base specificities of the B_2 and P_0 sites of bovine pancreatic ribonuclease A and turtle pancreatic ribonuclease. *Biochim. Biophys. Acta* **873**, 367-371.

Kauzmann, W. (1959). Some factors in the interpretation of protein denaturation. *Adv. Prot. Chem.* **14**, 1-63.

Kelemen, B. R. & Raines, R. T. (1997). One-dimensional diffusion of a protein along a single-stranded nucleic acid. In *Techniques in Protein Chemistry VIII* (D. R. Marshak, Ed.), pp. 565-572, Academic Press, San Diego, CA.

Kim, J.-S. & Raines, R. T. (1993). Bovine seminal ribonuclease produced from a synthetic gene. *J. Biol. Chem.* **268**, 17392-17396.

Kim, J.-S. & Raines, R. T. (1993). Ribonuclease S-peptide as a carrier in fusion proteins. *Protein Sci.* **2**, 348-356.

Kokesh, F. C. & Westheimer, F. H. (1971). A reporter group at the active site of acetoacetate decarboxylase. II. Ionization constant of the amino group. *J. Am. Chem. Soc.* **93**, 7270-7274.

Kong, X. P., Onrust, R., O' Donnell, M. & Kuriyan, J. (1992). Three-dimensional structure of the β subunit of E. coli DNA polymerase III holoenzyme: A sliding DNA clamp. *Cell* **69**, 425-437.

Kraulis, P. J. (1991). MOLSCRIPT: A program to produce both detailed and schematic plots of protein structures. *J. Appl. Crystallogr.* **21**, 916-924.

Kuhara, S., Ezaki, E., Fukamizo, T. & Hayashi, D. (1982). Estimation of the free energy change of substrate binding in lysozyme-catalyzed reactions. *J. Biochem. (Tokyo)* **92**, 121-127.

Kunkel, T. A., Roberts, J. D. & Zakour, R. A. (1987). Rapid and efficient site-specific mutagenesis without phenotypic selection. *Methods Enzymol.* **154**, 367-382.

Kuriyan, J. & O' Donnell, M. (1993). Sliding clamps of DNA polymerase. *J. Mol. Biol.* **234**, 915-925.

Kurth, T., Ullmann, D., Jakubke, H.-D. & Hedstrom, L. (1997). Converting trypsin to chymotrypsin: Structural determinants of S1' specficity. *Biochemistry* **36**, 10098-10104.

Kyte, J. (1995). *Structure in Protein Chemistry*, Garland Publishing, New York.

Labhardt, A. M. & Baldwin, R. L. (1979). Recombination of S-peptide with S-protein during folding of ribonuclease S. *J. Mol. Biol.* **135**, 231-244.

Layne, E. (1957). Spectrophotometric and turbidimetric methods for measuring proteins. *Methods Enzymol.* **3**, 447-454.

Lennette, E. P. & Plapp, B. V. (1979). Transition-state analysis of the facilitated alkylation of ribonuclease A by bromoacetate. *Biochemistry* **18**, 3938-3946.

Lequin, O., Thüring, H., Robin, M. & Lallemand, J.-Y. (1997). Three-dimensional solution structure of human angiogenin determined by ^{1}H,^{15}N-NMR spectroscopy. Characterization of histidine protonation states and pK_a values. *Eur. J. Biochem.* **250**, 712-726.

LeTilly, V. & Royer, C. A. (1993). Fluorescence anisotropy assays implicate protein–protein interactions in regulating *trp* repressor DNA binding. *Biochemistry* **32**, 7753-7758.

Levine, I. N. (1983). *Quantum Chemistry*, Allyn and Bacon, Boston, MA.

Li, J. R. & Walz, F. G. (1974). A steady-state kinetic study of the ribonuclease a catalyzed hydrolysis of uridine-2':3'(cyclic)-5'-diphosphate. *Arch. Biochem. Biophys.* **161**, 227-233.

LiCata, V. J. & Ackers, G. K. (1995). Long-range, small magnitude nonadditivity of mutational effects in proteins. *Biochemistry* **34**, 3133-3139.

Linderstrøm-Lang, K. (1924). On the ionization of proteins. *Compt. Rend. Trav. Lab. Carlsberg* **15**, 1-29.

Loewenthal, R., Sancho, J., Reinikainen, T. & Fersht, A. R. (1993). Long-range surface charge–charge interactions in proteins. Comparison of experimental results with calculations from a theoretical method. *J. Mol. Biol.* **232**, 574-583.

Lohman, T. M. (1986). Kinetics of protein-nucleic acid interactions: Use of salt effects to probe mechanisms of interaction. *CRC Crit. Rev. Biochem.* **19**, 191-245.

Lohman, T. M. & Overman, L. B. (1985). Two binding modes in *Escherichia coli* single strand binding protein–single stranded DNA complexes. *J. Biol. Chem.* **260**, 3594-3603.

Malcolm, B. A., Rosenberg, S., Corey, M. J., Allen, J. S., de Baetselier, A. & Kirsch, J. F. (1989). Site-directed mutagenesis of the catalytic residues Asp-52 and Glu-35 of chicken egg white lysozyme. *Proc. Natl. Acad. Sci. U.S.A.* **86**, 133-136.

Markley, J. L. (1975). Correlation proton magnetic resonance studies at 250 MHz of bovine pancreatic ribonuclease. I. Reinvestigation of the histidine peak assignment. *Biochemistry* **14**, 3546-3553.

Markley, J. L. (1975). Correlation proton magnetic resonance studies at 250 MHz of bovine pancreatic ribonuclease. II. pH and inhibitor-induced conformational transitions affecting histidine-48 and one tyrosine residue of ribonuclease A. *Biochemistry* **14**, 3554-3561.

Markley, J. L. (1975). Observation of histidine residues in proteins by means of nuclear magnetic resonance spectroscopy. *Accts. Chem. Res.* **8**, 70-80.

Markley, J. L. & Finkenstadt, W. R. (1975). Correlation proton magnetic resonance studies at 250 MHz. III. Mutual electrostatic interaction between histidine residues 12 and 119. *Biochemistry* **14**, 3562-3566.

Mascotti, D. P. & Lohman, T. M. (1997). Thermodynamics of oligoarginines binding to RNA and DNA. *Biochemistry* **36**, 7272-7279.

Matthews, C. K. & van Holde, K. E. (1990). *Biochemistry*, Benjamin/Cummings Publishing, Redwood City, CA.

Mauk, M. R., Barker, P. D. & Mauk, A. G. (1991). Proton linkage of complex formation between cytochrome c and cytochrome b_5: Electrostatic consequences of protein-protein interactions. *Biochemistry* **30**, 9873-9881.

McIntosh, L. P., Hand, G., Johnson, P. E., Joshi, M. D., Körner, M., Plesniak, L. A., Ziser, L., Wakarchuk, W. W. & Withers, S. G. (1996). The pK_a of the general acid/base carboxyl group of a glycosidase cycles during catalysis: ^{13}C-NMR study of *Bacillus circulans* xylanase. *Biochemistry* **35**, 9958-9966.

McPherson, A., Brayer, G., Cascio, D. & Williams, R. (1986). The mechanism of binding of a polynucleotide chain to pancreatic ribonuclease. *Science* **232**, 765-768.

Meadows, D. H., Roberts, G. C. K. & Jardetzky, O. (1969). Nuclear magnetic resonance studies of the structure and binding sites of enzymes. VIII. Inhibitor binding to ribonuclease. *J. Mol. Biol.* **45**, 491-511.

Mehler, E. L. & Eichele, G. (1984). Electrostatic effects in water-accessible regions of proteins. *Biochemistry* **23**, 3887-3891.

Messmore, J. M., Fuchs, D. N. & Raines, R. T. (1995). Ribonuclease A: Revealing structure – function relationships with semisynthesis. *J. Am. Chem. Soc.* **117**, 8057-8060.

Mildvan, A. S., Weber, D. J. & Kuliopulos, A. (1992). Quantitative interpretations of double mutations of enzymes. *Arch. Biochem. Biophys.* **294**, 327-340.

Mitsui, Y., Urata, Y., Torii, K. & Irie, M. (1978). Studies on the binding of adenylyl-3′,5′-cytidine to ribonuclease. *Biochim. Biophys. Acta* **535**, 299-308.

Mossing, M. C. & Record, M. T., Jr. (1985). Thermodynamic origins of specificity in the *lac* repressor-operator interaction: Adaptability in the recognition of mutant operator sites. *J. Mol. Biol.* **186**, 295-305.

Nakamura, H. (1996). Roles of electrostatic interaction in proteins. *Quart. Rev. of Biophys.* **29**, 1-90.

Nicholls, A., Sharp, K. A. & Honig, B. (1991). Protein folding and association: Insights from the interfacial and thermodynamic properties of hydrocarbons. *Proteins: Struct., Funct., and Genet.* **11**, 281-296.

Nogués, M. V., Vilanova, M. & Cuchillo, C. M. (1995). Bovine pancreatic ribonuclease A as a model of an enzyme with multiple substrate binding sites. *Biochim. Biophys. Acta* **1253**, 16-24.

Ogilvie, K. K., Beaucage, S. L., Schifman, A. L., Theriault, N. Y. & Sadana, K. L. (1978). The synthesis of oligoribonucleotides. II. The use of silyl protecting groups in nucleoside and nucleotide chemistry. VII. *Can. J. Chem.* **56**, 2768-2780.

Olmsted, M. C., Anderson, C. F. & Record, M. T., Jr. (1989). Monte Carlo description of oligoelectrolyte properties of DNA oligomers: Range of the end effect and the approach of molecular and thermodynamic properties to the polyelectrolyte limits. *Proc. Natl. Acad. Sci. U.S.A.* **86**, 7766-7770.

Orttung, W. H. (1969). Interpretation of the titration curve of oxyhemoglobin. Detailed consideration of Coulomb interactions at low ionic strength. *J. Am. Chem. Soc.* **91**, 162-167.

Orttung, W. H. (1970). Proton binding and dipole moment of hemoglobin. Refined calculations. *Biochemistry* **9**, 2394-2402.

Osterhout, J. J., Jr., Baldwin, R. L., York, E. J., Stewart, J. M., Dyson, H. J. & Wright, P. E. (1989). [1]NMR Studies of the solution conformations of an analogue of the C-peptide of ribonuclease A. *Biochemistry* **28**, 7059-7064.

Osterman, A. L., Brooks, H. B., Rizo, J. & Phillips, M. A. (1997). Role of Arg-277 in the binding of pyridoxal 5'-phosphate to *Trypanosoma brucei* ornithine decarboxylase. *Biochemistry* **36**, 4558-4567.

Overman, L. B., Bujalowski, W. & Lohman, T. M. (1988). Equilibrium binding of *Escherichia coli* single-strand binding protein to single-stranded nucleic acids in the $(SSB)_{65}$ binding mode. Cation and anion effects and polynucleotide specificty. *Biochemistry* **27**, 456-471.

Overman, L. B. & Lohman, T. M. (1994). Linkage of pH, anion and cation effects in protein-nucleic acid equilibria. *Escherichia coli* SSB protein-single stranded nucleic acid interactions. *J. Mol. Biol.* **236**, 165-178.

Pace, C. N., Shirley, B. A. & Thomson, J. A. (1989). Measuring the conformational stability of a protein. In *Protein Structure* (T. E. Creighton, Ed.), pp. 311-330, IRL Press, New York.

Page, M. I. (1977). Entropy, binding energy, and binding catalysis. *Angew. Chem. Int. Ed. Engl.* **16**, 449-459.

Parés, X., Llorens, R., Arus, C. & Cuchillo, C. M. (1980). The reaction of bovine pancreatic ribonuclease A with 6-chloropurineriboside 5'-monophosphate. Evidence on the existence of a phosphate-binding site. *Eur. J. Biochem.* **105**, 571-579.

Parés, X., Nogués, M. V., de Llorens, R. & Cuchillo, C. M. (1991). Structure and function of ribonuclease A binding subsites. *Essays Biochem.* **26**, 89-103.

Pauling, L. (1960). *The Nature of the Chemical Bond*, Cornell University Press, Ithaca, NY.

Pincus, M., Thi, L. L. & Carty, R. P. (1975). The kinetics and specificity of the reaction of 2'(3')-O-bromoacetyluridine with bovine pancreatic ribonuclease A. *Biochemistry* **14**, 3653-3661.

Quirk, D. J. Role of the His⋯Asp Catalytic Dyad of Ribonuclease A, *Ph.D. Thesis*, University of Wisconsin–Madison (1996).

Radzicka, A. & Wolfenden, R. (1995). A proficient enzyme. *Science* **267**, 90-92.

Radzicka, A. & Wolfenden, R. (1995). Transition state and multisubstrate analog inhibitors. *Methods Enzymol.* **249**, 284-312.

Raines, R. T. (1998). Ribonuclease A. *Chem. Rev.* **98**, 1045-1065.

Raman, C. S., Allen, M. J. & Nall, B. T. (1995). Enthalpy of antibody–cytochrome *c* binding. *Biochemistry* **34**, 5831-5838.

Record, M. T., Jr., deHaseth, P. L. & Lohman, T. M. (1977). Interpretation of monovalent and divalent cation effects on the *lac* repressor–operator interaction. *Biochemistry* **16**, 4791-4796.

Record, M. T., Jr., Lohman, T. M. & De Haseth, P. (1976). Ion effects on ligand-nucleic acid interactions. *J. Mol. Biol.* **107**, 145-158.

Relan, N. D., Jenuwine, E. S., Gumbs, O. H. & Shaner, S. L. (1997). Preferential interactions of the *Escherichia coli* LexA repressor with anions and protons are coupled to binding the *RecA* operator. *Biochemistry* **36**, 1077-1084.

Resnick, R. & Halliday, D. (1966). *Physics*, John Wiley and Sons, New York.

Ribó, M., Fernández, E., Bravo, J., Osset, M., Fallon, M. J. M., de Llorens, R. & Cuchillo, C. M. (1991). Purification of human pancreatic ribonuclease by high performance liquid chromatography. In *Structure, Mechanism and Function of Ribonucleases* (R. de Llorens, C. M. Cuchillo, M. V. Nogués & X. Parés, Ed.), pp. 157-162, Universitat Autónoma de Barcelona, Bellaterra, Spain.

Richards, F. M. & Vithayathil, P. J. (1959). The preparation of subtilisin-modified ribonuclease and the separation of the peptide and protein components. *J. Biol. Chem.* **234**, 1459-1465.

Richards, F. M. & Wyckoff, H. W. (1971). Bovine pancreatic ribonuclease. *The Enzymes* **IV**, 647-806.

Richardson, R. M., Parés, X. & Cuchillo, C. M. (1990). Chemical modification by pyridoxal 5'-phosphate and cyclohexane-1,2-dione indicates that Lys-7 and Arg-10 are involved in the p_2 phosphate-binding subsite of bovine pancreatic ribonuclease A. *Biochem. J.* **267**, 593-599.

Rico, M., Gallego, E., Santoro, J., Bermejo, F. J., Nieto, J. L. & Herranz, J. (1984). On the fundamental role of the glu 2⁻...arg 10⁺ salt bridge in the folding of isolated ribonuclease S-peptide. *Biochem. Biophys. Res. Comm.* **123**, 757-763.

Righetti, P. G. (1984). *Isoelectric Focusing: Theory, Methodology, and Applications*, Elsezier Science, Amsterdam.

Righetti, P. G., Gianazza, E., Gelfi, C. & Chiari, M. (1990). Isoelectric focusing. In *Gel Electrophoresis of Proteins: A Practical Approach* (B. D. Hames & D. Rickwood, Ed.), pp. 149-216, Oxford University Press, Oxford.

Rose, G. D. & Wolfenden, R. (1993). Hydrogen bonding, hydrophobicity, packing, and protein folding. *Annu. Rev. Biomol. Struct.* **22**, 381-415.

Royer, C. A. (1993). Improvements in the numerical analysis of thermodynamic data from biomolecular complexes. *Anal. Biochem.* **210**, 91-97.

Royer, C. A. & Beechem, J. M. (1992). Numerical analysis of binding data: Advantages, practical aspects, and implications. *Methods Enzymol.* **210**, 481-505.

Royer, C. A., Smith, W. R. & Beechem, J. M. (1990). Analysis of binding in macromolecular complexes: A generalized numerical approach. *Anal. Biochem.* **191**, 287-294.

Rushizky, G. W., Knight, C. A. & Sober, H. A. (1961). Studies on the preferential specificity of pancreatic ribonuclease as deduced from partial digests. *J. Biol. Chem.* **236**, 2732-2737.

Russell, A. J. & Fersht, A. R. (1987). Rational modification of enzyme catalysis by engineering surface charge. *Nature* **328**, 496-500.

Russell, A. J., Thomas, P. G. & Fersht, A. R. (1987). Electrostatic effects on modification of charged groups in the active site cleft of subtilisin by protein engineering. *J. Mol. Biol.* **193**, 803-813.

Rüterjans, H. & Witzel, H. (1969). NMR-studies on the structure of the active site of pancreatic ribonuclease A. *Eur. J. Biochem.* **9**, 118-127.

Sawada, F. & Irie, M. (1969). Interaction of uridine-(2'(3'),5'-diphosphate with ribonuclease A and carboxymethylribonuclease A. *J. Biochem. (Tokyo)* **66**, 415-418.

Schmidt, D. E. & Westheimer, F. H. (1971). pK of the lysine amino group at the active site of acetoacetate decarboxylase. *J. Am. Chem. Soc.* **10**, 1249-1253.

Scholtz, J. M., Qian, H., Robbins, V. H. & Baldwin, R. L. (1993). The energetics of ion-pair and hydrogen-bonding interactions in a helical peptide. *Biochemistry* **32**, 9668-9676.

Schultz, L. W., Hargraves, S. R., Klink, T. A. & Raines, R. T. (1998). Structure and stability of the P93G variant of ribonuclease A. *Protein Sci.* **7**, In press.

Schultz, L. W., Quirk, D. J. & Raines, R. T. (1998). His···Asp catalytic dyad of ribonuclease A: Structure and function of the wild-type, D121N, and D121A enzymes. *Biochemistry* **37**, In press.

Scopes, R. K. (1994). *Protein Purification: Principles and Practice*, Springer-Verlag, New York.

Sela, M., Anfinsen, C. B. & Harrington, W. F. (1957). The correlation of ribonuclease activity with specific aspects of tertiary structure. *Biochim. Biophys. Acta* **26**, 502-512.

Sharp, K., Fine, R. & Honig, B. (1987). Computer simulations of the diffusion of a substrate to an active site of an enzyme. *Science* **236**, 1460-1463.

Shiao, D. D. F. & Sturtevant, J. M. (1976). Heats of binding protons to globular proteins. *Biopolymers* **15**, 1201-1211.

Shoemaker, K. R., Kim, P. S., Brems, D. N., Marqusee, S., York, E. J., Chaiken, I. M., Stewart, J. M. & Baldwin, R. L. (1985). Nature of the charged-group effect on the stability of the C-peptide helix. *Proc. Natl. Acad. Sci. U.S.A.* **82**, 2349-2353.

Shrager, R. I., Cohen, J. S., Heller, S. R., Sachs, D. H. & Schechter, A. N. (1972). Mathematical models for interacting groups in nuclear magnetic resonance titration curves. *Biochemistry* **11**, 541-547.

Smith, J. S. & Scholtz, J. M. (1998). Energetics of polar side-chain interactions in helical peptides: Salt effects on ion pairs and hydrogen bonds. *Biochemistry* **37**, 33-40.

Sorrentino, S. & Libonati, M. (1994). Human pancreatic-type and nonpancreatic-type ribonucleases: A direct side-by-side comparison of their catalytic properties. *Arch. Biochem. Biophys.* **312**, 340-348.

Spolar, R. S. & Record, M. T., Jr. (1994). Coupling of local folding to site-specific binding of proteins to DNA. *Science* **263**, 777-784.

Steitz, T. A. (1993). *Structural Studies of Protein – Nucleic Acid Interaction: The Sources of Sequence-Specific Binding*, Cambridge University Press, Cambridge.

Steyaert, J. (1997). A decade of protein engineering on ribonuclease T_1. Atomic dissection of the enzyme-substrate interactions. *Eur. J. Biochem.* **247**, 1-11.

Takahashi, K. (1968). The reaction of phenylglyoxal with arginine residues in proteins. *J. Biol. Chem.* **243**, 6171-6179.

Tanford, C. (1957). Theory of titration curves. II. Calculations for simple models at low ionic strength. *J. Am. Chem. Soc.* **79**, 5340-5347.

Tanford, C. (1962). The interpretation of hydrogen ion titration curves of proteins. *Adv. Prot. Chem.* **17**, 69-165.

Tanford, C. & Kirkwood, J. G. (1957). Theory of protein titration curves. I. General equations for impenetrable spheres. *J. Am. Chem. Soc.* **79**, 5333-5339.

Tanford, C. & Roxby, R. (1972). Interpretation of protein titration curves. Application to lysozyme. *Biochemistry* **11**, 2192-2198.

Tarragona-Fiol, A., Eggelte, H. J., Harbron, S., Sanchez, E., Taylorson, C. J., Ward, J. M. & Rabin, B. R. (1993). Identification by site-directed mutagenesis of amino acids in the B2 subsite of bovine pancreatic ribonuclease A. *Protein Eng.* **6**, 901-906.

Tartof, K. D. (1992). Cloning vectors and techniques for exonuclease hybridization restriction mapping. *Methods Enzymol.* **216**, 574-584.

Taylor, J. D. & Halford, S. E. (1989). Discrimination between DNA sequences by the *Eco*RV restriction endonuclease. *Biochemistry* **28**, 6198-6207.

Thompson, J. E. Catalysis by Bovine Pancreatic Ribonuclease A – Energetics and Contributions from the Active-Site Histidines, *Ph.D. Thesis*, University of Wisconsin–Madison (1995).

Thompson, J. E., Kutateladze, T. G., Schuster, M. C., Venegas, F. D., Messmore, J. M. & Raines, R. T. (1995). Limits to catalysis by ribonuclease A. *Bioorg. Chem.* **23**, 471-481.

Thompson, J. E. & Raines, R. T. (1994). Value of general acid-base catalysis to ribonuclease A. *J. Am. Chem. Soc.* **116**, 5467-5468.

Thompson, J. E., Venegas, F. D. & Raines, R. T. (1994). Energetics of catalysis by ribonucleases: Fate of the 2',3'-cyclic intermediate. *Biochemistry* **33**, 7408-7414.

Thompson, R. C. (1974). Binding of peptides to elastase: Implications for the mechanism of substrate hydrolysis. *Biochemistry* **13**, 5495-5501.

Tishmack, P. A., Bashford, D., Harms, E. & Van Etten, R. L. (1997). Use of ^{1}H NMR spectroscopy and computer simulations to analyze histidine pK_a changes in a protein tyrosine phosphatase: Experimental and theoretical determination of electrostatic properties in a small protein. *Biochemistry* **36**, 11984-11994.

Travers, A. (1993). *DNA – Protein Interactions*, Chapman and Hall, London.

Tronrud, D. E., Ten-Eyck, L. F. & Matthews, B. W. (1987). An efficient general-purpose least-squares refinement program for macromolecular structures. *Acta Crystallogr., Sect A* **43**, 489-501.

Ui, N. (1971). Isoelectric points and conformation of proteins. II. Isoelectric focusing of α-chymotrypsin and its inactive derivative. *Biochim. Biophys. Acta* **229**, 567-581.

Vallee, B. L. & Williams, R. J. P. (1968). Metalloenzymes: The entatic nature of their active sites. *Proc. Natl. Acad. Sci. U.S.A.* **59**, 498-505.

Varani, G. (1997). RNA–protein intermolecular recognition. *Accts. Chem. Res.* **30**, 189-195.

von Hippel, P. H. & Berg, O. G. (1989). Facilitated target location in biological systems. *J. Biol. Chem.* **264**, 675-678.

von Hippel, P. H. & Schleich, T. (1969). The effects of neutral salts on the structure and conformational stability of macromolecules in solution. In *Structure and Stability of Biological Macromolecules* (S. N. Timasheff & G. D. Fasman, Ed.), pp. 417-574, Marcel Dekker, New York.

Wallace, R. B. & Miyada, C. G. (1987). Oligonucleotide probes for the screening of recombinant DNA libraries. *Methods Enzymol.* **152**, 432-442.

Walz, F. G. (1971). Kinetic and equilibrium studies on the interaction of ribonuclease A and 2'-deoxyuridine 3'-phosphate. *Biochemistry* **10**, 2156-2162.

Warshel, A. & Åqvist, J. (1991). Electrostatic energy and macromolecular function. *Annu. Rev. Biophys. Biophys. Chem.* **20**, 267-298.

Williams, R. J. P. (1971). The entatic state. *Cold Spring Harbor Symp. Quant. Biol.* **36**, 53-62.

Winter, R. B., Berg, O. G. & von Hippel, P. H. (1981). Diffusion-driven mechanisms of protein translocation on nucleic acids. 3. The *Escherichia coli lac* repressor–operator interaction: Kinetic measurements and conclusions. *Biochemistry* **20**, 6961-6977.

Wiseman, T., Williston, S., Brandts, J. F. & Nan, L.-N. (1989). Rapid measurement of binding constants and heats of binding using a new titration calorimeter. *Anal. Biochem.* **179**, 131-137.

Wittmayer, P. K. & Raines, R. T. (1996). Substrate binding and turnover by the highly specific I-*Ppo*I endonuclease. *Biochemistry* **35**, 1076-1083.

Wlodawer, A., Anders, L. A., Sjölin, L. & Gilliland, G. L. (1988). Structure of phosphate-free ribonuclease A refined at 1.26 Å. *Biochemistry* **27**, 2705-2717.

Wlodawer, A., Miller, M. & Sjölin, L. (1983). Active site of RNase: Neutron diffraction study of a complex with uridine vanadate, a transition-state analog. *Proc. Natl. Acad. Sci. U.S.A.* **80**, 3628-3631.

Wolfenden, R., Ridgeway, C. & Young, G. (1998). Spontaneous hydrolysis of ionized phosphate monoesters and diesters and proficiencies of phosphatases and phosphodiesterases as catalysts. *J. Am. Chem. Soc.* **120**, 833-834.

Wyman, J. & Gill, S. J. (1990). *Binding and Linkage: Functional Chemistry of Biological Macromolecules*, University Science Books, Mill Valley, CA.

Zegers, I., Maes, D., Dao-Thi, M., Poortmans, F., Palmer, R. & Wyns, L. (1994). The structures of RNase A complexed with 3'-CMP and d(CpA): Active site conformation and conserved water molecules. *Protein Sci.* **3**, 2322-2339.

Zhang, W., Bond, J. P., Anderson, C. F., Lohman, T. M. & Record Jr., M. T. (1996). Large electrostatic differences in the binding thermodynamics for a cationic peptide to oligomeric and polymeric DNA. *Proc. Natl. Acad. Sci. U.S.A.* **93**, 2511-2516.